Detailed Comparison of CPP's Uptake Properties for Pro-Apoptotic Cargo Delivery

D i s s e r t a t i o n

zur Erlangung des akademischen Grades

d o c t o r r e r u m n a t u r a l i u m
(Dr. rer. nat.)

im Fach Biologie

eingereicht an der
Mathematisch-Naturwissenschaftlichen Fakultät I
der Humboldt-Universität zu Berlin

von
Diplom-Biologin Judith Müller

Präsident der Humboldt-Universität zu Berlin
Prof. Dr. Jan-Hendrik Olbertz

Dekan der Mathematisch-Naturwissenschaftlichen Fakultät I
Prof. Dr. Andreas Herrmann

Gutachter/innen: 1. Prof. Dr. Hans-Dieter Volk

2. Prof. Dr. Andreas Herrmann

3. Prof. Dr. Gerald Grütz

Tag der mündlichen Prüfung: 02. Juli 2012

TABLE OF CONTENTS

TABLE OF CONTENTS

TABLE OF CONTENTS

ZUSAMMENFASSUNG

Limitierend für pharmakologische Therapien ist oft die Unfähigkeit des Wirkstoffes, biologische Membranen zu überwinden, weswegen häufig Transportmoleküle wie z.B. zellpenetrierende Peptide (CPPs, cell penetrating peptides) benutzt werden. Von den über 100 beschriebenen CPPs wurde bisher nur eine kleine Anzahl systematisch verglichen, was die Auswahl des „richtigen“ CPPs für eine Anwendung erschwert.
Ziel dieser vorliegenden Arbeit war es, das pro-apoptotische Peptid KLA mittels CPPs spezifisch in Krebszellen zu transportieren. Untersucht wurden: (I) Verschiedene CPPs in unterschiedlichen Zelltypen zur Selektion der „besten“ CPPs; (II) Der Einflusses des CPP C-Terminus auf die Internalisierung und zelluläre Verteilung; (III) Der zelluläre KLA-Transport mittels CPPs via einer nicht-kovalenten Administration.
22 verschiedene CPPs wurden in sieben Zelltypen untersucht, wobei Toxizität, Zellaufnahme und zelluläre Lokalisation mittels Fluorescein markierten CPPs in Fluoreszenzspektroskopie und konfokaler Mikroskopie betrachtet wurden. Abhängig von der Zellaufnahme wurden die CPPs in drei Gruppen klassifiziert. Die Untersuchung carboxylierter und carboxyamidierter CPP C-Termini ergab, dass in den meisten Fällen ein Carboxyamid die zelluläre Aufnahme begünstigte.
Drei CPPs (MPG, Penetratin und Integrin) wurden ausgewählt, um das pro-apoptotische KLA Peptid in zwei Krebszelllinien (MCF-7 Brustkrebszellen und leukämische RAW264.7 Makrophagen) im Vergleich zu Fibroblasten (Cos-7) nicht-kovalent zu transportieren. Der erfolgreiche KLA-Transport hing vom CPP, dessen C-Terminus und der Zelllinie ab. Die Analyse der Viabilität nach CPP:KLA Administration ergab, dass MPG-$CONH_2$:KLA (1:2) toxisch für Makrophagen und Brustkrebszellen, aber nicht für Fibroblasten war. Die Toxizität konnte der Apoptose zugeordnet werden.
Die vorliegende Arbeit liefert wichtige Informationen über die Auswahl des passenden CPPs für den nicht-kovalenten Transport des pro-apoptotischen KLA-Peptids.

Schlagwörter: Zellpenetrierendes Peptid, KLA Peptid, pro-apoptotisch, nicht-kovalent, Peptidtransport

SUMMARY

Limitations in a pharmacological therapy are often due to the inability of drugs to overcome the cellular membrane and therefore transporting molecules are being used, e.g. cell penetrating peptides (CPPs). Only a few of the over 100 described CPPs have been compared systematically making the choice of "the" CPP for a given application difficult.

The goal of the presented work is the CPP mediated delivery of the pro-apoptotic peptide KLA in breast cancer cells as proof of principle for a therapeutical application. Analysed were (I) Different CPPs in various cell types to select the "best" one, (II) The influence of the CPP C-termini on uptake and localisation, (III) The cellular KLA delivery via a non-covalent CPP administration.

22 CPPs were compared in seven cell types thereby looking at toxicity, cellular uptake and subcellular localisation using fluorescein labelled CPPs for fluorescence spectroscopy and confocal microscopy. The resulting uptake information allowed the classification of the CPPs in three main groups. The evaluation of carboxylated and carboxyamidated CPP C-termini revealed that a carboxyamide mostly enhanced the cellular CPP uptake.

Three CPPs were selected (MPG, penetratin and integrin) to deliver the pro-apoptotic KLA peptide in two cancer cell lines (breast cancer MCF-7 cells and RAW264.7 macrophages) compared to fibroblasts (Cos-7) via the non-covalent strategy. A successful KLA delivery depended on the applied CPP, its C-terminus and the used cell line.

The biological activity of the pro-apoptotic KLA peptide was determined via the cell viability (MTT assay). The co-incubation of MPG-$CONH_2$:KLA (1:2) was able to induce toxicity in breast cancer cells and leukaemic macrophages, but not in fibroblasts. The viability reductions were then assigned to apoptosis.

This work provides important information for the choice of an adequate CPP for the pro-apoptotic KLA peptide delivery and presents the advantage of the non-covalent delivery strategy.

Keywords: cell penetrating peptide, KLA peptide, pro-apoptotic, non-covalent, peptide delivery

1. INTRODUCTION

The observation and modulation of intracellular processes in the context of physiological and molecular-pharmaceutical studies is the basis of a specific and targeted development of active pharmaceutical agents. Necessary for that end as well as for an effective pharmacotherapy, a sufficient concentration of the biological active substance is needed at the site of action, which therefore requires an efficient internalisation. One of the main obstacles is the translocation over the cell membrane. Furthermore, depending on the target site, pharmaceuticals need to be distributed to different parts of the body while overcoming additional absorption barriers (e.g. blood-brain barrier).

1.1. Problems of Drug Delivery

The cell membrane protects the cell from the invasion of pathogens and other harmful molecules and is needed for the maintenance of the cells inner homeostasis, resulting in a well controlled import and export. Only small lipophilic molecules (< 600 Da) are able to pass the membrane by passive diffusion, whilst bigger ones have to be transported in energy-dependent and independent events [reviewed in (Sawant *et al.*, 2009)].

For a better understanding of intracellular biochemical processes, scientists need to translocate various molecules into living cells whilst influencing the cell as little as possible in its viability and homeostasis. Different methods have been developed, which either permeabilise the plasma membrane for a short amount of time or make use of transport molecules, so called carriers.

A method to overcome the plasma membrane is the microinjection of molecules by glass needles into the cytoplasm or nucleus (Capecchi, 1980). Cell plasma membrane permeabilisation is done by electroporation (Knight *et al.*, 1986; Rols, 2006) or sonoporation (Wyber *et al.*, 1997), in which an externally applied electrical field or ultrasonic sound induces pores in the membrane, respectively. Furthermore, pore forming molecules (Walev *et al.*, 2001), laser irradiation (Zeira *et al.*, 2003) or the "gene pistol" (Wells, 2004) can be used to overcome the cell membrane. These methods are unfortunately mostly inapplicable to the therapeutic utilisation for humans and are therefore primarily used in laboratories.

In pharmacology, carriers are therefore highly important and used to transport cargoes efficiently to the site of action, which can be a specific cell type, cell compartment or

cellular component. In contrast to free, unbound small molecules that passage the cell membrane mostly by diffusion or unspecific, adsorptive pinocytosis, carrier-bound molecules mostly internalise by receptor-mediated endocytosis. Examples of carriers include pH sensitive liposomes and polymers, cationic liposomes, lipids and polymers, viral vectors, polymeric nanoparticles and fusogenic peptides (Rawat *et al.*, 2007).

1.2. Cell Penetrating Peptides

An increasing popular class of membrane translocating agents is represented by the cell penetrating peptides (CPPs), also called protein transduction domains (PTDs) [reviewed in (Deshayes *et al.*, 2005; Jarver *et al.*, 2006)]. CPPs are able to translocate over the cellular membrane into different cell types *in vitro* (cell lines, primary cultures or tissues) and have even been applied *in vivo* (mouse, rat) transporting a range of different molecules e.g. nucleic acids, PNA, peptides, proteins, liposomes and nanoparticles [overview: (Dietz *et al.*, 2004; Langel, 2002; Lindsay, 2002; Sawant *et al.*, 2009)].

Work in the CPP area stemmed from the discovery that the third helix of the Antennapedia homeodomain, pAntp (43–58) (Derossi *et al.*, 1994) and the trans-activating transcriptional activator, Tat, a protein encoded by human immunodeficiency virus-1 (HIV-1) (Frankel *et al.*, 1988; Green *et al.*, 2003), can cross biological membranes. Up to the turn of the millennium, the number of peptides assigned to the family of CPPs has increased tremendously (Lindgren *et al.*, 2000). Nowadays, they can be divided into three classes: protein-derived peptides, model peptides and designed peptides (Zorko *et al.*, 2005). Protein-derived CPPs usually comprise the minimal effective sequence segment of the parent translocation protein and are also known as protein transduction domains or membrane translocation sequences. Examples are the Tat peptide (48–60) derived from the 86-mer Tat protein (Vives *et al.*, 1997) or penetratin (43–58) derived from the homeodomain Antennapedia of *Drosophila* (Joliot *et al.*, 2008). Model CPPs comprise sequences designed with the aim of producing well-defined amphipathic α-helical structures, or mimicking the structures of known CPPs. Examples are the model amphipathic peptide (MAP) (Oehlke *et al.*, 1998) or polyarginine sequences (Futaki *et al.*, 2001). Designed CPPs are usually chimeric peptides containing a hydrophilic and a hydrophobic domain of different origins, such as transportan, a fusion peptide of galanin and mastoparan (Pooga *et al.*, 1998a).

However, no unambiguous definition of CPPs has been proposed, only common features have been agreed on; such as (I) CPPs carry a net positive charge at

physiological pH and (II) CPPs facilitate the rapid translocation of molecules across cellular membranes. Generally, they comprise less than 30 amino acids and contain between approximately 17 % [e.g. hCT(9-32)] to 100 % [polyarginines] positively charged amino acids. With some exceptions such as polyarginine and integrin, most CPPs are amphipathic. Some of them acquire amphipathic characteristics when adopting an α-helical structure, as for instance the model peptide MAP (Oehlke *et al.*, 1998), while others have distinct hydrophobic and hydrophilic parts, such as transportan (Yandek *et al.*, 2008).

As mentioned, CPPs reveal remarkable properties of cell penetration either on their own, or as conjugates with a range of other types of biomolecules [reviewed in (Lindsay, 2002)]. However, the endocytic mechanism used - clathrin-mediated endocytosis (Richard *et al.*, 2005), caveolae-mediated endocytosis (Ferrari *et al.*, 2003; Fittipaldi *et al.*, 2003) or macro-pinocytosis (Kaplan *et al.*, 2005; Wadia *et al.*, 2004) - defines the migration of these peptides into cells and depends on parameters such as the nature of the cationic agent itself and complex formation with cargo, as well as the nature and distribution of proteoglycans expressed on the cell surface (Duchardt *et al.*, 2007; Poon *et al.*, 2007). Most likely CPPs utilise multiple internalisation mechanisms in combination (Duchardt *et al.*, 2007). Besides the translocation by endocytosis, it is thought that they are also able to overcome the cell membrane by energy-independent mechanism, such as micelle and pore formation (Deshayes *et al.*, 2004).

1.3. The CPPs of This Study

In this study, 22 different CPPs were chosen as representative cadidates from the three different CPP classes (Table 1, page 29).

SynB1 derives from the antimicrobial peptide protegrin, which was isolated from porcine leukocytes and acts against a broad spectrum of microorganisms (Steinberg *et al.*, 1997). The amphipathic, linear SynB1 is able to pass biological membranes as well as the blood brain barrier and is therefore involved in the development of peptide-conjugated pharmaceuticals (Rousselle *et al.*, 2000).

Polyomavirus Vp1 originates from the capsid protein VP1 of this virus. It is able to translocate into the nucleus, because the peptide contains a nuclear localisation sequence (NLS) as well as a DNA-binding motif (Chang *et al.*, 1993; Murray *et al.*, 2001).

Penetratin results from the *Drosophila* homeoprotein Antennapedia. Homeoproteins belong to the trans-activating factors and were described first in *Drosophila melanogaster* (Gehring, 1987). They consist a DNA-binding motif, the 60 amino acid long homeodomain, structured in three α-helices (Qian *et al.*, 1989). The amphipathic CPP penetratin (amino acid 43-58) derives from the third helix of this homeodomain (Derossi *et al.*, 1994).

Tat, also called HIV-1 Tat-(48-60), is the most frequently used CPP and stems from the transcriptional activator protein of HIV-1, is known to internalise into cells as well as the nucleus (Frankel *et al.*, 1988) and can be used as a vehicle for heterologic proteins (Fawell *et al.*, 1994). The cell penetrating peptide Tat contains a cluster of basic amino acids 49-58 with a nuclear localisation sequence (Ruben *et al.*, 1989).

Bac1-15 originates from Bac7, which is a bactenicin isolated from the granules of bovine neutrophils (Gennaro *et al.*, 1989). Its antimicrobial activity results from the increase in membrane permeability resulting in the inhibition of the bacterial respiration and ATP (adenosine-5'-triphosphate)-synthesis and therefore also of the protein biosynthesis (Skerlavaj *et al.*, 1990). Cationic Bac1-15 was found in the cytoplasm as well as the nucleus (Sadler *et al.*, 2002).

NF-κB is a positively charged NLS of the nucleus factor kappa B, which is involved in the regulation of cellular and viral genes (Lenardo *et al.*, 1989) and exhibits cell penetrating properties (Ragin *et al.*, 2002).

SV40, a short, seven amino acid long NLS, stems from the Simian Virus 40 large tumour antigen and is able to promote the nuclear accumulation of usually cytoplasmic proteins like the β-galactosidase (Kalderon *et al.*, 1984).

HATF3 is the NLS of the basic region of the human activating transcription factor (ATF)-3 (Hai *et al.*, 1989) and internalises into the cell probably by endocytosis (Ragin *et al.*, 2002).

hCT(9-32) derives from the C-terminal domain of human calcitonin, a hormone involved in the regulation of the calcium and phosphate balance (Copp, 1970). In comparison to the other CPPs its charge is relatively low at physiological pH. After the penetration of the cell membrane it is found in the cytoplasm in a punctuated pattern, but not in the nucleus (Trehin *et al.*, 2004).

Rev, also called HIV-1 Rev-(34-50), originates from the trans-activating Rev protein of HIV-1 and contains a nuclear localisation sequence (Cochrane *et al.*, 1990) as well as a RNA (ribonucleic acid)-binding motif (Bohnlein *et al.*, 1991).

pVEC is a peptide stemming from murine, endothelial cadherin, which is a transmembrane protein mediating cell contact between neighbouring cells and anchoring the actin cytoskeleton with the plasma membrane (Huber *et al.*, 1996). The peptide sequence consists of 13 amino acids, which are usually located near the cell membrane and five hydrophobic amino acids of the C-terminus of the transmembrane region (Elmquist *et al.*, 2001).

Integrin derives from the hydrophobic region of the cytoplasmic part of the human transmembrane protein integrin β_3. So far, its cell penetrating properties were described being cell type unspecific (Hawiger, 1999).

DPV6 (Diatos Peptide Vector) stems from PDGF (platelet-derived growth factor), belongs to the human Vectocell® penetrating peptides and can interact with aminoglycans, like heparin, on the cell surface. It has been described as non-toxic *in vitro* and *in vivo* and was found in the cytoplasm together with the cargo protein maleimid without the detection of a nuclear localisation (De Coupade *et al.*, 2005).

$S4_{13}$PV is from a 13 amino acid sequence of the dermaseptin S4 peptide, which has cell penetrating properties attached to the NLS of SV40 large T antigen (Hariton-Gazal *et al.*, 2002). Dermaseptin was isolated from the skin of the frog *Phyllomedusa bicolor*, adopts a α-helical conformation and inhibits the growth of a number of pathogenic microorganisms (Mor *et al.*, 1994).

Transportan consists of amino acids from the neuropeptide galanin and the wasp toxin mastoparan linked via a lysine residue. During the cellular uptake transportan is found first at the outer membrane and cytoplasmic membrane structures, and later at the nuclear membrane and inside the nucleus, where it condenses in sub-structures, probably in the nucleoli (Pooga *et al.*, 1998a).

Pep-1, also known as Chariot™, belongs to the newly constructed peptides. It has a hydrophobic tryptophan-rich domain to interact with proteins on the cell membrane and a hydrophilic, lysine-rich domain, the NLS of SV-40 large T-Antigen, to reach the nucleus fast. Pep-1 is able to penetrate various cell lines and accumulates fast in the nucleus (Morris *et al.*, 2001).

MPG (FP-NLS MPG, model amphipathic peptide) is a synthetic peptide, in which the hydrophobic domain of the fusion protein gp41 of HIV was combined with the hydrophilic domain of the SV40 large T antigen NLS (Morris *et al.*, 1997). MPG is able to transport single and double-stranded oligonucleotides into the nucleus independent of endosomal pathways (Vidal *et al.*, 1998).

MAP is a designed, amphipathic peptide containing lysine, leucine and alanine residues (Oehlke *et al.*, 1996). Its penetration was reported being cell type independent and it was found in the nucleus (Oehlke *et al.*, 1998).

Poly-P, a peptide containing many prolines, is found in the cytoplasm after peptide incubation and is reported to show no toxic effects even at high concentrations (Fernandez-Carneado *et al.*, 2004).

R7 and **R9**, the poly-arginine peptides, are the only non-amphipathic peptides, which are able to pass the cell membrane. R9 is able to translocate 100-times more efficient than Tat and both peptides are even more resistant to proteases (Wender *et al.*, 2000).

pVEC-scrambled is the mixed sequence of pVEC and used as a negative control in this study, since it is unable to pass the cell membrane (Elmquist *et al.*, 2003).

1.4. Strategies of CPP Delivery

1.4.1. Covalent Delivery

The main purpose of CPPs is their use as delivery vehicle for biological active substances into living cells. For that, the cargo is usually attached to the CPP either by covalent linkage or tandem synthesis/expression, when the cargo is a peptide or protein (Gait, 2003; Nagahara *et al.*, 1998). Here the final localisation of the chimeric molecule depends on both cargo and carrier.

CPPs have been shown to efficiently improve intracellular delivery of various biomolecules, including plasmid DNA, oligonucleotides, siRNA (short interfering RNA), PNA (peptide nucleic acid), proteins and peptides, as well as liposome nanoparticles, into cells both *in vivo* and *in vitro*. Short synthetic CPPs have been designed to overcome both extracellular and intracellular limitations, trigger the movement of a cargo across the cell membrane into the cytoplasm and improve its intracellular trafficking, thereby facilitating interactions with the target (Brasseur *et al.*, 2010; Sawant *et al.*).

When CPPs are used to transport other peptides, they are usually synthesised continously. Snyder and colleagues synthesised a tumour suppressor p53-derived peptide linked to Tat and were able to restore p53 protein activity in cancer cells (Snyder *et al.*, 2004). They showed that the CPP did not hinder the therapeutical effectiveness of the p53-derived peptide and that it was proteolytically stable.

If the conjugates are longer than about 50 amino acids, they are either genetically expressed in tandem or chemically conjugated. One of the first reports stated the

120 kDa β-galactosidase protein expressed in tandem with the Tat peptide was able to translocate in all tissue of the mice and even passaged the blood-brain barrier (Schwarze *et al.*, 1999).

Chemical conjugation through disulfide bond formation is particularly interesting. It can form between thiol groups of cysteine residues and will be reduced when entering the cytoplasm due to the intracellular redox environment followed by the release of the cargo (Hallbrink *et al.*, 2001). Efficient and specific coupling, thereby preventing the formation of homodimers, can be done by the use of 2-pyridinesulfenyl (SPyr)-protected cysteine-containing peptides with thiol-unprotected peptides (Schulz *et al.*, 2000). Unfortunately, due to the lack of glutathione and therefore thiolate anions, disulfide cleavage is disfavoured in the acidic endosome, but happens at the cell surface and may happen in the early endosome (Feener *et al.*, 1990; Jones, 2007). This needs to be taken into consideration, since the CPPs are often endocytosed.

Coupling proteins or peptides to CPPs with a short proteolytic cleavage site in between is another possibility. Recombinant Tat-delivered alpha B-crystallin, a small heat shock protein, was delivered into cells and proteolytically cleaved by matrix metalloproteinase-1 (MMP-1), which then could be blocked by the treatment with a MMP inhibitor (Yang *et al.*, 2011). MMP-2 and -9 activities are associated with tumour invasion and metastasis (Egeblad *et al.*, 2002). A specific linker, predominantly sensitive to these MMPs, has been used to attach a short cationic CPP sequence to neutralising anions (Olson *et al.*, 2009). When the molecule is cleaved by MMP-1 and -9, the masking anion is detached releasing the cell membrane adhesive CPP sequence as well as the cargo and promoting cellular uptake of both. Tsien's group used dendrimers to display many activatable CPPs, which transport magnetic resonance and fluorescent probes for tomographic imaging as well as superficial intraoperative guidance during surgery. They were able to detect very small tumours and metastasis of 200 μm. This potential diagnostic agents is promising, since it can be used (I) for a wide range of tumours, (II) for all tumour markers, (III) for whole-body scanning as well as (IV) for precise, fluorescence-guided surgery.

One main purpose of CPPs is the delivery of oligonucleotides for a therapeutical application. For example, RNA interfering (RNAi) technology is a powerful technique for post transcriptional gene silencing, in which short interfering double stranded (ds) RNAs (siRNAs) are loaded into the RNA-induced silencing complec (RISC) siRNAi complex in the cytoplasm, which then recognises and degrades target mRNA. The

delivery of siRNAs remains a problem, since they are highly negatively charged and therefore rejected by the cell membrane. Eguchi and Dowdy linked a RNA-binding domain to a CPP, thereby masking the negative charge of the siRNA and were able to completely knockdown the target gene in the whole cell population in over 30 cell types including primary cells [reviewed in (Eguchi *et al.*)]. Their peptide transduction domain-dsRNA binding domain (PTDDRBD) represents a promising tool for RNAi therapy in the future.

Furthermore, uncharged oligonucleotide analogues, peptide nucleic acids (PNA) and phosphorodiamidate morpholino oligomers (PMO, morpholino) are widely used for antisense applications, such as steric block ONs for the inhibition of translation. In principle, PNAs can be coupled to CPPs either by synthesis in tandem (Simmons *et al.*, 1997) or through conjugation by thioether or disulfide linkages (Abes *et al.*, 2007; Moulton *et al.*, 2004). Here as well the disulfide linkage is very popular and was first used by Pooga *et al.* (Pooga *et al.*, 1998b), who linked PNA, complementary to the human galanin receptor type 1 mRNA, to transportan and penetratin suppressing the expression of functional galanin receptors. Thioether, disulfide or amide conjugated CPP-PMOs have similar nuclear antisense activity (Moulton *et al.*, 2004), but the amide linkage might be advantageous, since it requires only one step synthesis and purification in comparison to a two step process. In addition, it was found to be more stable in human serum than disulfide-linked CPP-PMO (Youngblood *et al.*, 2007). One of the most promising CPP-PMO conjugates is used in the treatment of Duchenne muscular dystrophy. Avi Biopharma, a company working with CPPs, uses 6-aminohexanoic acid spaced oligoarginine [$(R\text{-}Ahx\text{-}R)_4$] for *in vivo* steric block splicing correction in the treatment of Duchenne Muscular dystrophy (Wang *et al.*, 2010). Further CPPs have even made it into clinical trials. CellGate Inc. initiated phase II clinical trials with cyclosporine linked to polyarginines in 2003 to treat patients with psoriasis (Rothbard *et al.*, 2000; Smith *et al.*, 2003). A phase IIa clinical trial is now in progress in patients suffering from acute myocardial infarction for testing PKC (protein kinase C) peptidic inhibitors known to be cardioprotective (Bates *et al.*, 2008). In particular the δ-PKC inhibitor KAI-9803 (also known as δ-V1-1) leads to reduced damages in cardiomyocytes (> 60 % infarct size reduction) and endothelial cells after an ischemic insult (Inagaki *et al.*, 2003).

Although conjugation methods offer several advantages for *in vivo* applications, including rationalisation and control of the CPP-cargo, they remain limited from the chemical point of view, as they risk altering the biological activity of the cargoes.

1.4.2. Non-Covalent Delivery

The non-covalent delivery of biomolecules has been reported for several CPPs (Morris *et al.*, 2008). It is advantageous, because it simplifies conjugation protocols and different cargoes can be delivered without the adjustment of them (although the mixing ratio might need some consideration). Furthermore, the non-covalent delivery decreases the likelihood of unwanted influences of the CPP on cargo activity as well as of the cargo on the cell penetrating properties of the CPPs.

Different approaches for gene-delivery have been used. Peptides, which are able to complex with DNA, associate with peptides that facilitate endosomal escape, such as the fusion peptide of HA_2 subunit of influenza haemagglutinin (Wagner *et al.*, 1992). Other successful gene carriers are MPG (Morris *et al.*, 1999) or the synthetic peptide analogue GALA (Gottschalk *et al.*, 1996). Furthermore, Pep-1 was able to deliver peptides and proteins non-covalently *in vitro* (Morris *et al.*, 2001) and *in vivo* (Gros *et al.*, 2006). MPG formed stable non-covalent complexes with siRNA and delivered it efficiently into the nucleus of mammalian cells, for which the NLS was essential for nuclear delivery, but not for cytoplasmic targeting (Simeoni *et al.*, 2003). Electrostatic and hydrophobic interactions are responsible for stable complex-formation of Pep-1 and MPG with oligonucleotides or peptides and proteins (Morris *et al.*, 2001; Simeoni *et al.*, 2003).

The novel CPP Rath was also able to deliver proteins and nucleic acids in a temperature-independent mechanism hereby avoiding endosomal entrapment (Bais *et al.*, 2008). It was also capable of delivering large antibodies into primary cells, which is thought to be more difficult than the delivery into immortalised cell lines and was non-cytotoxic at high concentrations (75 μM). Another approach is the inclusion of RNA binding domains in the Tat sequence, which then specifically recognises a short RNA sequence. The siRNA cargo is designed including the matching RNA sequence and is transported into the cells by complex formation (Endoh *et al.*, 2009). The attachment of the CPP to the cargo can also be done by using the interactions of avidin and biotin-CPP constructs (Pooga *et al.*, 2001).

1.4.3. CPP-Modified Liposomes

Liposomes for the carriage of water-soluble drugs and micelles delivering poorly soluble therapeuticals are probably the most popular and well-investigated drug carriers (Torchilin, 2005; Torchilin, 2007). When Tat was incorporated in liposomes via a spacer molecule, which allowed the Tat peptide to interact with the cell surface, cells displayed an enhanced uptake (Pittet *et al.*, 2006). Furthermore, the number of CPP molecules (Tat and penetratin) attached to the liposomal surface was proportional to the translocation and was dependent on peptide and cell type used. The conjugation of CPPs (such as R8) to liposomes was found to enhance their uptake into airway cells upon inhalation (Cryan *et al.*, 2006). The incorporation of Tat into micelles was used to deliver anticancer drugs to acidic, solid tumours (Sethuraman *et al.*, 2007).

Besides the incorporation of CPPs in liposomes and micelles, they have been used for the modification of solid lipid nanoparticles (no inner aqueous space) and were able to enhance the gene transfection in vitro and in vivo compared to polyethylenimine nanocarriers (Suk *et al.*, 2006).

Surprisingly, Tat peptide-modified liposomes (Tatp-lipoplexes), which were prepared with small amounts of cationic lipids, complexed with DNA showing higher transfection and less toxicity than Lipofectamine® in mouse fibroblasts and cardiac myocytes. When injected intratumourally, Tat-liposome-DNA complexes showed efficient transfection (Torchilin *et al.*, 2003). For the delivery of siRNA, liposomes modified with R8 have been used, which showed very high blood serum stability as well as transfection in Lipofectamine 2000-resistant SK-MES-1 lung tumour cells (Zhang *et al.*, 2006).

1.4.4. Internalisation Mechanisms of CPPs

The internalisation mechanism of many CPPs remains unclear, possibly due to the use of different methods in different laboratories, which are probably not comparable, but is thought to involve a wide range of possibilities (see Figure 1).

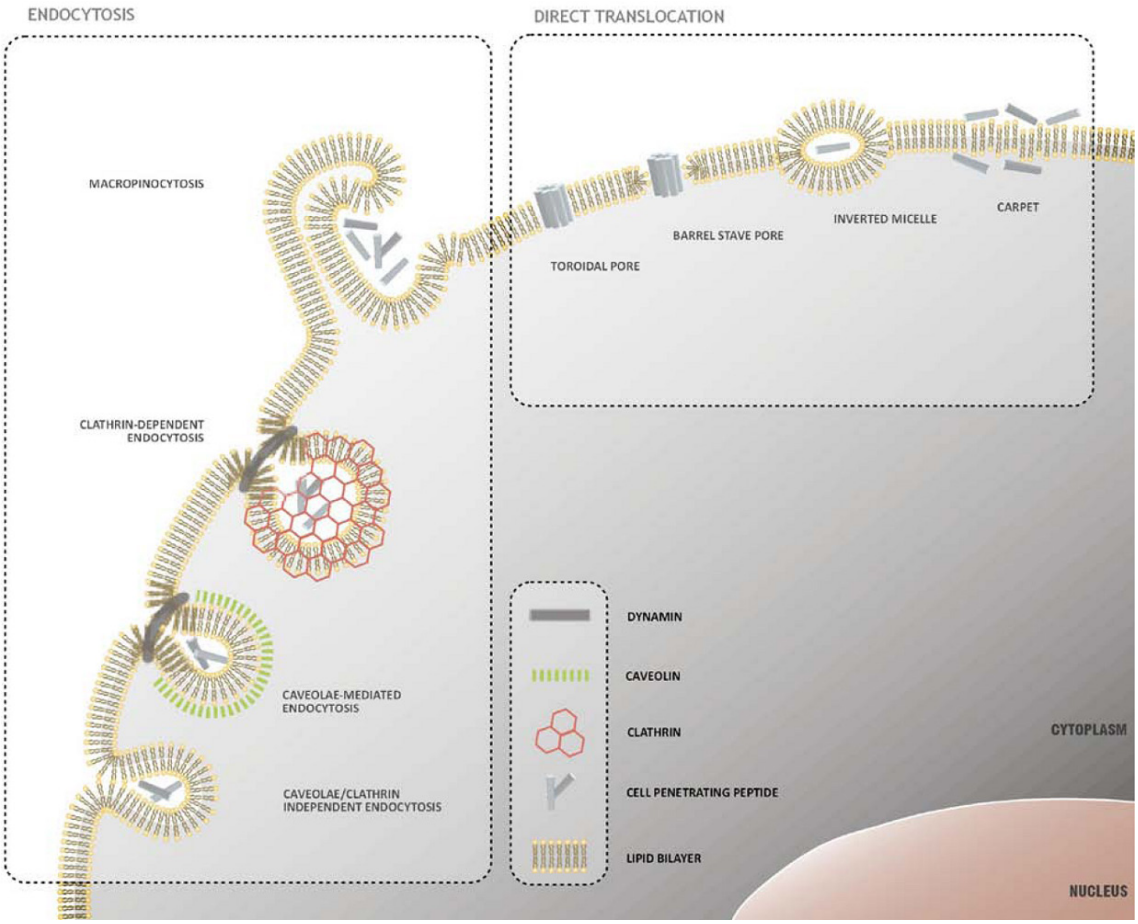

Figure 1. Mechanisms of CPP Uptake.
Many internalisation mechanisms for the cellular uptake of cell penetrating peptides have been suggested. They include energy-dependent endocytotic pathways as well as energy-independent translocation by pore formation of lipid membrane destabilisation. The figure is taken from (Trabulo *et al.*, 2010).

The first contact of the CPPs with the cell membrane is driven by electrostatic interactions with proteoglycans and syndecans, which are the major components of the extracellular matrix. The clustering of glucosaminoglycans (GAGs) triggers the remodelling of the actin network and guanosine triphosphate hydrolase (GTPase) activation and impacts the membrane fluidity (Gerbal-Chaloin *et al.*, 2007; Ziegler, 2008). Primary amphipathic peptides, consisting of a sequentially hydrophobic and cationic domain such as MPG (Morris *et al.*, 1997), transportan (Pooga *et al.*, 1998a) and Pep-1 (Morris *et al.*, 2001) bind to neutral anionic lipid membranes, probably through hydrophobic interactions and reduce the surface tension (Ziegler, 2008). They penetrate deep in the hydrophobic core without spanning the bilayer. Primary amphipathic peptides often self-associate in the head group region, insert into the membrane and translocate directly by e.g. pore formation (Deshayes *et al.*, 2006). Transportan and MPG lead to membrane leakage already at submicromolar concentrations (Barany-Wallje *et al.*, 2007), whereas Pep-1 crosses the membrane

without inducing leakage (Weller *et al.*, 2005). Besides the formation of pores, other direct penetration mechanisms, which are most likely for primary amphipathic CPPs, are the formation of inverted micelles (Derossi *et al.*, 1996), the carpet-like (Pouny *et al.*, 1992) and the membrane-thinning model (Lee *et al.*, 2005).

Secondary amphipathic peptides, such as penetratin (Derossi *et al.*, 1996), show their amphipathic secondary structure after the interaction with lipids as helixes (Futaki *et al.*, 2001) or β-sheets (Oehlke *et al.*, 1997). Their insertion into the bilayer is not very pronounced. At low micromolar CPP concentrations high fractions of anionic lipids (> 10 %) are needed for membrane binding, not typical in eukaryotic cells (Ziegler, 2008). The same was reported for non-amphipathic CPPs such as R9 - direct translocation was not seen at low micromolar concentrations. Instead it has been reported that penetratin and polyarginines bind to the membrane mainly through electrostatic interactions and trigger the cellular uptake of energy-dependent endocytosis (Murriel *et al.*, 2006). Endocytosis can be subdivided in phagocytosis (large particle uptake) and macropinocytosis (solute uptake). In macropinocytosis the outer surface of the plasma membrane folds inwards, forming an external macropinocytic structure that is enclosed and internalised: the macropinosome. It is unknown whether CPPs induce specific macropinocytotic pathways, but quite likely that they utilise multiple pathways in the fluid phase as well as non-specific adsorptive endocytosis. In receptor-mediated endocytosis, clathrin- or caveolin-mediated mechanisms are involved, which bind the extracellular molecule followed by an invagination of the membrane and the formation of phagosomes (Jones, 2007). Depending on the experimental conditions, a CPP uses mostly more than one pathway (Letoha *et al.*, 2003). After cellular uptake, the endosomal escape remains a major limitation, but is has been reported that CPPs traffic through the endoplasmic reticulum and Golgi network into the cytosol (Fischer *et al.*, 2004) and that NLS motifs can localise the cargo to the nucleus (Simeoni *et al.*, 2003). The incorporation of endosomal breakers is a possibility to escape the endosome through proton sponge effects (Yamaguchi *et al.*). Another possibility is the use of endosomolytic reagents like chloroquine (Veldhoen *et al.*, 2006) or endosomolytic peptides, which acidic residues get protonated at a result of endosomal acidification leading to the formation of an α-helix, which hydrophobic side interacts and destabilises the endosomal membrane (Lundberg *et al.*, 2007). Using photosensitisers, which localise in the endosomal membrane and destabilise the

membrane upon photostimulation to release the entrapped molecules has also been done (Hogset *et al.*, 2004).

In summary, even after two decades of CPP applications *in vitro* and *in vivo* the internalisation mechanism of the CPPs alone or together with their cargo remains controversial and a main subject in research areas.

1.5. Pro-Apoptotic Peptides as Therapeutic Tools

Therapeutic peptides mimicking or inhibiting protein-protein interactions have become a promising new class of drugs, because of potential great target specificity, easy development and low-prized production (Raucher *et al.*, 2009; Vlieghe *et al.*). This is especially relevant in tumour therapy where the delivery of therapeutic peptides is limited due to rapid degradation and poor tumour cell penetration. As a result D-amino acids can be introduced to improve stability or they can be attached to carriers to improve cellular uptake, e.g. CPPs. Therapeutic peptides are classified in three main groups: signal transduction-inhibiting, cell cycle-arresting and necrosis- or apoptosis-inducing peptides.

1.5.1. Peptides for Signal Transduction Inhibition

Peptides that interfere with the proliferative signal transduction cascade either inhibit mitogenic signals or restore the activity of tumour suppressor proteins. For example, researchers developed peptide inhibitors of extracellular signal-regulated kinase (ERK), which is one of the most studied transduction cascades transmitting extracellular signals to the nucleus, resulting in the activation of transcription factors which are essential for proliferation and differentiation (Kelemen *et al.*, 2002). Attaching penetratin or Tat to the inhibitor facilitated the uptake and inhibited ERK activation in stimulated NIH 3T3 (mouse embryo fibroblast) cells or nerve growth factor-treated PC12 (pheochromocytoma) cells followed by the inhibition of the activation of E twenty-six (ETS)-like transcription factor 1 (Elk-1).

The tumour suppressor protein p53, whose gene is very often deleted or mutated in cancer cells, is a transcription factor important for cell cycle regulation and apoptotic response to DNA damage. A C-terminal peptide of p53 (peptide 46) fused to penetratin was able to activate p53-mediated transcription in cell lines expressing wild-type and certain mutant p53 proteins, but not in null p53 cell lines (Selivanova *et al.*, 1997). It could restore the growth-inhibition and apoptosis-induction function of two often mutated p53 proteins, which was due to the binding of the peptide to the core as well as

to the C-terminal domain of p53, which rehabilitated the sequence-specific DNA binding of the p53 protein (Selivanova *et al.*, 1999). Furthermore, the peptide induced cell death in several cancer cell lines, such as MCF-7 cells (overexpression of wild-type p53), but not in non-malignant cell lines containing wt p53 (Kim *et al.*, 1999). This therapeutic anticancer peptide is a promising agent for the induction of apoptosis in cancer cells carrying p53 abnormalities.

1.5.2. Peptides for Cell Cycle Inhibition

Peptides inhibiting cell cycle progression modulate cyclin and cyclin-dependent kinase (Cdk) activity. Cdks are activated by cyclin binding or by other Cdk-activating kinases (CAKs) and phosphorylate target proteins, which control cell-cycle specific events like spindle formation or chromosome condensation. Cdks are therefore great targets for anticancer drugs. The inhibition of Cdks is either due to phosphorylation of inhibitory sites or due to the binding of Cdk inhibitors (CKIs). Gondeau *et al.* designed a peptide derived from cyclin A, which was able to form stable complexes with Cdk2-cyclin A and inhibited its kinase activity (Gondeau *et al.*, 2005). When coupled to the Tat peptide, it inhibited the proliferation of several tumour cell lines (including MCF-7 cells) with IC_{50}s between 2 μM and 14.2 μM in 48 h incubations.

1.5.3. Peptides for Apoptosis Induction: the Bcl-2 Protein Family

The pro-apoptotic peptides inhibit members of the Bcl-2 protein family, mimic Bcl-2 family members or modulate caspase activity. Apoptosis is crucial for the body's homeostasis and for the elimination of cells containing damaged DNA. It is often dysfunctional in cancer cells resulting in uncontrolled proliferation. Therefore the development of pro-apoptotic peptides for the selective induction of apoptosis in cancer cells is of great interest (Ellerby *et al.*, 1999).

One possibility is to target protein kinase B (Akt kinase). Completely phosphorylated, membrane anchored, activated Akt inhibits key apoptosis proteins by phosphorylation (Cardone *et al.*, 1998) and regulates NF-κB-mediated transcription of other inhibitors of apoptosis (IAPs) (Barkett *et al.*, 1999), which leads to cellular apoptosis protection and uncontrolled cancer cell growth. Akt-mediated protection against apoptosis can be stopped by its interaction with the cell membrane or by inhibiting its substrate phosphorylation activity. Indeed, Hiromura *et al.* (Hiromura *et al.*, 2004) was able to deliver an Akt-inhibitor peptide by fusing it to the CPP Tat in human T cells, which interacted with it and specifically inhibited its kinase activity. This peptide chimer was

able to inhibit cell proliferation and anti-apoptosis activity *in vitro* as well as tumour growth *in vivo*.

Furthermore, pro-apoptotic peptides can target the anti-apoptotic B-cell lymphoma 2 (Bcl-2) family proteins (Lutz, 2000). The family of Bcl-2 proteins consists of pro- and anti-apoptotic regulator proteins all sharing the Bcl-2 homology 3 (BH3) domain. Pro-apoptotic Bcl-2 proteins contain either only the BH3 domain [e.g. Bcl-2-associated death promoter (BAD) protein] or several domains [e.g. BH1-BH3 in Bcl-2-associated X protein (Bax)] which induce apoptosis by promoting cytochrom c release from the mitochondria, followed by the activation of caspases mediating the cell death. In cancer cells the anti-apoptotic side of the Bcl-2 proteins is overexpressed. Anti-apoptotic proteins such as Bcl-2 or Bcl-xL neutralise pro-apoptotic Bax or BH3-only proteins and decrease the cell's susceptibility to cell death.

In one study, BH3 peptides derived from the pro-apoptotic Bcl-2 family members were conjugated to Antennapedia and introduced into head and neck squamous carcinoma cell lines, which overexpress the anti-apoptotic protein Bcl-XL (Li *et al.*, 2007). The Antp-BH3 peptides colocalised with the mitochondria and induced viability reduction and apoptosis.

With the goal to restore apoptosis in cancer cells, Valero *et al.* designed a peptide encompassing two central helices of the membrane pore-forming domain of the pro-apoptotic Bcl-2 protein Bax (Valero *et al.*, 2011). This peptide alone was sufficient to insert in the mitochondrial outer membrane resulting the loss of the transmembrane potential, membrane disruption and cytochrome c release. Furthermore, the peptide itself delivered GFP to the mitochondria, induced caspase-dependent apoptosis and was even more effective than the widely used pro-apoptotic KLA peptide (discussed in more detail later). When coupled to the CPP octaarginine it efficiently penetrated HeLa cells and induced toxicity with a LC_{50} of 15 µM after 24 h, which could be assigned to apoptosis induced by the Bax-derived peptide. Moreover, the R8-Bax [106-134] peptide showed anticancer activity in tumour-bearing mice.

1.5.4. Peptides for Apoptosis Induction: The Pro-Apoptotic KLA Peptide

A widely used pro-apoptotic peptide is the polycationic KLA peptide with the sequence $(KLAKLAK)_2$ (Ellerby *et al.*, 1999). Due to their positive charge, pro-apoptotic KLA peptides are attracted by negatively charged membranes e.g. mitochondrial membranes, where they distort the lipid matrix. Losing the membrane barrier function, mitochondria swell and cells undergo apoptosis. Since the eukaryotic plasma membrane has a low

transmembrane potential, these peptides usually remain non-toxic outside the cell, but induce apoptosis when transported across the plasma membrane (Lemeshko, 2010). When KLA was coupled to hepta-arginine, both isoforms (L- and D-) induced permeabilisation of the inner and outer membranes of rat liver mitochondria at 3.6 μM. Furthermore, they induced mitochondrial aggregation thereby stopping their metabolic activity, which was strongly dependent on the inner membrane potential of the mitochondria. Therefore, the higher anti-cancer activity of R7-KLA and r7-kla (D-isoform) in comparison to just KLA or kla alone is not only due to a better plasma membrane penetration (Law *et al.*, 2006), but also due to the presence of arginine-rich CPPs, which increase the direct permeabilisation of mitochondrial membranes in a potential dependent mechanism. This finding might be important, taking into account that plasma and mitochondrial membrane potentials are usually higher in tumour cells than in normal cells (about 60 mV higher in the mitochondria of cancer cells) (Chen, 1988). Coupling the KLA-peptide to tumour homing devices resulted in the disruption of mitochondrial membranes, the growth inhibition of human dermal microvessel endothelial cells (DMECs) under angiogenic conditions of proliferation and cord formation, but not under angiostatic ones and even induced anti-cancer activity in mice (Ellerby *et al.*, 1999).

In another approach the KLA peptide was delivered using a multimeric RGD-containing scaffold, which released KLA by disulfide bridge cleavage after internalisation by receptor-mediated endocytosis (Foillard *et al.*, 2009). In a different study, KLA was coupled to R8 and induced toxicity (IC_{50}) at 2 μM and 4 μM in human myeloid KG1a and HeLa cells (Watkins *et al.*, 2009). Furthermore, researchers reckoned some of the cytotoxic effects mediated by r8-kla were due to direct effects on the plasma membrane and its increased permeability, since they observed cellular propidium iodide entry after 10 minutes as well as membrane blebbing.

To selectively induce apoptosis in malignant cells whilst showing little cytotoxicity in normal cells, the cytokine TRAIL (tumour necrosis factor-a related apoptosis inducing ligand) has been widely used (Hopkins-Donaldson *et al.*, 2000). TRAIL binds to death receptors and induces apoptosis. Unfortunately, many tumour cells are resistant to TRAIL-induced apoptosis due to e.g. loss of caspase-8 activity (Hopkins-Donaldson *et al.*, 2000) or constitutively active Akt protein kinase (Chen *et al.*, 2001). Therefore, the use of KLA is of high importance, since it can be used to overcome TRAIL resistance (Barua *et al.*, 2010). KLA was used for the chemosensitisation of two TRAIL-resistant

human prostate cancer cell lines to death receptor (DR) agonistic antibodies. KLA alone had no effect at low concentrations (1-15 μM), but induced swelling necrosis (oncosis) at > 30 μM. A KLA concentration of 15-25 μM was then used to sensitise the cells to the apoptotic effects of the DR agonists. Pre-incubation with KLA before treatment with DR agonistic antibodies resulted in an increase in caspaser-3 cleavage and cytochrome c levels. This shows that KLA can be used to sensitise TRAIL-resistant cells to DR-mediated apoptosis.

Another study used three triphenyl phosphonium (TPP) cations to deliver KLA (Kolevzon *et al.*, 2011). TPPs accumulate in the mitochondria due to the high negative mitochondrial potential (Murphy *et al.*, 2007), but are highly affected by its cargo: no mitochondrial localization after conjugation to CPPs (Ross *et al.*, 2004). The delivery of 3-TPP-KLA induced mitochondria-dependent apoptosis in HeLa cells with an IC_{50} of 25 μM after 3 hours incubation. Furthermore, the conjugation of three TPPs to the N- or C-terminus did not influence the cytotoxic KLA activity.

KLA has also been used in the fight of obesity (Kolonin *et al.*, 2004). It was coupled to a homing peptide of white fat vasculature and was able to ablate white fat in obese mice resulting in the upregulation of lipid turnover and an increased metabolic rate followed by the reversal of obesity and metabolic normalisation as well as no detection of adverse effects. Since the target of the homing peptide also exists in humans, this study is promising for the development of targeted drugs to treat human obesity.

These examples show, that mitochondrial membrane-disrupting peptides like KLA are promising tools for future cancer therapies, since they do not rely on the intrinsic expression of pro-apoptotic Bcl-2-like proteins and can be used in a wide range of cell types. Since they have proven applicability *in vivo* (Kolonin *et al.*, 2004), their future use as therapeutic peptides is very likely.

1.6. Objective and Strategy

Major limitations in the clinical implementation of peptide-based drugs have risen from their incapacity to cross biological membranes. Cell penetrating peptides are promising tools to improve the intracellular delivery of various cargoes including peptides and proteins [as reviewed in (Dietz *et al.*, 2004; Sawant *et al.*, 2009)]. However, for a therapeutical application (e.g. cancer treatment with pro-apoptotic peptides) it is still a challenge to choose “the” appropriated CPP.

Nowadays, only a few comparative studies of CPP internalisation have been performed (El-Andaloussi *et al.*, 2007; Fischer *et al.*, 2004; Fotin-Mleczek *et al.*, 2005; Maiolo *et al.*, 2005; Sarko *et al.*, 2010; Tunnemann *et al.*, 2008; Wender *et al.*, 2000). Nevertheless, differences in numerous variables relating to the experimental procedures used by various groups make it hard to compare studies and form any conclusions, especially about the mechanism of internalisation. These variables include: different sources and purity of CPP, label or cargo used, concentration of CPP, cell-type, density and stage of cell cycle, incubation time and final end point or read-out.

With regard to a clinical application of anti-cancer drugs such as biological active peptides, the best CPP suited for that application should be determined *in vitro*. In this study the internalisation of the apoptosis-inducing KLA peptide is supposed to be achieved via a non-covalent strategy meaning a simple co-incubation procedure of both - CPP and KLA peptide. This approach represents a huge advantage for the future therapeutic utilisation: (I) It is much easier and quicker to mix the appropriate CPP with the corresponding therapeutic peptide instead of newly synthesising the chosen set; (II) It is possible to change the pro-apoptotic peptide quickly in case resistance occurs. Furthermore, the likelihood of negative influences of the CPP on the activity of the cargo peptide, and vice versa, is hopefully reduced by the non-covalent approach.

Since there has been no large-scale systematic attempt to determine which CPP sequence shows optimal cellular uptake, the internalisation of 22 different CPPs will be compared in various commonly used cell types. In a first step, the standard assay conditions will be defined allowing direct comparison of the measured cellular uptake, toxicity and their subcellular localisation (vesicular or evenly distributed). To measure cellular CPP uptake, fluorescein labelled CPPs will be used, which can be measured in the lysate using a microplate reader and visualised by confocal microscopy. The toxicity of the peptides will be assessed by a MTT assay. The resulting uptake information should allow the classification of the CPPs by their internalisation rates and help to select promising CPPs for efficient KLA-peptide delivery.

Besides the search for the most promising CPP, the internalisation mechanism will be analysed using different endocytosis modulators (e.g. chlorpromazine or nystatin) or depleting energy-dependent processes (4°C). Furthermore, the influence of CPP C-termini (carboxylated *versus* carboxyamidated) on the peptide's uptake, cellular localisation and toxicity will be analysed due to the fact that CPPs with different C-termini have been used in various studies (Weller *et al.*, 2005; Zorko *et al.*, 2005).

After this intense comparative exploration, a subset of CPPs showing no toxicity, good uptake and cytosolic localisation will be chosen for a successful KLA peptide delivery in cancer cell lines, such as breast cancer MCF-7 cells and RAW 264.7 macrophages in comparison to fibroblasts (Cos-7). Using the co-incubation strategy, the optimal molecular mixing ratio of CPP:KLA will be determined. Thereafter, KLA-delivery will be assessed by measuring intracellular Cy5-labelled KLA in cell lysates as well as by the detection in live cells with confocal microscopy. Since it has been stated that a cysteamide at the C-terminus is required for efficient gene transfection (Simeoni *et al.*, 2003) as well as for protein delivery (Simeoni *et al.*, 2003; Wells, 2004), the influence of carboxylated and carboxyamidated CPP C-termini on the delivery of the KLA peptide should be evaluated. Finally the activity of the pro-apoptotic peptide will be determined using different routinely used methods such as nucleus condensation (microscopy), DNA fragmentation (ELISA) or caspase-3 activity (western blot, specific substrate cleavage).

Altogether, this work should give important background information in the choice of the adequate CPP for an anti-apoptotic peptide delivery with regards of future *in vivo* and/or clinical applications.

2. EXPERIMENTAL PROCEDURES

2.1. Peptide Synthesis

The peptides used were synthesised by the Molecular Libraries and Recognition Group (Charité, Berlin) automatically (Syro II, MultiSynTech) using the Fmoc standard protocol. Peptides with a C-terminal carboxyl group were generated using TentaGel S PHB-aa-Fmoc (Rapp Polymere) and with a C-terminal carboxyamide group using TentaGel S Ram resin (Rapp Polymere). For standard synthesis Fmoc-aa-OH were used with the following side-chain protections: E-, D-(OtBu); S-, T-, Y-(tBu); K-, W-(Boc); N-, Q-, H-(Trt); R-(Pbf) (Novabiochem; Bachem). 5(6)-carboxyfluorescein (CF, Fluka) coupling was achieved using 1 equiv. N-hydroxybenzotriazole (HOBt) and 1 equiv. di-isopropylcarbodiimide (DIC) as activators, as reported in (Fischer *et al.*, 2003). Coupling of Cyanine 5 (Cy5) was done with 1 equiv. O-Benzotriazole-1-yl-N,N,N',N'-tetramethyluronium tetrafluoroborate (TBTU) and 2 equiv. N,N-Diisopropylethylamine (DIPEA). The crude peptides were purified to > 95 % by preparative HPLC (Waters) and their identity was determined by analytical RP-HPLC (Waters) and MALDI TOF mass spectrometry (LaserTec BenchTopII, PerSeptive Biosystems).
The amino acids are mostly given in the single-letter code, but sometimes in the three letter code.

2.2. Cell Culture

African green monkey kidney (Cos-7), human embryonal kidney (HEK293), human cervix carcinoma (HeLa) and Madin-Derby canine kidney (MDCK) cells were cultured in phenol red-free (prf) Dulbecco's Modified Eagle medium (DMEM, Invitrogen) supplemented with 10 % fetal bovine serum (FBS, Invitrogen) and 1 % penicillin/streptomycin (pen/strep, Biochrom AG). Human breast adenocarcinoma cells (MCF-7) were cultured in phenol red-free (prf) RPMI 1640 (Invitrogen), 10 % FBS, 1 % non-essential amino acids (MEM NEAA, Gibco), 1 mM sodium pyruvate (Gibco), and 1 % pen/strep. Mouse leukaemic macrophages (RAW 264.7) were cultured in RPMI 1640 (prf), 10 % heat inactivated FBS, 0.05 mM L-glutamine (Gibco) and 1 % pen/strep.
RAEC cells were cultured in Endothelial Basal Medium (EBM, PAA), 10 % FBS, 1 % pen/strep. All surfaces, e.g. bottom of culture flasks or well-plates, were coated with 0.2 % gelatine (Invitrogen).

The cells were seeded in the appropriate concentrations (see experimental section below) and grown until ~ 80 % confluence at the day of the experiment. Unless otherwise indicated, solutions were tempered to 37 °C and all incubations were performed at 37 °C, 5 % CO_2.

2.3. Cellular Uptake

Uptake measurements were performed in 6- or 12-well plates (Falcon, BD Biosciences). Cells were rinsed twice with PBS (phosphate buffered saline) and 1 ml 10 µM CF-labelled CPP solutions in medium without FBS were applied for 30 min at 37°C, 5 % CO_2. Excess CPPs were carefully removed by two rinses with PBS buffer and cells were trypsinated for 10 min at 37°C with 200 µl trypsin [0.05 % trypsin/0.02 % EDTA (ethylenediaminetetraacetic acid) (w/v) solution (Biochrom AG)]. Cell solutions were transferred to eppendorf tubes. Following two washing steps with PBS and centrifugation at 4,000 rpm at 4°C for 10 min, cells were lysed in 500 µl RIPA [50 mM Tris, 1 mM EDTA, 150 mM NaCl, 1 % (v/v) NP40, 0.5 % (v/v) deoxycholat, 0.1 % (w/v) SDS (sodium dodecyl sulfate), pH 7.5; Complete Mini, EDTA-free (Roche Diagnostica GmbH) freshly added] for 1 hour at 4°C. Finally, the samples were centrifuged at 8,200 rpm at 4°C for 10 min.

Signal intensities of CF-CPP were determined using 100 µl lysate in a 96 well plates (U96PP, Nunc) with a microplate reader [FLUOstar OPTIMA – BMG Labtech (excitation: 485 nm and emission: 520 nm)].

Later on, 12-well plates were used with half the volumes for each incubation step.

The total protein contents were determined by a BCA (bicinchoninic acid) assay where 5 µl sample and 200 µl BCA-reagent (Reagent A: 1 % (w/v) BCA-Na_2, 2 % (w/v) Na_2CO_3, 0.16 % (w/v) Na_2-Tatrat, 0.4 % NaOH, 0.95 % (w/v) $NaHCO_3$, pH 11.25 and reagent B: 4 % (w/v) $CuSO_4*5H_2O$; A:B = 50:1) were mixed and incubated for 30 min at 37°C in a 96-well plate (Nunc Maxi Sorb). The absorbance at 620 nm was measured and thereafter the concentration was calculated using a bovine serum albumin (BSA, Sigma-Aldrich) calibration curve.

2.4. Endocytosis Inhibitor Test

All endocytosis inhibitors were purchased from Sigma-Aldrich and used with the following concentrations: 30 µM chlorpromazine hydrochloride, 100 µM chloroquine

diphosphate salt, 10 µM heparin sodium salt all dissolved in H_2O, as well as 100 µM nystatin dehydrate and 100 nM wortmannin dissolved in DMSO (dimethyl sulfoxide).
Cells were pre-incubated with different endocytosis inhibitors for 30 min in medium without FBS. Then CPPs were added to a final concentration of 10 µM and incubated for 30 min.
Besides the 37°C CPP incubation, incubations at 4°C were also performed. To minimise possible side effects, all solutions were pre-chilled to 4°C.
Excess CPPs and inhibitors were removed by two rinses with PBS and then the cells were trypsinated and lysed with RIPA. As described before, CF-intensities and protein concentrations were assessed using microtiter plate reader measurements (FLUOstar Optima – BMG Labtech).

2.5. Cellular Delivery of Peptides

The basic procedure was done as in described in the chapter "2.3 Cellular Uptake". Cells were seeded, washed and co-incubated with CF-CPPs, cyanine 5 (Cy5)-labelled KLA or PRC and CF-labelled CPP-KLA or CPP-PRC peptides for 30 min. Different concentrations or mixing ratios are shown in the respective figures (Figure 8 and Figure 9). If not otherwise indicated, the CPPs and KLA peptide were directly co-incubated with the cells without a previous pre-incubation step of both peptides only. Finally, the peptide solutions were washed off, the cells were lysed and Cy5-intensities were measured in the lysate via a microplate reader (FLUOstar Optima – BMG Labtech; excitation 640 nm, emission 680 nm). The CF-CPP uptake was monitored as well to ensure consistency. The protein content in the lysate was determined using a BCA assay.

2.6. Confocal Laser Scanning Microscopy

The cellular localisations of CF-labelled CPPs were detected together with the membrane-labelling dye trypan blue with a confocal microscope [inverted IX81 fluorescence microscope equipped with a Fluoview 1000 scanhead (Olympus) and a 60× (N.A. 1.35) oil-immersion objective at 25°C]. The green CF fluorescence was excited with the 488 nm laser line of an Argon-ion laser, while the red trypan blue fluorescence was excited with a 543 nm Helium–Neon laser. The system was run in sequential scanning mode, where only one laser was active at a time to avoid spectral

overlap. The emission of CF was recorded between 500 nm and 530 nm. For trypan blue, the emission was recorded from 570 nm to 670 nm.

To detect the KLA delivery by CPPs, the KLA peptide was labelled with Cy5. Cells were incubated with KLA and CPPs at respective concentrations (Cos-7: 10 μM Integrin + 10/20 μM KLA; MCF-7: 1 μM Integrin + 1/2 μM KLA; RAW 264.7: 1 μM MPG + 1/2 μM KLA) for 30 min, washed and analysed in complete growth medium. HOECHST 33342 (Molecular Probes) was used to stain nuclei. The pictures were then obtained using a Zeiss Axiovert 200M fluorescence microscope (Carl Zeiss).

For nuclear morphology analysis, cells (8×10^4 cells per dish) were seeded and the next day incubated with indicated CPP:KLA complexes. Directly after or after 24 h or 48 h the cells were stained with 10 μg/ml HOECHST 33342 (Molecular Probes) for 30 min. The nuclear morphology was analysed with a Zeiss Axiovert 200M fluorescence microscope (Carl Zeiss).

All measurements were performed with living, non-fixed cells grown in glass bottom dishes (World Precision Instruments).

2.7. MTT Assay

A good cellular tolerance is highly important for the use of CPPs as delivery reagents. Cell viability was determined using the CCK-8 kit (Fluka) as described by the manufacturer. In a few words, to test the cytotoxicity of CPPs 5×10^5cells were seeded in 96-well microtiter plates (Falcon) and cultivated over night (37°C, 5 % CO_2). Then they were incubated with peptides for 2 h in FBS-free medium, washed and further incubated with the appropriate medium containing FBS and the MTT dye for 4 h. This measurement of cell viability is based on the principle that the WST-8 (water soluble tetrazolium salt) dye is reduced in cells by dehydrogenases giving a yellow coloured product (formazan), which is soluble in the tissue culture medium. The amount of the formazan generated by the activity of dehydrogenases in cells is directly proportional to the number of living cells. The absorbance of the formazan product at 570 nm was measured using a microplate reader (FLUOstar Optima – BMG Labtech). The results were normalised to the control (without peptide) which corresponds to 100 % viability.

Measurements of the pro-apoptotic KLA peptide activity were performed using the MTT test as well. Therefore cells were incubated with CPPs (10 μM for Cos-7, 1 μM for MCF-7 and RAW 264.7) and KLA (10 or 20 μM for Cos-7, 1 or 2 μM for MCF-7 and RAW 264.7) alone or as a mixture. The incubation time was 3 h for Cos-7 cells and

1 h for MCF-7 and RAW 264.7 cells. The MTT-test was performed after 3 days for Cos-7, MCF-7 cells and after different time points (0 to 3 days) for RAW 264.7 cells. The results were normalised to the control (without peptide) which corresponds to 100 % viability.

2.8. Western Blot Analysis

To detect cleaved caspase-3, cells were subjected to western blot analysis. MCF-7 and Cos-7 cells were seeded 3.2×10^4 cells/well in 6 well plates. The next day, MCF-7 cells were incubated with 1 µM MPG-$CONH_2$ and 2 µM KLA for 1 h or 3 h. Cos-7 cells were incubated with 10 µM MPG-$CONH_2$ or Int-COOH and 20 µM KLA for 3 h in FBS-free medium. Thereafter, the cells were washed with PBS and left in FBS-containing medium. Either directly after incubation or after 3 days, cells were harvested and lysed with RIPA buffer (Sigma-Aldrich) containing protease inhibitor cocktail tablets (Sigma-Aldrich) for 30 min shaking at 4°C. Cell lysates were centrifuged at 8,000 rcf for 10 min at 4°C. 50 µg proteins [BCA Protein Assay Reagent, Pierce] were separated by SDS-PAGE electrophoresis and transferred to a polyvinylidene fluoride (PVDF) membrane (BioRad). Blots were blocked with 5 % non-fat dry milk in PBS (Gibco), 0.05 % Tween-20 (ICN Biomedicals Inc.) for 1 h and incubated with cleaved caspase-3 rabbit monoclonal antibody (Cell Signaling - 1:1,000) as recommended by the manufacturer. The next day membranes were incubated with the secondary anti-rabbit IgG-peroxidase antibody (Sigma-Aldrich - 1:1,000). Afterwards membranes were washed and incubated with the anti-actin-peroxidase antibody (Sigma-Aldrich - 1:50,000). The blots were detected with an enhanced chemiluminescence western blotting substrate (Pierce).

2.9. Caspase-3 Assay

Cos-7 cells were seeded (8×10^3 cells/well), washed and incubated with 10 µM Int-COOH and 10/20 µM KLA for 3 h. Using the Caspase-3 Fluorescence Assay Kit (Cayman), the caspase-3 activation was measured the same day using the specific caspase-3 substrate N-Ac-DEVD-N'-MC-R110, which generates a fluorescent substrate upon cleavage by active caspase-3. Active caspase-3 included in the kit was used as a positive control. For detailed instructions see the kit protocol. To ensure that the KLA peptide's Cy5-label is not the cause of cell death, the KLA peptide without the

fluorophore was tested in this assay. The caspase-3 inhibitor (N-Ac-DEVD-CHO) was diluted in assay buffer and used as described by the manufacturer.
In parallel, MCF-7 cells were seeded (8×10^3 cells/well), washed, co-incubated with 1 μM MPG-$CONH_2$ and 1/2 μM KLA for 3 h and caspase-3 activity was accessed in the same way as described for Cos-7 cells.

2.10. DNA-Fragmentation Assay

Using the Cell Death Detection ELISA kit (Roche Diagnostics), the DNA fragmentation in MCF-7 lysates after CPP and KLA incubation was detected with antibodies against histones and DNA as described by the manufacturer. Briefly, MCF-7 cells were seeded (2×10^4 cells/well) in 24-well plates (Falcon) and incubated the next day with 1 μM MPG-$CONH_2$ and 2 μM KLA for 1 h. DNA fragmentation was measured using the supernatants of MCF-7 lysates after 1 day, 2 days or 3 days at 405 nm and 490 nm (Tecan). The absorbance values (A_{405}-A_{490}) were normalised to those of untreated cells to calculate the nucleosomal enrichment factor. 0.5 μM staurosporine (STS, Sigma-Aldrich) was used as a positive control.

2.11. Annexin V/Propidium Iodide Flow Cytometric Analysis

In apoptotic cells phosphatidylserine (PS) is translocated from the cytoplasmic side of the cell membrane to the extracellular side, where fluorescein isothiocyanate (FITC)-labelled annexin V can bind to it with high affinity. Including propidium iodide (PI) in the staining procedure ensures a discrimination between dead, necrotic and apoptotic cells. MCF-7 cells were seeded (1.6×10^5 cells/well) in 12-well plates and the next day incubated with 1 μM MPG-$CONH_2$ and 2 μM KLA for 1 h. Cells were harvested directly after peptide incubation or after 1 day or 2 days, stained using the FITC-annexin V/Dead Cell Apoptosis Kit V13242 (Invitrogen) and analysed with a BDFACSCanto (BD). 0.5 μM STS were included as positive controls.

2.12. Statistical Analysis

All values are expressed as mean ± SEM. Multiple comparisons between groups were assessed by one-way ANOVA with Newman-Keuls post hoc test. Probability values < 0.05 were accepted as statistically significant and the P values were noted as: not significant (ns) for $P > 0.05$ and * for $P < 0.05$, ** $P < 0.001$ and *** $P < 0.0001$. Data was analysed using GraphPad Prism (GraphPad Software, San Diego California USA).

3. RESULTS

3.1. Basic Conditions

22 different CPPs (Table 1, page 29) were selected covering the three main CPP families (protein-derived, designed or model CPPs) to evaluate their cellular uptake in four most utilised epithelial cell lines (Cos-7, HEK293, HeLa, MDCK). As negative control one CPP was synthesised in a scrambled version (pVEC-scrambled). A literature screen showed that groups used different concentrations ranging from 1 µM to 50 µM (Lebleu *et al.*, 2008; Pujals *et al.*, 2008) without getting toxic side effects (Duchardt *et al.*, 2007; Tunnemann *et al.*, 2008). By using a concentration of ≥ 10 µM Durchardt *et al.* showed a significant enhancement of cellular uptake. After the performance of time dependent assays, a 30 min incubation time proved sufficient and that longer incubation times of 45 min or 60 min only increased the CPP uptake little (factor 1.4, data not shown). Therefore and keeping toxicity in mind, the analytical evaluation of the CPP uptake was started using a CPP concentration of 10 µM and an incubation time of 30 min as standard incubation condition unless otherwise stated.

CPPs are highly positively charged peptides and therefore stick very well to the negatively charged plasma membrane on the cellular outside. To avoid these false positive uptake signals a trypsinisation step should be carried out before fluorescence measurements (flow cytometry or plate reader). For the microscopic evaluation an extra-cellular fluorescence quencher should be added to the cells (e.g. trypan blue to quench green fluorescence) (Green *et al.*, 1988; Mueller *et al.*, 2008; Richard *et al.*, 2003).

Also, the use of living, non-fixed cells during microscopy is highly important, because formaldehyde or methanol fixation prior to a microscopic analysis can lead to an artificial redistribution of the CPP in the nucleus (Melikov *et al.*, 2005; Richard *et al.*, 2003). At low CPP-concentration (≤ 10 µM), fixation can lead to broad cytoplasmic and nuclear localisation instead of a vesicular distribution in live-cell imaging.

Table 1: Peptide Names and Sequences

Peptide	Name	Sequence	AA	pI	MW [Da]	Reference
Protein-derived CPPs	SynB1	RGGRLSYSRRRFSTSTGR	18	12.30	2460	(Rousselle *et al.*. 2000)
	Polyomavirus Vp1	APKRKSGVSK	10	11.26	1417	(Saphire *et al.*, 2000)
	Penetratin	RQILIWFQNRRMKWKK	16	12.31	2591	(Derossi *et al.*, 1994)
	Tat	GRKKRRQRRRPPQ	12	12.70	2078	(Vives *et al.*, 1997)
	Bac1-15	RRIRPRPPLPRPRP	14	12.70	2123	(Sadler *et al.*, 2002)
	NF-kB	VQRKRQKLMP	10	12.02	1643	(Ragin *et al.*, 2002)
	SV40 T antigen	PKKKRKV	7	11.33	1242	(Lanford *et al.*, 1986)
	HATF3	ERKKRRRE	8	11.55	1517	(Ragin *et al.*, 2002)
	hCT(9-32)	LGTYTQDFNKFHTFPQTAIGVGAP	24	6.74	2970	(Trehin *et al.*, 2004)
	Rev	TRQARRNRRRRWRERQR	17	12.60	2797	(Futaki *et al.*, 2001)
	pVEC	LLIILRRRIRKQAHAHSK	18	12.48	3206	(Elmquist *et al.*, 2001)
	Integrin	VTVLALGALAGVGVG	15	5.49	2456	(Zhang *et al.*, 1998)
Designed CPPs	DPV6	GRPRESGKKRKRKRLKP	17	12.19	1656	(De Coupade *et al.*, 2005)
	$S4_{13}PV$	ALWKTLLKKVLKAPKKKRKV	20	11.51	2437	(Mano *et al.*, 2005)
	Transportan	GWTLNSAGYLLGKINLKALAALAKKL	27	10.18	2736	(Pooga *et al.*, 1998a)
	Pep-1	KETWWETWWTEWSQPKKKRKV	21	9.82	3201	(Morris *et al.*, 2001)
	MPG	GALFLGWLGAAGSTMGAWSQPKKKRKV	27	11.33	2237	(Morris *et al.*, 1997)
Model CPPs	MAP	KLALKLALKALKAALKLA	18	10.60	3208	(Oehlke *et al.*, 1998)
	poly-P	VRLPPPVLRPPPVLRPPP	18	12.30	2357	(Fernandez-Carneado *et al.*, 2004)
	R7	RRRRRRR	7	12.78	1471	(Wender *et al.*, 2000)
	R9	RRRRRRRRR	9	12.90	1783	(Wender *et al.*, 2000)
Others	pVEC-scrambled	IAARIKLRSRQHIKLRHL	18	12.48	2569	(Elmquist *et al.*, 2003)

Footnote: CPPs were synthesised as amide (-$CONH_2$) or as carboxyl (-COOH). Furthermore, CPPs were N-terminally labelled with (5/6) carboxyfluorescein (CF-) for uptake and microscopic analyses. The theoretical isoelectric point (pI) was calculated with the ProtParam tool (http://web.expasy.org/protparam/).

3.2. Evaluation of Cellular Uptake: 22 CPPs in 4 Cell Lines

3.2.1. Viability Test of the 22 CPPs

First of all, the potential cellular toxicity of the 22 different CPPs was examined, since this is crucial to their use as effective delivery vehicles. To provide information about acute toxicity, cells were incubated for two hours with 22 CF-labelled CPPs at concentrations of 1 µM - 50 µM (Annex - Table 5). Afterwards, the cells were washed, incubated with the vital MTT dye and the formazan formation was detected at 570 nm.

Most of the CPPs showed no cytotoxicity even at high concentrations (100 ± 20 % viability). $S4_{13}PV$ was the only peptide that lowered the viability substantially at 10 µM (HeLa 64 ± 24 % viability and MDCK 33 ± 16 % viability) and at ≥ 25 µM for all cells. Also, at 25 µM transportan and MAP decreased the cell viability. For example, transportan caused strong reductions at 25 µM in Cos-7, HeLa and MDCK cells (20 – 0 %) but had a lower effect on HEK293 cells (~ 50 %). The decreasing cell viabilities induced by these three CPPs are not surprising due to the fact that they are postulated to penetrate the cell by pore formation (Matsuzaki, 1996). However, to assess cytotoxic effects of the CPPs in the MTT assay, the incubation time was prolonged to 2 h. Most CPPs seem to have no influence on cell viability even under these extreme conditions.

Altogether, these results substantiate the used standard conditions (10 µM CPP for 30 min) to analyse the internalisation properties of the 22 CPPs.

3.2.2. Comparing Cellular CPP Uptake and Distribution

The cellular uptake rates of the 22 CPPs were quantified in Cos-7, HEK293, HeLa and MDCK cells by fluorescence measurements using a microplate reader (Figure 2, page 31). Although all 22 CPPs are known from the literature and are supposed to have cell penetrating properties, they do not show the same degree of cellular uptake.

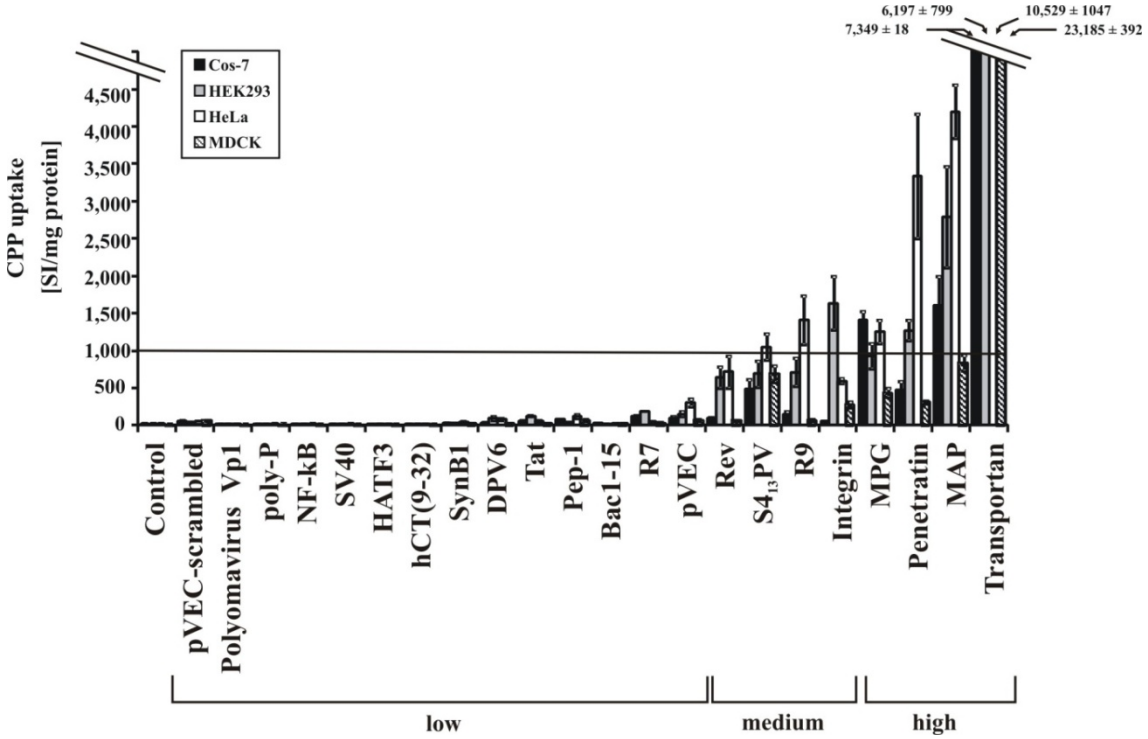

Figure 2. CPP Uptake in Cos-7, HEK293, HeLa and MDCK Cells.
Cells, which were 80 % confluent, were washed and incubated with 10 µM CF-CPPs for 30 min at 37°C. After further washing and trypsinisation (10 min at 37°C) to avoid the measurement of membrane bound, but not internalised CPPs, the cells were lysed. The CPP amount in the lysate was quantified via the peptide's CF-label (excitation: 485 nm and emission: 520 nm) and normalised to the total protein content using a BCA assay (absorbance measurement at 620 nm). Classification corresponds to low (< 500 SI/mg protein), medium (500 – 1,000 SI/mg protein) and high (> 1,000 SI/mg protein) internalisation. The data represents the mean ± S.E.M. (n≥3).

Figure 2 shows that the degree of cellular penetration varies highly. First of all, the used negative control pVEC-scrambled did not show any internalisation compared to untreated cells. Altogether, the CPPs can be classified in three groups showing low (< 500 SI/mg protein), medium (500 – 1,000 SI/mg protein) and high (> 1,000 SI/mg protein) cellular uptake. Surprisingly there are a large number of 14 CPPs in the first group with low or nearly no cellular penetration in the tested cell lines (for instance hCT(9-32), Tat or Pep-1). The second group with medium cellular uptake in most cell lines comprises four CPPs including Rev, S4$_{13}$PV, R9 and integrin. CPPs with high uptake rates in most cells are the four commonly used CPPs MPG, penetratin, MAP and transportan. The overall lower cellular uptake of Tat compared to penetratin and the polyarginines was confirmed (Fischer *et al.*, 2004; Wender *et al.*, 2000) as well as the efficiency of R9 compared to R7 for HeLa and HEK293 cells, which is in accordance with Tunnemann et al. (Tunnemann *et al.*, 2008).

Interestingly, integrin prefers HEK293 cells (3-fold higher SI/mg protein compared to the other cells), penetratin HeLa cells (3-fold higher uptake) and transportan MDCK cells (2-fold higher uptake). Amongst the 22 CPPs used, none internalises in Cos-7 cells better than in the other cell lines.

To investigate the subcellular localisation of the 22 CPPs, microscopic experiments were performed using representing candidates from the three determined uptake-groups: polyomavirus Vp1 as an example of a CPP with low cellular uptake, integrin and R9 as examples of medium uptake and MAP, MPG, penetratin and transportan as examples of high uptake rates (Figure 2). Tat was included, because it is widely used in the scientific community.

Figure 3 (page 33) summarises the distribution of an exemplarily subset of eight CPPs within the four cell lines. In the control picture (without CPPs) no self-fluorescence of the cells was measured (Figure 3, 1st panel). Additionally, to avoid misinterpretation due to extracellular CPP fluorescence bound to cell membranes or working materials, trypan blue solution was added during each CLSM (confocal laser scanning microscopy) measurement (only shown in the last panel). Trypan blue is unable to translocate intact cell membranes, which makes it a selective quencher for extracellular bound fluorophores (Foerg *et al.*, 2007; Hed *et al.*, 1987).

First of all, by subjectively comparing the fluorescence pictures, the results obtained by the microplate reader could clearly be reproduced (Figure 2). CPPs showing low (polyomavirus Vp1) and high (penetratin, transportan, and MAP) cellular uptake also show low or bright green fluorescent signals in the CLSM pictures.

Tat mainly shows a vesicular distribution in all cells, and furthermore, a diffuse cytoplasmic and additionally nucleic localisation in the case of HeLa and MDCK cells (Figure 3, 3rd panel). Due to the additional cytoplasmic and nucleic distribution in HeLa and MDCK cells, the quantity of internalised CPPs seems to be higher than in the other two cell lines, which does not correspond to the approximately equal distribution measured by the microplate reader (Figure 2). At this juncture, it can only be postulated that nuclear located CPP could not be exactly measured in cell lysates.

Penetratin (Figure 3, 4th panel) displays a punctuated dispersion within the three cells, as is also observed for the smac-penetratin construct used in HeLa cells (Fotin-Mleczek *et al.*, 2005). A similar distribution of R9 was observed in Cos-7, HEK293 and HeLa cells, with a pronounced cytoplasmic and nucleic distribution found most strongly in MDCK cells (Figure 3, 5th panel).

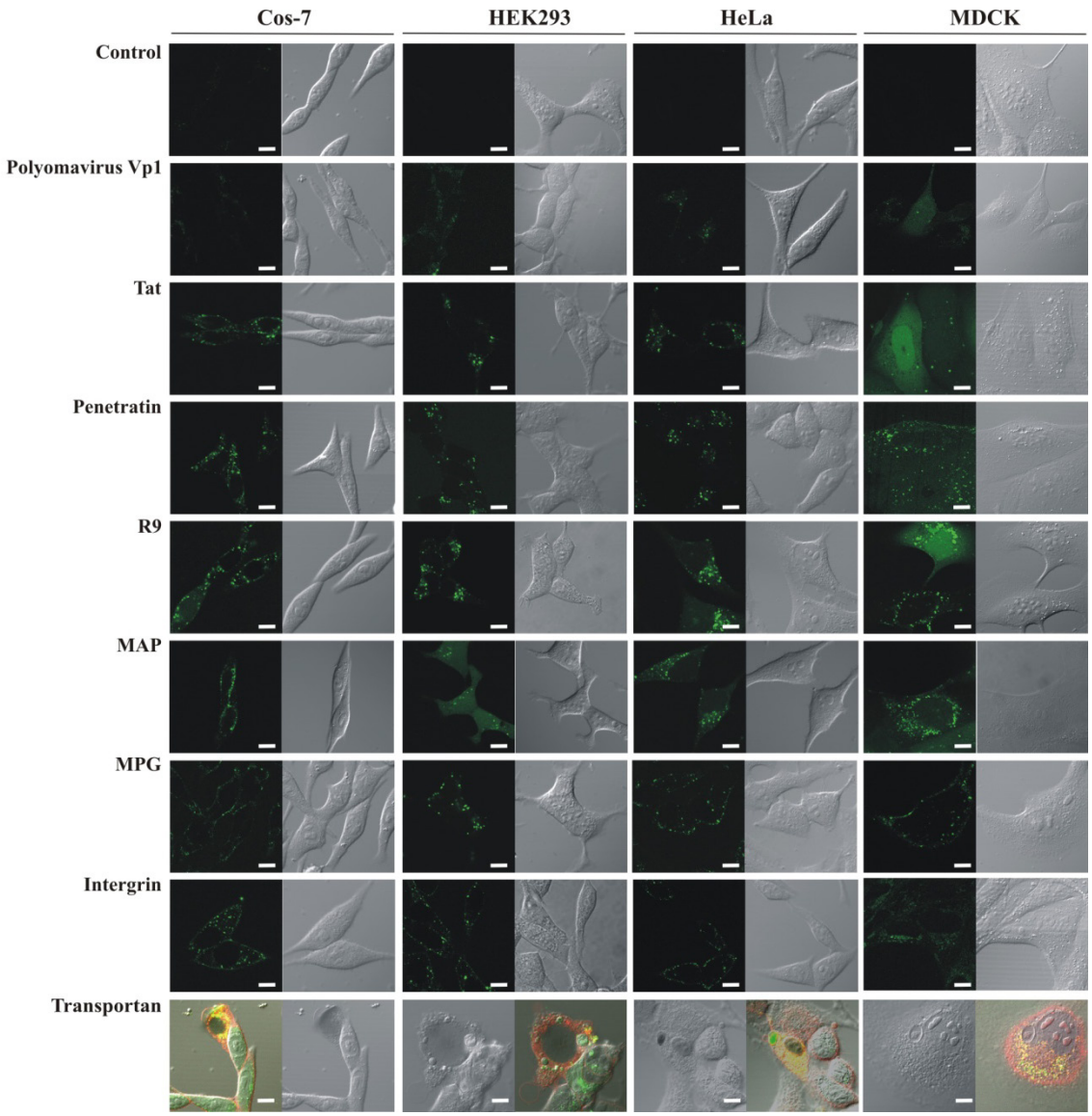

Figure 3: Cellular Distribution of Eight Example CPPs in Cos-7, HEK293, HeLa and MDCK Cells.
As control, the four cell lines without peptide incubations are shown (no CF-staining at 488 nm) with the corresponding phase contrast images. The four different cell types are treated with 10 µM of the CF-labelled CPPs for 30 min. For each condition CF-fluorescence (488 nm) and phase contrast images are shown. For transportan (last row) the vital trypan blue staining (543 nm) is merged with the CF-images. The white bars represent 10 µm.

The fluorescence of MAP (Figure 3, 6th panel) and of MPG (Figure 3, 7th panel) in the CSLM pictures appears evenly distributed throughout the cytosol and nucleus, accompanied by a punctuated pattern, suggesting that non-endocytotic as well as endocytotic modes of uptake are involved.

Integrin seems to be mostly located close to the cell membrane, especially in Cos-7 and HeLa cells, which is in agreement with Zhang et al. (Zhang *et al.*, 1998) (Figure 3, 8th panel). Transportan plays a special role in the cellular uptake. Using the microplate

reader, extremely high incorporations were recorded. Images of confocal microscopy show not only cytoplasmic vesicles, but also intense cell damages (Figure 3, 2nd shot of transportan). 20-30 % of the cells reveal a huge intracellular accumulation of transportan correlating with the trypan blue staining and independent of the cell types. This lytic characteristic of transportan was also clearly demonstrated in the viability test showing a high cytotoxic effect with a concentration up to 25 µM (Annex - Table 5). The similar phenomenon could be observed in 5 % of the HeLa cells incubated with MAP (data not shown).

3.2.3. Influence of Endocytosis Modulators on the Cellular Uptake

To gain more insights into the mechanism(s) by which CPPs are taken up by cells, eight CPPs from Figure 3 as well as four others were selected and tested with chemical inhibitors to block specific endocytotic pathways, compete with membrane associated HSPGs or inhibit endosome acidification or fusion. Cells were pre-treated with the chemicals (Table 2) for 30 min before the main incubation (10 µM CPPs + inhibitors) and analysed using a microplate reader.

Table 2: Endocytosis Modulation

Treatment	Concentration	Consequence
37°C	-	Standard condition
4°C	-	Inhibition of energy-dependent processes
Chlorpromazine	30 µM	Inhibition of clathrin-dependent endocytosis
Chloroquine	100 µM	Inhibition of endosome acidification
Nystatin	100 µM	Disrupt caveolar structure and function
Heparin	10 µM	Competitor of cell membrane-associated HSPGs
Wortmannin	100 nM	Inhibition of endosome fusion

Footnote: The concentrations given in the table are the concentrations used in this study. Additionally, a brief description of the proposed exerted effect on endocytosis is given for each substance. HSPGs: heparin sulfate proteoglycans.

Besides the standard conditions at 37°C, energy-dependant pathways were tested by measuring CPP uptakes at 4°C. Chlorpromazine was used as a clathrin-dependent endocytosis inhibitor and nystatin disrupts caveolar structures and functions. Chloroquine was utilised inhibiting the acidification of endosomes, and the fungal metabolite wortmannin inhibiting fluid phase uptake and the homotypic fusion of early endosomes (Jones, 2007). Furthermore, heparin was used as a competitor of cell membrane-associated heparin sulfate proteoglycans (HSPGs), which are known to mediate the first interaction with CPPs (Ziegler, 2008).

Comparing the four cell lines, the most positive effects were seen with heparin (58 %), chloroquine (58 %) and at 4 °C (48 %), suggesting an energy- and clathrin-dependent pathway for uptake. By looking at the overall results, the most frequent negative effects were observed in HEK293 cells, at temperatures of 4 °C (58 %), with nystatin (50 %) and wortmannin (58 %) reflecting an energy- and caveolin-dependent pathway. A more equal distribution of positive and negative effects was found for HeLa and MDCK cells. Altogether, most of the inhibitors used seem to have weak consequences for the cellular uptake: 44 % of the conditions have no effect on Cos-7, 50 % on HEK293, 63 % on HeLa and 70 % on MDCK cells. These results were confirmed by confocal microscopic analysis (Mueller *et al.*, 2008).

Altogether, adding different endocytosis modulators mostly did not change the cellular uptake as well as the subcellular CPP localisation.

3.3. Evaluation of CPP Uptake in Other Cell Types

Having completed the analytical evaluation of the 22 CPPs in four cell lines, three additional cell types were selected to confirm the results. The adenocarcinoma cell line MCF-7 and the leukaemic macrophagic cell line RAW 264.7 were chosen as examples of cancerous cell lines as well as the aortic endothelial cells RAEC [kindly provided by Dr. Martina Seifert (IMI, Charité)], as an example for primary cells. The same 22 CPPs were analysed quantitatively by microplate reader measurements and qualitatively by confocal microscopy as described in the previous chapter.

The cytotoxicity of CPPs is very important for their use as delivery vehicles. Therefore all three cell types were incubated with the peptides in different concentrations (1 µM – 50 µM) for two hours and the cellular viability was determined using the MTT assay. Fortunately, most of the CPPs did not influence the cellular viability even at a high concentration of 25 µM in MCF-7, RAW 264.7 and RAEC cells. Here again, especially $S4_{13}PV$ revealed toxic properties at 10 µM or 25 µM (Annex - Table 7). Since much shorter incubation times in the uptake experiments were used (30 min compared to 2 h applied here) a 10 µM peptide solution seems to be non-toxic.

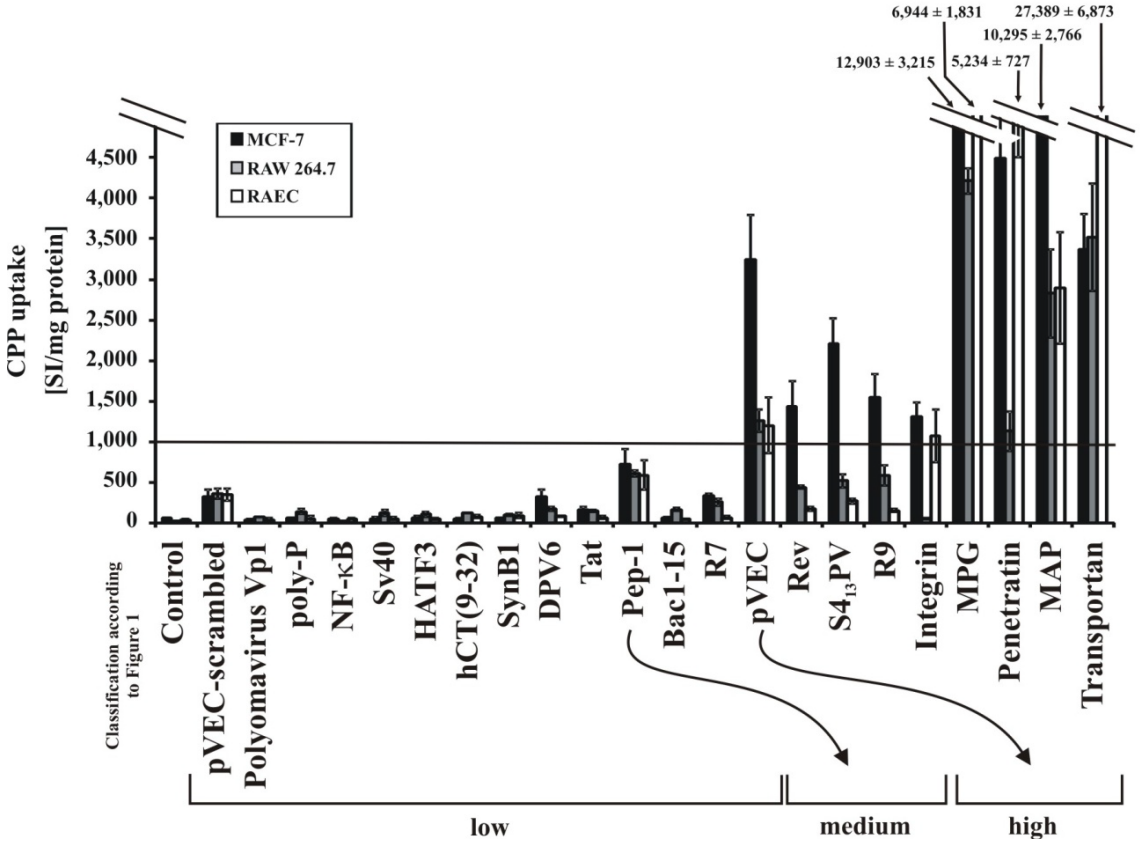

Figure 4. Comparison of CPP Uptake in MCF-7, RAW 264.7 and RAEC Cells.
80 % confluent cells were incubated with 10 µM CF-CPPs for 30 min at 37°C. The cells were then washed and treated with trypsin (10 min at 37°C) to avoid the measurement of membrane bound, but not internalised CPPs. After cell lysis, the CPP amount was quantified via the peptide's CF-label (excitation: 485 nm and emission: 520 nm) and normalised to the total cellular protein content using a BCA assay (absorbance measurement at 620 nm). The data represents the mean ± S.E.M. (n≥3).

As in the previously analysed cell lines (Figure 2), the 22 CPPs show very different uptake properties (Figure 4) and can be classified in the same three main internalisation groups although with some exceptions. The CPP group of high uptake rates (> 1,000 SI/mg protein for MPG, penetratin, MAP, transportan) also shows high penetration in the MCF-7, RAW264.7 and RAEC cells. Also, CPPs that internalised poorly in the previous four cell lines, (< 500 SI/mg protein), show mostly low uptake rates here as well (e.g. polyomavirus Vp1, hCT(9-32) and Tat). Only the two CPPs Pep-1 and pVEC switch their classification group showing here a higher cellular penetration in the new three analysed cell types (see arrows in Figure 4**)**.

Interestingly, some CPPs such as MPG, S4$_{13}$PV, MAP, R9, Rev and pVEC penetrated MCF-7 cells better compared to the other tested cells. Transportan penetrates primary aortic cells about 8-fold better than the other two cell lines (27,389 ± 6,873 SI/mg

protein *versus* 3,374 ± 433 SI/mg protein in MCF-7 and 3,520 ± 664 SI/mg protein in RAW 264.7) and even better than Cos-7, HEK293, HeLa and MDCK cells.

The cellular location of the CPPs was analysed by confocal microscopy using a subset of six CPPs. This time polyomavirus Vp1 and transportan were not included, because Vp1 shows no significant uptake and transportan seems to be cytotoxic as shown in Figure 3 (upper panel).

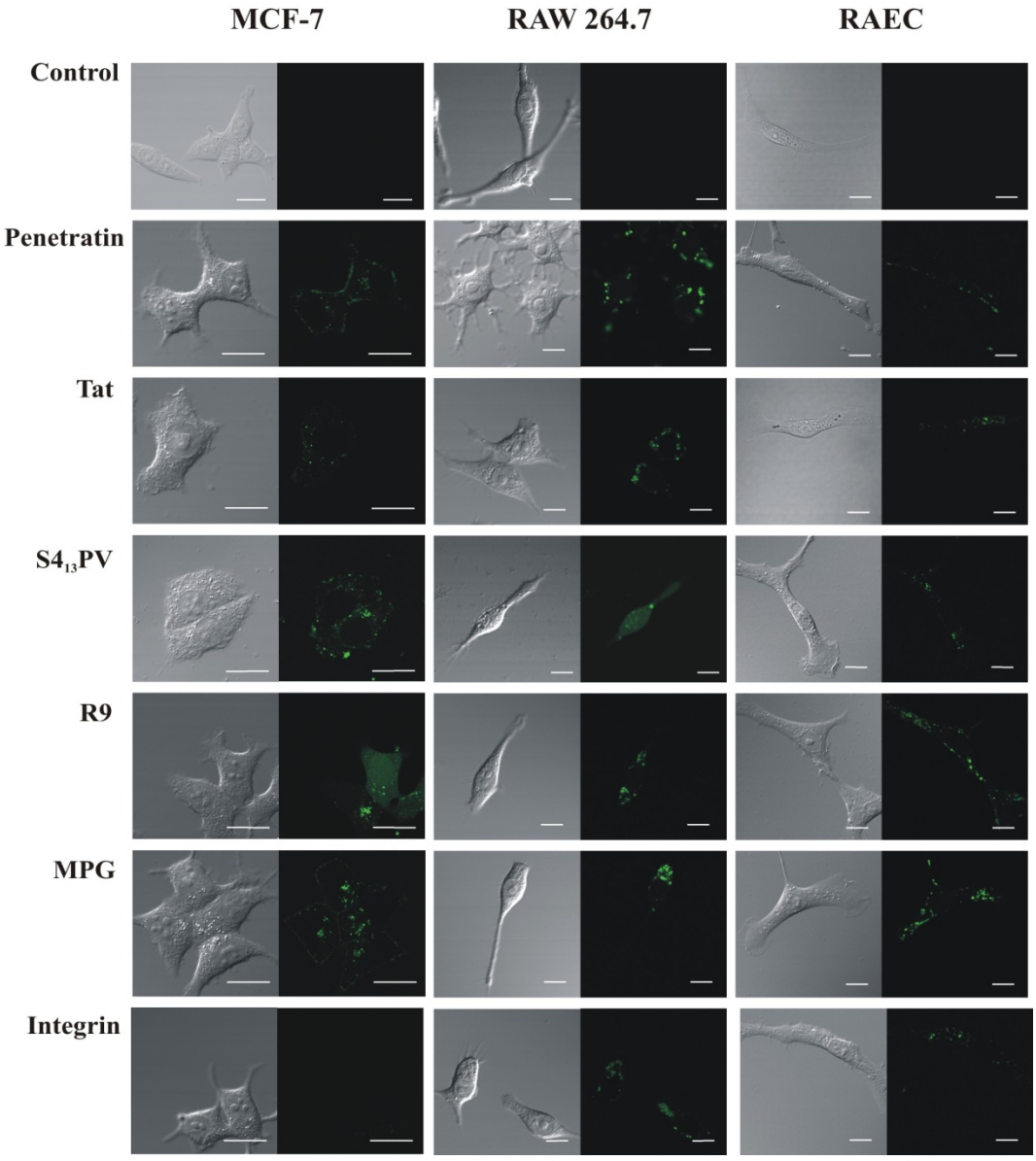

Figure 5. Cellular Distribution of Six CPPs in MCF-7, RAW 264.7 and RAEC Cells.

MCF-7, RAW 264.7 and RAEC cells were incubated with 10 µM CPPs for 30 min, washed and analysed by confocal microscopy. Trypan blue was added to quench extracellular fluorescence (data not shown). For each condition the phase contrast image as well as the CF-CPP staining (488 nm) is shown. The white bars represent 10 µm.

First of all, the control pictures (Figure 5, 1st panel) show no auto-fluorescence of the living, non-fixed cells and furthermore the cells incubated with the CPPs seem to be

healthy in every condition tested. The CLSM pictures confirmed the measurements done with the microplate reader. Strong uptake values as for penetratin in RAEC cells resulted in strong fluorescent signals. The only discrepancy was observed with integrin showing an internalisation in MCF-7 cells, but obviously no intracellular fluorescence by microscopic detection.

Altogether, the distribution of the CPPs in the three cell types exhibits a punctuated pattern throughout the cytoplasm, which suggests an entrapment of the peptides in endosomal vesicles. In some cases (R9 in MCF-7 and $S4_{13}PV$ in RAW264.7) a nuclear and cytoplasmic distribution of the CPPs was observed. However, the microscopically visualised results correspond mainly to the fluorescence measurements by microplate reader as previously shown for Cos-7, HEK293, HeLa and MDCK cells (Figure 3).

3.4. Influence of the CPPs C-Terminus on the Cellular Uptake

Different studies have been using CPPs with different C-termini (Weller *et al.*, 2005; Zorko *et al.*, 2005) and it has been stated that a cysteamide at the C-terminus is required for efficient transfection (Simeoni *et al.*, 2003). There has never been a systematic evaluation of the influence of the C-terminus on CPP uptake and intracellular localisation. Based on the analytical evaluation of 22 CPPs in seven cell type, six CPPs were selected (penetratin, Tat, integrin, $S4_{13}PV$, MPG and R9) and synthesised with a carboxyamidated (-$CONH_2$) or carboxylated (-COOH) C-terminus to analyse its influence on the cellular internalisation and its intracellular distribution. Tat was chosen as an example of a CPP with low uptake and also because it is often used in the CPP community, $S4_{13}PV$, R9, penetratin and integrin as examples of medium cellular uptake and MPG as a CPP with high internalisation properties (according to the classification in Figure 2 and Figure 4) (Mueller *et al.*, 2008; Mueller *et al.*, 2011). These CPPs were analysed in comparison to each other in the seven cell types used before (chapters 3.2 and 3.3).

First of all, the potential cytotoxic effects of the carboxyamidated CPPs were determined using the MTT-viability assay (Annex - Table 8). Interestingly, carboxyamidated CPPs appear more toxic than carboxylated CPPs. The most toxic effects are seen in HeLa cells, beginning at 25 µM (penetratin, Tat, $S4_{13}PV$, R9 and MPG). Again $S4_{13}PV$ - here in the carboxyamidated version - shows the highest toxicity in all cell lines (at 25 µM but sometimes also at 10 µM). Interestingly, integrin reveals the lowest influence on cell viability.

With the exception of $S4_{13}PV$, no toxicity was observed for carboxyamidated CPPs in primary RAEC cells, which is in contrast to carboxylated CPPs, where the most viablity reductions were seen in this cell line.

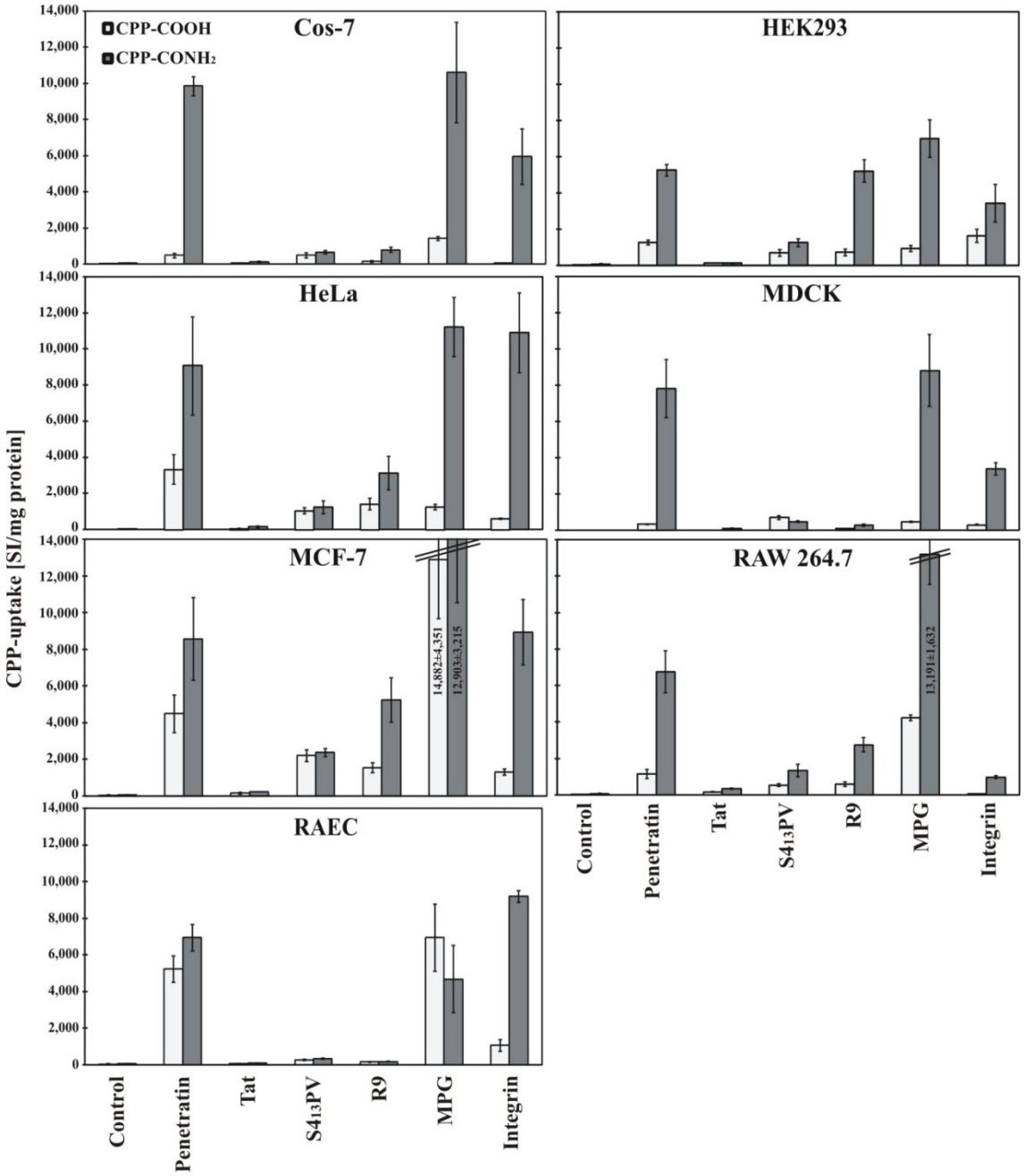

Figure 6. Cellular Uptake of CPPs with Carboxylated or Carboxyamidated C-Terminus.

Cos-7, HEK293, HeLa, MDCK, MCF-7, RAW 264.7 and RAEC cells were incubated for 30 min with the six selected CF-CPPs having either a carboxylated or carboxyamidated C-terminus. Then the cells were washed, trypsinised, lysed and analysed by microplate reader. The data shown are the mean ± SEM (n=3).

All together carboxyamidated CPPs are more toxic to the seven tested cell types than carboxylated CPPs, but surprisingly less cytotoxic to the primary RAEC cells than carboxylated CPPs.

Having found that 30 min incubations of 10 µM peptide solutions had no cytotoxic effect on most cell types independent of the CPPs' C-termini, their cellular uptake was evaluated and compared to the one of carboxylated CPPs. In analogue to previous experiments, cells were incubated with the CF-labelled CPPs and their internalisation was quantified by fluorescence measurements in the lysate using a microplate reader.

The uptake measurements shown in Figure 6 clearly revealed a strong influence of the CPP C-terminal character on CPP cellular uptake. The internalisation of the carboxyamidated form of penetratin, R9 and integrin is extremely improved in most cell types compared to the carboxylated form, e.g. CF-Pen-COOH is internalised with 311 ± 22 SI/mg protein whereas CF-Pen-$CONH_2$ penetrates at 7,811 ± 1,591 SI/mg protein in MDCK cells. In contrast, the uptake of Tat and $S4_{13}PV$ is nearly not influenced when changing the C-terminus in all analysed cells. Interestingly, the MPG uptake rises in most cell lines when carboxyamidated MPG is used (3-fold to 20-fold), but shows no significant difference in MCF-7 cells and the primary RAEC cells (e.g. 6,944 ± 1,831 SI/mg protein for CF-MPG-COOH *versus* 4,674 ± 1,344 SI/mg protein for CF-MPG-$CONH_2$ in RAEC cells). With the exception of RAEC cells, CF-MPG-$CONH_2$ is the CPP showing the highest uptake (from 7,008 ± 1,043 SI/mg protein in HEK293 to 14,882 ± 4,351 SI/mg protein in MCF-7) when compared to other CPPs in that cell type.

In summary, regarding the seven analysed cell types, the C-terminus change from a carboxylate to a carboxyamide enhances the cellular CPP uptake in about 59 % of the cases.

Here again, as mentioned before, the cells were incubated with CF-labelled CPPs and analysed by confocal microscopy to determine if the different C-termini might have an influence on the CPP's sub-cellular distribution. Before picture acquisition, the cells were incubated with trypan blue as vital dye and as a quencher of extracellular bound CF-CPPs. As exemplified in Figure 7, the cellular internalisation of penetratin, $S4_{13}PV$ and MPG (green fluorescence) in the seven cell lines as a merged picture with the trypan blue staining (red fluorescence) is shown as well as the bright field images. The uptake values of the CF-measurements by microplate reader are given in the left lower corners.

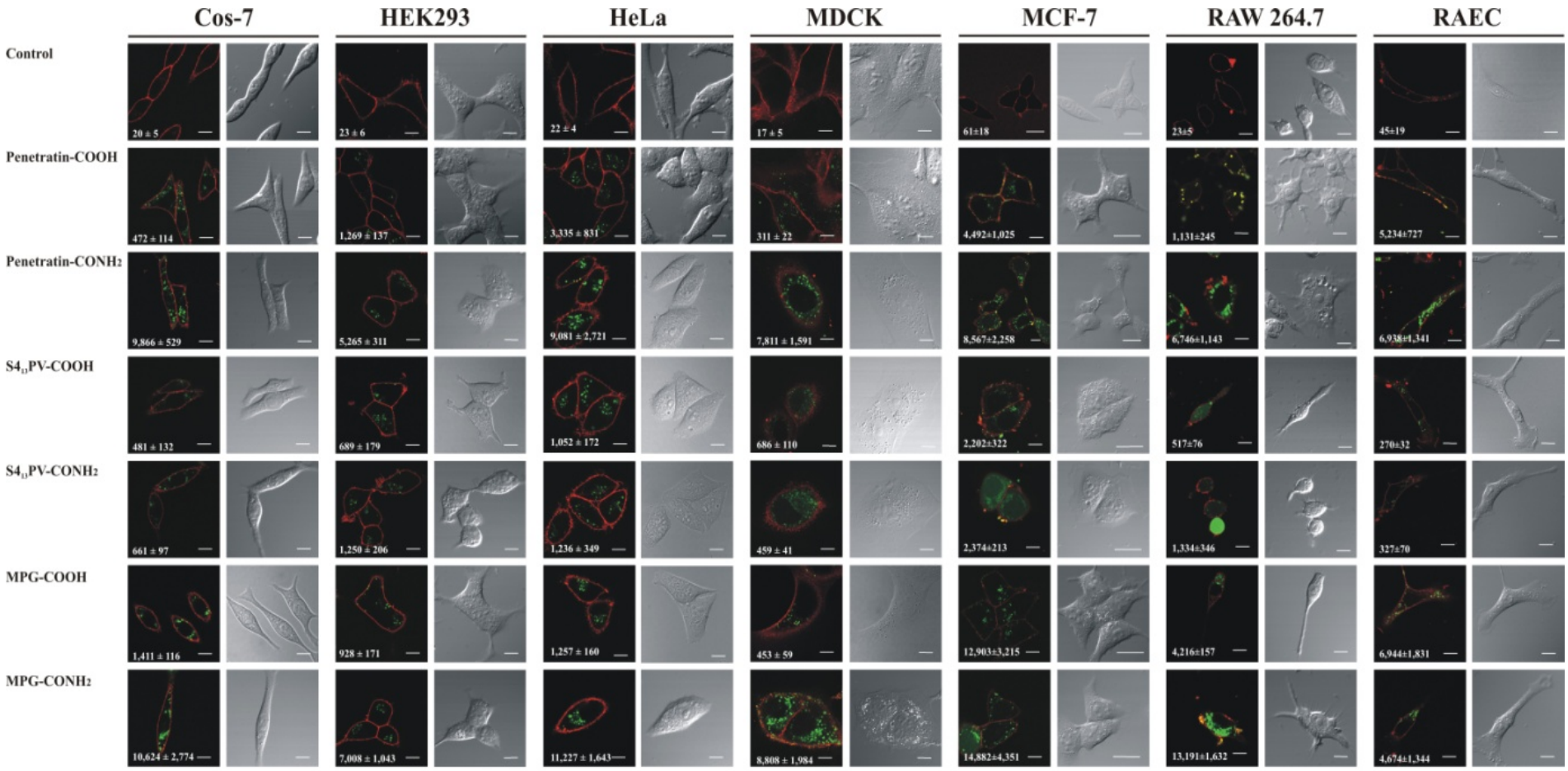

Figure 7. Cellular Distribution of Carboxylated or Carboxyamidated CPPs in Cos-7, HEK293, HeLa, MDCK, MCF-7, RAW 264.7 and RAEC Cells.

Cells were treated with 10 µM of the CF-labelled CPPs for 30 min. For each condition, the overlay of CF-staining (green fluorescence) and trypan blue stain (red fluorescence) as well as the phase contrast images are shown. The uptake values measured by microplate reader are given in the left lower corner. The white bars represent 10 µM.

First of all, the control pictures (Figure 7, 1st panel) show no intrinsic fluorescence in the green CF channel. Furthermore, intact cell membranes indicated by the trypan blue staining (red fluorescence) correspond to no toxicity of the used CPPs under the applied conditions (10 μM, 30 min incubation). Subjectively looking at the images of the different cell types, most of them confirmed the measurements done with the microplate reader, e.g. CF-Pen-$CONH_2$ in HeLa and CF-MPG-COOH in MDCK cells clearly show a stronger fluorescence signal.

It was not possible to identify a change in the subcellular localisation of the CPPs when altering the C-termini for most cell lines - they showed a punctuated pattern throughout the cytoplasm, which probably resulted from uptake via endocytosis (Jones, 2008). However, MCF-7 cells exhibit a different distribution for carboxylated and carboxyamidated penetratin, $S4_{13}PV$ and MPG. The carboxyamidated peptides were localised not only in the vesicles, probably the endosomes, as seen for their carboxylated forms, but also diffused in the cytoplasm as well as in the nucleus. The same can be observed for Tat and R9 in RAW 264.7 cells (data not shown) and for $S4_{13}PV$ in MDCK cells. Only RAEC cells show no altered subcellular distribution after a CPP C-terminal change.

In summary, the conformation of the C-terminus has an influence on (I) the cellular CPP uptake (carboxyamidated CPPs > carboxylated CPPs) and in a few cases on (II) the CPP's cellular localisation depending on the CPP and cell line.

3.5. Cellular Delivery of the Pro-Apoptotic KLA Peptide

The main purpose of CPPs is their use as delivery vehicles for e.g. biological active peptides. To prove their therapeutic applicability by a simple co-incubation with the CPPs (non-covalent strategy) into the mammalian breast cancer MCF-7 cells and the leukaemic macrophages RAW264.7 compared to the fibroblastic Cos-7, the pro-apoptotic peptide KLA (Table 3, page 43) (Ellerby *et al.*, 1999) was chosen to be delivered into cells keeping a potential application in cancer therapy in mind. Additionally, another peptide sequence was used (PRC) to analyse the influence of amino acid composition of the cargo for the CPP based cellular non-covalent delivery.

Table 3: Cargo Peptides

Name	Sequence	Reference
KLA	KLAKLAKKLAKLAK	(Raucher *et al.*, 2009)
PRC	ANSRWQTSII	(Vouilleme *et al.*, 2010)

Footnote: Peptides were synthesised with N-terminal Cy5-labels for uptake and microscopic analyses.

3.5.1. Optimal Mixing Ratio for the Non-Covalent Delivery of the KLA Peptide

To ensure the best cellular delivery of the KLA peptide, the optimal mixing ratio was determined using MPG-$CONH_2$:KLA and Int-$CONH_2$:KLA in Cos-7 cells (both CPPs show high internalisations in Figure 6). The cells were co-incubated with Cy5-labelled KLA and CF-labelled CPP-$CONH_2$ in different molar ratios (20:1 to 1:2 for CPP:KLA) as well as with KLA and CPP alone (Figure 8A). Interestingly, the internalisation was dramatically reduced using ratios of 10:1 or 20:1 (CPP:KLA) which are typical ratios for CPP:oligonucleotide mixtures (Said Hassane *et al.*, 2009). Furthermore, a 30 min pre-incubation of the CPP:KLA mixture before adding to the cells did not increase the KLA uptake (Figure 8A, page 44).

In detail, an increased cellular uptake of the KLA-peptide was observed when incubated with the appropriated same amount of CPP compared to the incubation without one. For example, incubating Cos-7 cells with KLA together with MPG-$CONH_2$ or Int-$CONH_2$ roughly doubled or tripled the amount of uptake [e.g. 390 ± 95 Cy5-SI/mg protein for KLA alone *versus* 1,106 ± 230 Cy5-SI/mg protein for Int-NH2:KLA (1:2)]. To check the transportation capacity of a CPP with low cellular uptake, the Tat peptide was chosen and applied using the co-incubation strategy. The results shown in Figure 8A clearly demonstrate that co-incubating Tat with KLA did not improve the internalisation, confirming the importance of the CPP selection for cargo delivery.

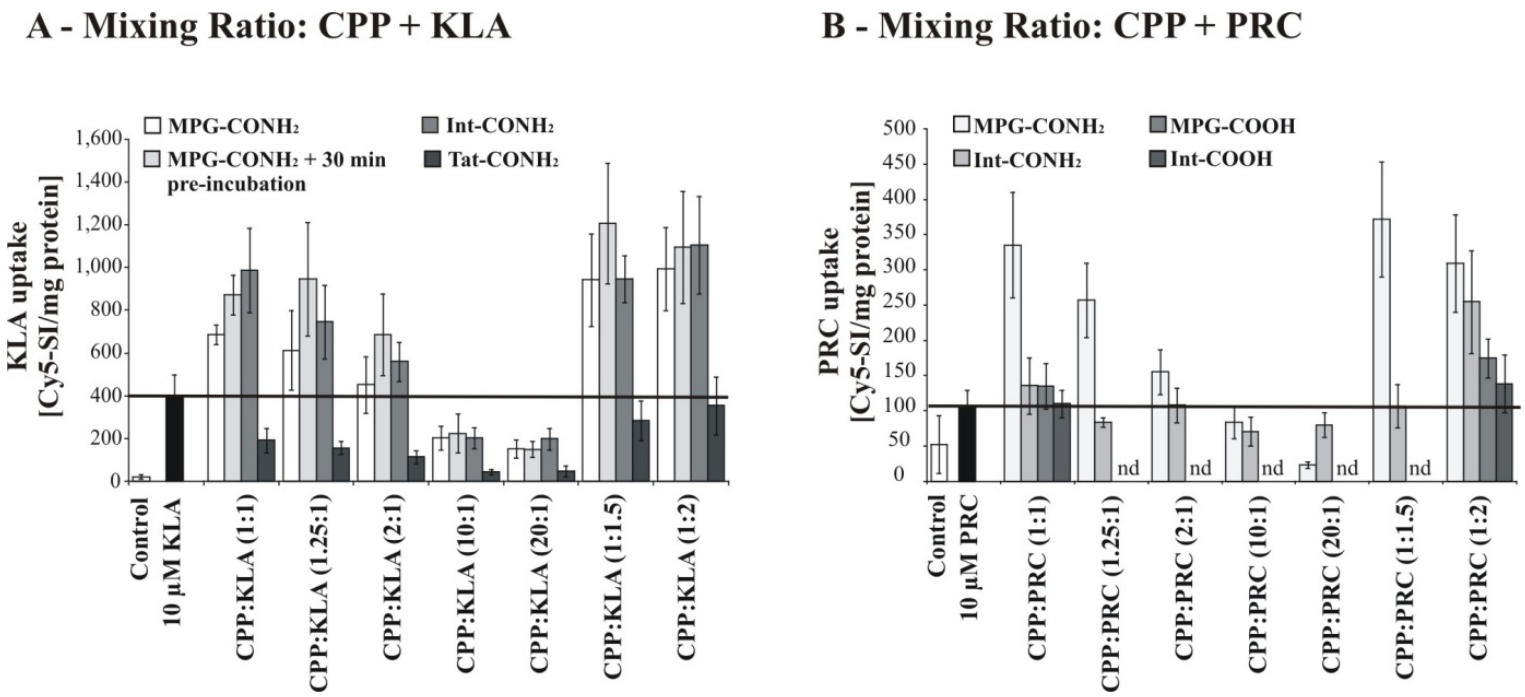

Figure 8. Mixing Ratios of the KLA (A) or PRC (B) Peptide and CPPs.
Mixing ratios of the (A) KLA or (B) PRC peptide and CPPs: Cos-7 cells were incubated with 10 µM CPP and different concentrations of the KLA or PRC peptide for 30 min. For all conditions, the peptides were co-incubated; only in (A) MPG-$CONH_2$:KLA solutions were pre-incubated for 30 min. The Cy5-KLA/PRC uptake was measured and normalised to the total protein concentration (Cy5-SI/mg protein). The CF-CPP uptake was also monitored to ensure consistency (data not shown). The maximal uptake was reached using CPP:KLA mixture ratios of 1:1 and 1:2. n.d. means 'not determined'. Data shown are the mean ± SEM (n=3).

The same mixing ratios resulted in high uptake amounts when a different arbitrary chosen peptide was used (PRC, Table 3, Figure 8B). Therefore it is likely that this phenomenon was not dependent on the KLA sequence as cargo (positively charged, helix conformation) (Ellerby *et al.*, 1999). Even though the overall uptake amounts were much smaller for PRC than for KLA, its internalisation was doubled or tripled when co-incubated with MPG-$CONH_2$ or Int-$CONH_2$ at a ratios of 1:1 or 1:2 compared to the internalisation without a CPP as vehicle [104 ± 26 Cy5-SI/mg protein for Cy5-PRC alone *versus* 310 ± 69 Cy5-SI/mg protein for MPG-$CONH_2$:Cy5-KLA (1:2)]. Here as well, the internalisation was rather dependent on the used CPP as well as on its C-terminal conformation.

These results suggest that mixing ratios of 1:1 and/or 1:2 (CPP:peptide) are the best choices for the delivery of a peptide co-incubated with a CPP. However to find the best CPP for peptide delivery into a certain cell type using the simple co-incubation strategy seems to be rather difficult. It can be believed that a high CPP uptake and a carboxyamidated C-terminus are advantageous for a successful peptide delivery – however, this should always be tested.

For all following experiments the ratios CPP:KLA (1:1) and (1:2) were chosen to evaluate the uptake and induce pro-apoptotic effects of the transduced KLA peptide.

3.5.2. Cellular Delivery of the KLA Peptide

Having found the optimal mixing ratios (1:1 or 1:2), Cos-7, MCF-7 and RAW 264.7 cells were incubated with KLA together with MPG, integrin or penetratin. Here as well the influence of the C-terminus was evaluated, since it has been stated, that a C-terminal cysteamide is important for plasmid and cysteamine for protein delivery (Simeoni *et al.*, 2003; Wells, 2004). To evaluate the influence of the CPP C-terminus on peptide delivery, it was tested in both versions (carboxylated *versus* carboxyamidated) (Figure 9).

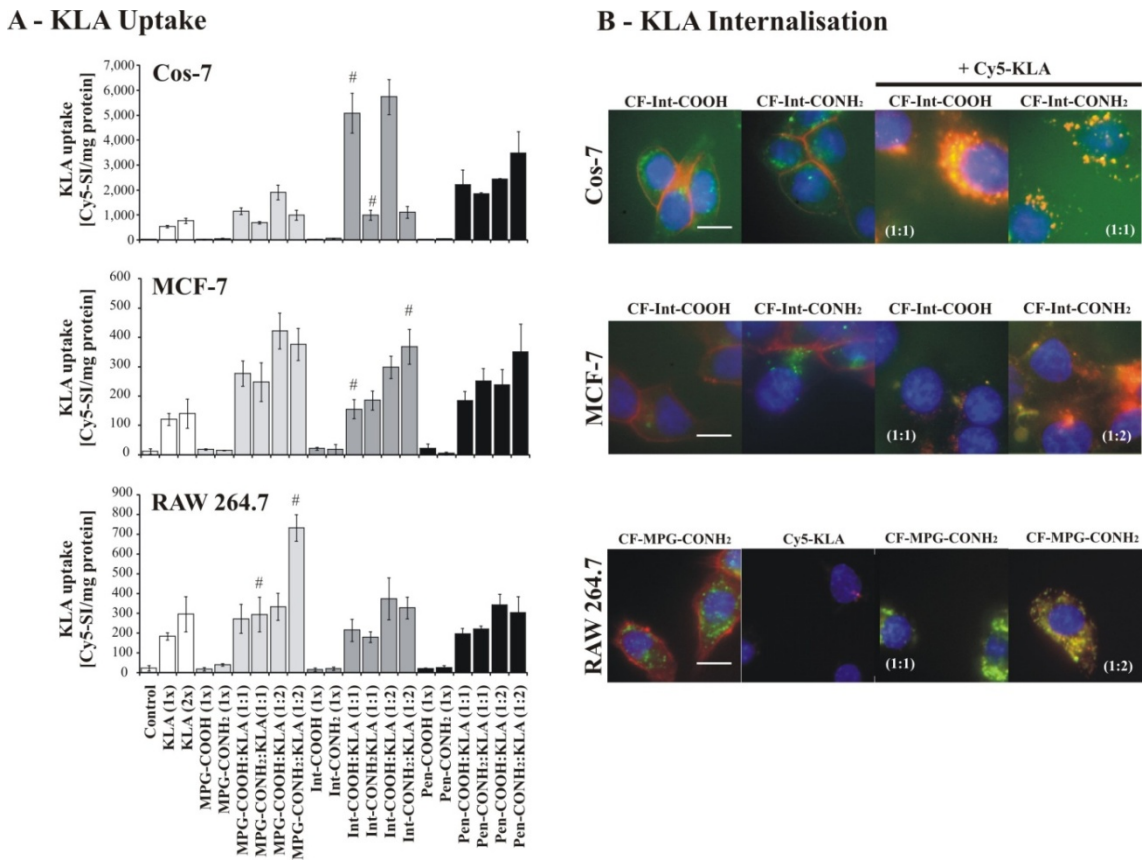

Figure 9. Cellular Delivery and Distribution of the Pro-Apoptotic KLA Peptide Co-Incubated with a CPP.

(**A**) KLA delivery by CPPs in Cos-7, MCF-7 and RAW 264.7 cells: Cos-7, MCF-7 and Raw 264.7 cells were incubated with CPPs and KLA as described before. "1×" means 1 µM or 10 µM and "2×" means 2 µM or 20 µM peptide concentration depending on the cell lines. The delivery of the KLA peptide was successfully enhanced when co-incubating it with a CPP in all cell lines. Notice the strong enhancement with Int-COOH in Cos-7 and MPG-$CONH_2$ in RAW 264.7 cells. Data shown are the mean ± SEM (n=3).

(**B**) Cellular distribution of the KLA peptide: Combinations of CF-CPP and Cy5-KLA with the symbol # in Figure 9A were analysed under the microscope. Trypan blue was added to ensure cell viability, but omitted when KLA was present to avoid spectral overlaps. Nuclei were stained with HOECHST 33342. CF-CPPs are visualised in green, trypan blue and Cy5-KLA in red. The scale bars represent 10 µm.

The KLA-delivery in Cos-7 cells is mainly possible with penetratin and integrin. However, the internalisation depends on the C-terminus of the CPP, especially in the case of integrin. A 5- to 6-fold increase was observed in the KLA uptake with Int-COOH compared to Int-$CONH_2$ at both ratios (5,085 ± 803 Cy5-SI/mg protein *versus* 987 ± 197 Cy5-SI/mg protein for ratio 1:1 and 5,737 ± 705 Cy5-SI/mg protein *versus* 1,106 ± 230 Cy5-SI/mg protein for ratio 1:2).

When applying the same conditions of KLA delivery (10 µM CPP with 1:1 or 1:2 ratios) in MCF-7 and RAW 264.7 cells, they rapidly detached making the analysis of the results difficult. For that reason, these assays were performed using a 10-fold diluted

concentrate (1 µM CPP with ratio 1:1 or 1:2). As observed for the Cos-7 cells, an enhancement of the KLA internalisation was seen in both cell lines depending on the CPP C-terminus, even if the signal was weaker due to lower peptide concentrations. The best results were seen with MPG-COOH:KLA (1:2) (423 ± 61 Cy5-SI/mg protein; 3-fold increase compared to KLA alone) for MCF-7 and MPG-$CONH_2$:KLA (1:2) (73 ± 67 Cy5-SI/mg protein 2.5-fold increase compared to KLA alone) for RAW 264.7 cells.

Using confocal microscopy the results found by microtiter plate reader measurements were confirmed: high uptake corresponded to high fluorescence signals in the analysed cells (Figure 9B). For example, the vast difference in transportation capability of both forms of integrin was confirmed for Cos-7 cells (Int-COOH:KLA >> Int-$CONH_2$:KLA). The higher delivery by Int-$CONH_2$ at a ratio of 1:2 compared to 1:1 in MCF-7 cells as well as MPG-$CONH_2$ 1:2 in relation to 1:1 in RAW 264.7 cells were also validated.

Looking at the pictures in greater detail, a huge accumulation of CF-Int-COOH:Cy5-KLA around the nucleus of Cos-7 cells appeared (merged distribution in orange, Figure 9B). Also a strong cellular accumulation of CF-Int-$CONH_2$:Cy5-KLA (1:2) in MCF-7 and CF-CPP:Cy5-KLA (1:2) in RAW 264.7 cells were seen, which correspond to the values measured in the uptake tests - even at a low concentration (1 µM CPP). Interestingly, the cellular distribution seemed to be mainly cytosolic, hinting towards a potential entrapment in endosomal vesicles. Since there was also a diffuse signal detectable surrounding the vesicles, it is also assumable that KLA is able to escape the endosomal entrapment.

In summary, the KLA peptide was successfully delivered in adenocarcinoma cells (MCF-7), leukaemic macrophages (RAW 264.7) and fibroblasts (Cos-7) using the non-covalent co-incubation approach. In order to obtain high delivery rates, different cell lines required different CPPs. The conformation of the CPP's C-terminus also played a crucial role for an effective translocation of the KLA peptide over the cell membrane.

3.5.3. Activity of the CPP-Delivered Pro-Apoptotic KLA Peptide

To evaluate the activity of the pro-apoptotic KLA peptide introduced by MPG, integrin or penetratin, the MTT-test was utilised to assess the cell viability using the same conditions as in the KLA delivery experiments (Figure 10, page 49). A value of 100 % corresponds to no cytotoxic effect of the peptides and viable cells, whereas values lower than 80 % viability represent a cytotoxic effect.

First of all, CPPs and the KLA peptide themselves caused no toxicity in the tested cell lines.

In Cos-7 cells, most combinations of CPPs and KLA did not lower the cell viability significantly (Figure 10A). A detectable pro-apoptotic effect with a cell viability reduction of 32 % ($P < 0.001$ *versus* KLA alone) was only observed with the combination of 10 µM Int-COOH and 20 µM KLA.

In MCF-7 cells, seven out of the twelve different applied conditions show a reduction in cell viability although using 10-fold lower concentrations than in Cos-7 cells (Figure 10B). The highest effects were given by MPG-COOH:KLA (1:2) and MPG-$CONH_2$:KLA (1:2) with reductions of 32 % ($P < 0.001$ *versus* KLA alone) and 42 % ($P < 0.001$ *versus* KLA alone), respectively. This is in agreement with the results of the cellular uptake, where both were amongst the combinations with the highest delivery rates.

In RAW 264.7 cells, the toxic effects of KLA delivered by different CPPs and changing ratios were not as obvious as in MCF-7 cells. Using the same condition as applied for the MCF-7 cells (MTT detection after 3 days), no pro-apoptotic effect could be observed for any of the used mixing partners (Annex - Figure 15). Therefore, the toxicity of the KLA peptide was evaluated with reduced periods after peptide incubation. Measuring the cell viability directly after peptide incubation, a viability reduction of 27 % ($P < 0.05$ *versus* KLA alone) with 1 µM MPG-$CONH_2$ + 2 µM KLA was determined (Müller *et al.*, 2011); a combination which caused toxicity in MCF-7 cells as well. Toxicity was also observed using 1 µM Pen-$CONH_2$ + 2 µM KLA with a viability reduction of 26 % ($P < 0.05$ *versus* KLA alone).

Cancerous MCF-7 and macrophagic RAW 264.7 cells showed the highest induction of apoptosis with MPG-$CONH_2$:KLA (1:2), which was not found in fibroblastic Cos-7 cells even at a 10-fold higher concentration.

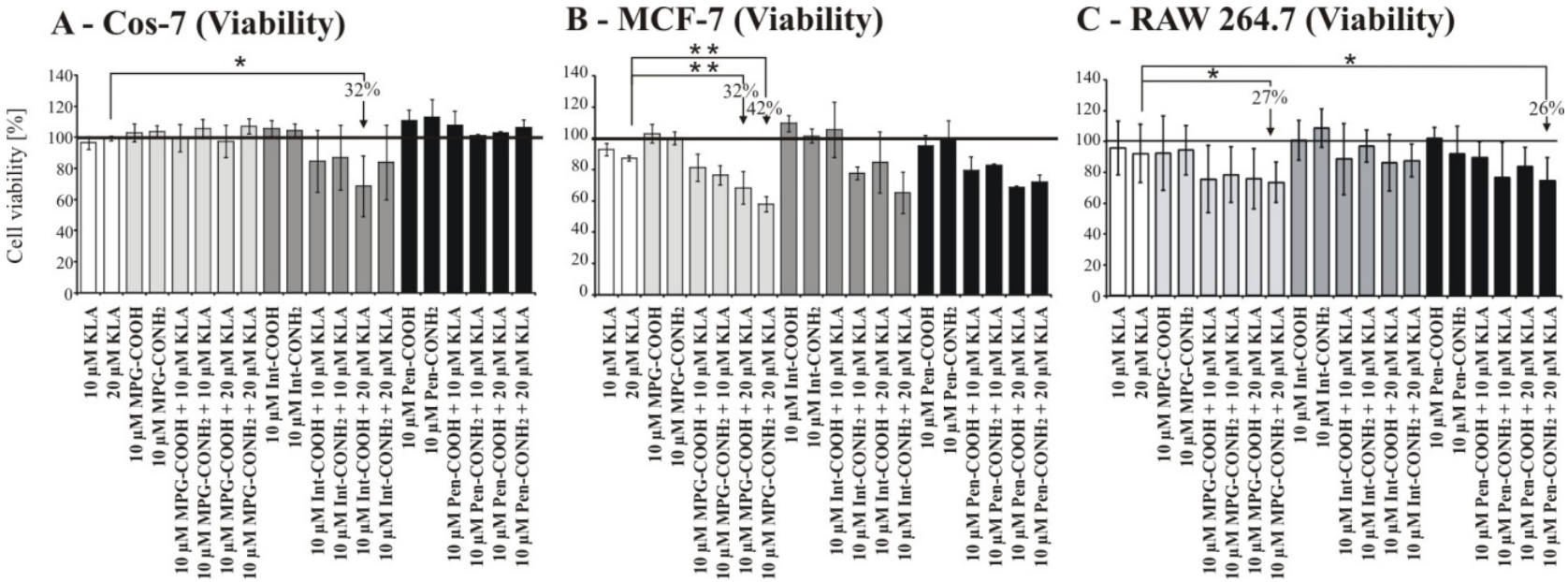

Figure 10. Viability after CPP:KLA Incubation.
Cells were incubated with the CPP:KLA mixture and the cell viability was detected after 3 days (Cos-7 and MCF-7) or directly after peptide incubation (RAW 264.7) using the MTT-test. 100 % cell viability corresponds to no toxic effect of the peptides. In Cos-7 cells the mixture of 10 µM Int-COOH + 20 µM KLA reveals a toxic effect of 32 % ($P < 0.05$). The mixture of 1 µM MPG-$CONH_2$ + 2 µM KLA reveals a toxic effect of 42 % ($P < 0.001$) for MCF-7 and of 27 % ($P < 0.05$ %) for RAW 264.7. Data shown are the mean ± SEM (n=3).

To ascribe the viability reductions measured with the MTT tests to pro-apoptotic effects of the CPP:KLA mixtures, the nuclear morphology of Cos-7, MCF-7 and RAW 264.7 cells was observed to detect nuclear pyknosis, which is a sign of cells undergoing apoptosis. Cells were treated with the conditions that showed toxic effects in the MTT assay and stained with HOECHST 33342 (Figure 11).

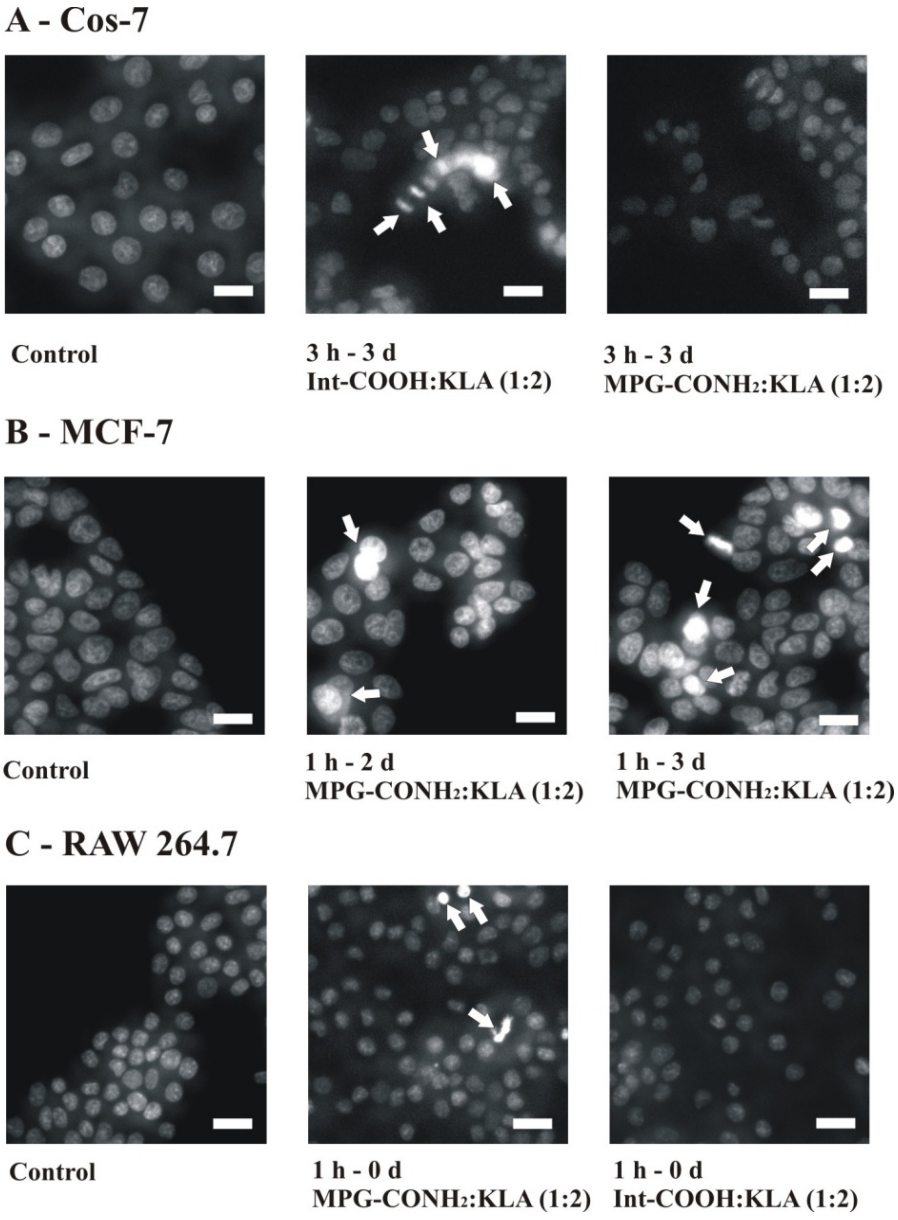

Figure 11. Nuclear Condensation after CPP:KLA Incubation.
Cells were incubated with the CPP:KLA mixtures and stained with Hoechst 33342 after the indicated time periods. Arrows point to condensed chromatin. Condensed chromatin was revealed in cells treated with the conditions that showed toxic effects in the MTT tests. The scale bar represents 20 µm.

Cos-7 cells showed no altered nuclei in the control picture or when incubated with MPG-$CONH_2$:KLA (1:2) (no effect in MTT assay), but condensed chromatin was found after the incubation with Int-$CONH_2$:KLA (1:2) (white arrows in Figure 11A). In

MCF-7 cells nuclear pyknosis was clearly visible after the incubation with MPG-$CONH_2$:KLA (1:2) after 2 days and even more pronounced after 3 days (Figure 11B). When incubating RAW 264.7 cells with MPG-$CONH_2$:KLA (1:2), degenerated cell nuclei were only detectable at the day of the incubation (Figure 11C), but not after 3 days (data not shown). Furthermore, using the Int-COOH:KLA (1:2) condition no effect was identifiable, which coincides with the MTT assays. All tested conditions showing reduced cell viabilities in the MTT assays were correlated to apoptosis as revealed by nuclear pyknosis.

3.5.4. Caspase-3 Detection: No Activation in MCF-7 Cells

In respect to the treatment of cancer, a main goal was to deliver the pro-apoptotic KLA peptide in breast adenocarcinoma cells. The induction of apoptosis mainly results in the activation of caspases and finally in DNA fragmentation. Previously it has been reported that the KLA peptide activates caspase-3 in cell-free systems (rat liver mitochondria in cytosolic extracts of DMECs) (Ellerby *et al.*, 1999). On that account, the identification of caspase-3 activity by measuring its substrate specific cleavage was promoted (Caspase-3 Fluorescence Assay Kit, Cayman) or its activation by self-proteolysis or cleavage by other upstream caspases (western blot using cleaved-caspase-3 antibody) in MCF-7 cells. Unfortunately, there was no caspase-3 activity detectable with both assays even with different incubation periods (partly shown in Figure 12A).

To confirm the functionality of both assays, Cos-7 cells were used as reference and also to show that both methods can be used to detect activated caspase-3.

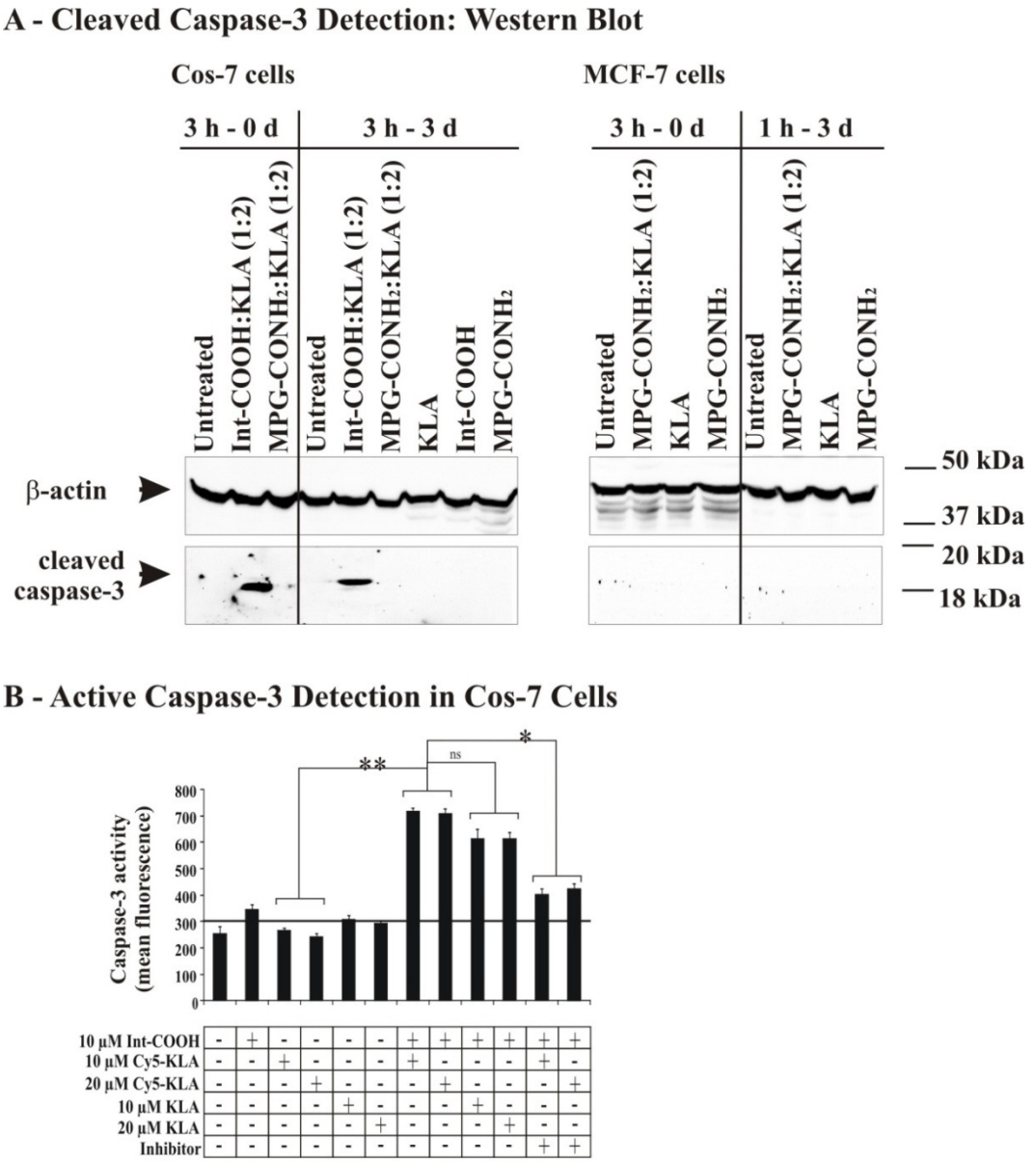

Figure 12. Caspase-3 Detection after the Incubation with CPP:KLA.
(A) Cleaved caspase-3 detection by western blot: Cos-7 and MCF-7 cells were incubated with the peptides (1 hour or 3 hours) and cell lysates (directly after or after 3 days incubation) were subjected to western blot analysis. Antibodies against ß-actin (internal control) and cleaved caspase-3 were used. Cleaved caspase-3 was detected in Int-COOH:KLA (1:2) treated Cos-7 cells directly after the incubation (0 days) and after 3 days. All lysates of MCF-7 cells were negative for cleaved caspase-3.
(**B**) Caspase-3 activity measurements: Cos-7 cells were treated with the peptides, lysed and the given to the specific caspase-3 substrate. A 2-fold increase using Int-COOH:KLA-Cy5 ($P < 0.001$ *versus* KLA-Cy5 alone) was detected, which could be inhibited using N-Ac-Asp-Glu-Val-Asp-CHO as inhibitor ($P < 0.05$). Cy5-labelling of KLA has no effect on caspase-3 activity. Data shown are the means ± SEM (n=3).

In Cos-7 cell lysates active caspase-3 was not detectable in untreated cells at day 0 and 3, as well as when incubated with the peptides alone (Figure 12A). After the incubation with MPG-$CONH_2$:KLA (1:2) Western blots show no cleaved caspase-3 after 0 and 3 days. Caspase-3 was only activated by the mixture of Int-COOH:KLA (1:2) at both

time points measured. Both results are in agreement with the viability reductions in the MTT assay (Figure 10) and nuclear condensation (Figure 11).

The incubation with the CPP and the KLA peptide alone had no effect on caspase-3 activation in Cos-7 cells determined by the Caspase-3 Fluorescence Assay Kit (Figure 12B). By using the combination Int-COOH:KLA (1:2) we detected elevated levels of caspase-3 activity. Curiously, the difference between ratios 1:1 and 1:2 is not as pronounced as observed in Figure 9B and Figure 10A. Nevertheless, the activation of caspase-3 is specific and could be reversed using the caspase-3 inhibitor (N-Ac-Asp-Glu-Val-Asp-CHO; $P < 0.05$). Finally, by using unlabelled KLA peptide co-incubated with Int-COOH the caspase-3 activity was not significantly reduced ($P > 0.05$) showing that Cy5-labelling has no influence on the assay procedure.

However, to determine if apoptosis is induced in MCF-7 cells after MPG-$CONH_2$:KLA treatment other methods should be applied (see next section).

3.5.5. KLA-Peptide Induced Apoptosis

The mixture MPG-CONH2:KLA (1:2) caused toxicity in MCF-7 cells (MTT test: 42 % toxicity) and led to nuclear chromatin condensation. To further investigate this viability reduction and to assign it to apoptosis, the annexin V labelling and the detection of DNA fragmentation was assessed using the peptide mixture in comparison with the apoptosis inducing agent staurosporin (STS) (Liu et al., 2008). Early apoptosis can lead to the displacement of phosphatidylserine at the outer cell membrane which can be detected by FITC-labelled annexin V staining and analysed by flow cytometry. Co-staining with propidium iodine (PI) allows the clear determination of apoptotic cells (in contrast to necrotic ones).

MPG-$CONH_2$:KLA treated MCF-7 cells revealed in the annexin V/PI stain the same amount of induced apoptosis as compared to STS-treated cells at day 0 (0.5 µM STS: 50 ± 27 % *versus* MPG-$CONH_2$:KLA: 41 ± 8 %) and at day 1 (0.5 µM STS: 85 ± 27 % *versus* MPG-$CONH_2$:KLA: 68 ± 22 %) (Figure 13A, page 54). However, the pro-apoptotic effect of the KLA-peptide on early apoptosis is lost after day 2 (0.5 µM STS: 124 ± 54 % *versus* MPG-NH_2:KLA: 26 ± 16 %).

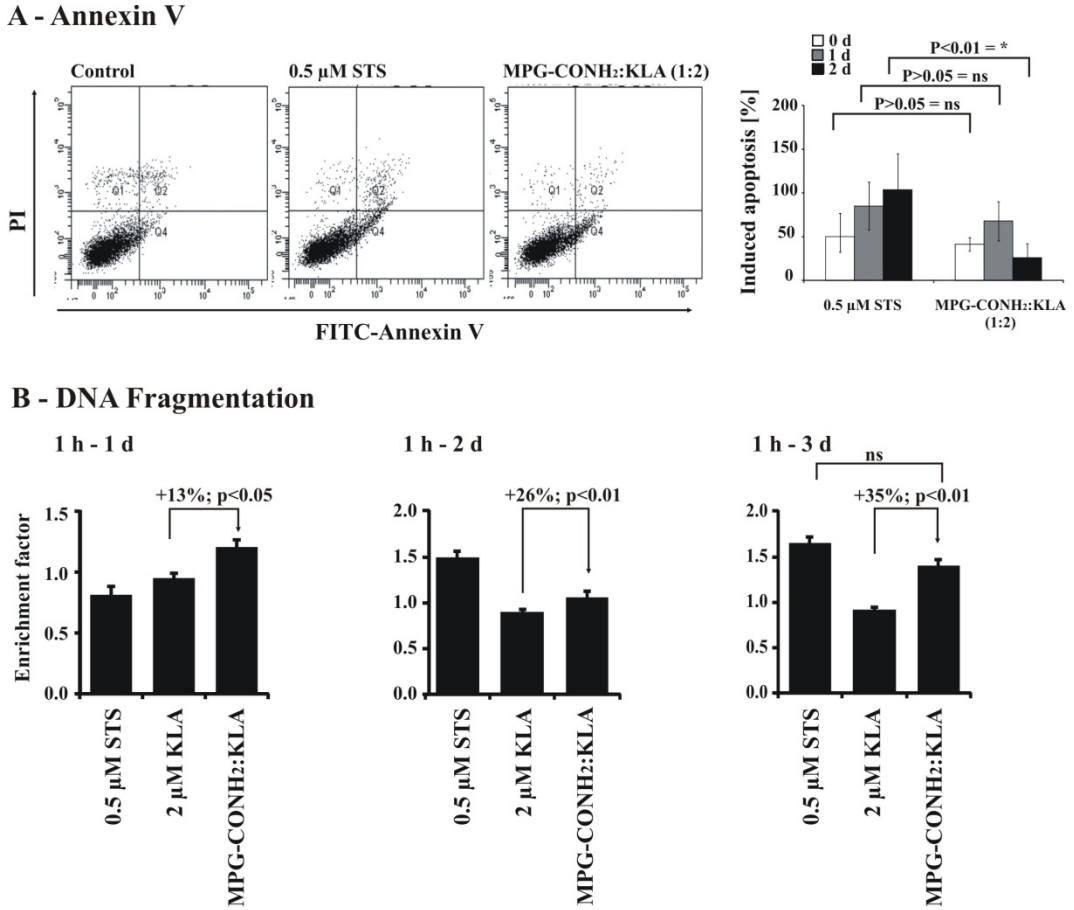

Figure 13. Apoptosis Detection in MCF-7 Cells.
(**A**) Annexin V: 0, 1 and 2 days after the incubation with 0.5 µM STS and MPG-$CONH_2$:KLA (1:2) MCF-7 cells were stained with annexin V/PI. The percentage of apoptotic cells is shown in the right graph. At day 0 and 1, the amount of apoptotic cells is equally induced with 0.5 µM STS or with the pro-apoptotic peptide mixture (P=ns).
(**B**) DNA fragmentation (ELISA): A quantitative immunoassay using anti-histone/anti-DNA antibodies was performed after the incubation with the conditions stated in the figure. MCF-7 cells show an increase in mono- and oligonucleosomes up to 3 days after the incubation with MPG-$CONH_2$:KLA (1:2) (+ 35 % related to 2 µM KLA, P=0.01).

Apoptotic cell death goes along with the cleavage of double stranded DNA into mono- and oligonucleosomes tightly complexed with core histones. To reassure the pro-apoptotic properties of the MPG-$CONH_2$:KLA (1:2) mixture in MCF-7 cells, DNA fragmentation was measured with the Cell Death Detection ELISA kit. The enrichment factors of mono- and oligonucleosomes were significantly increased 3 days after the incubation with MPG-$CONH_2$:KLA (1:2) compared to just the incubation with 2 µM KLA (+35 % increase in relation to 2 µM KLA, $P < 0.01$; Figure 13B).

Using annexin V stain and DNA fragmentation assay, signs of early as well as late apoptosis in MCF-7 cells were measured induced by the MPG-$CONH_2$:KLA (1:2) mixture, which corresponds to the first results of the MTT assays and nucleus condensation measurements.

4. DISCUSSION

Successful and effective cellular delivery remains one of the main obstacles in the medical field. The use of cell penetrating peptides (CPPs) has become one of the most important tools for the internalisation of a wide range of molecules including pharmaceuticals (Dietz *et al.*, 2004; Langel, 2011; Sawant *et al.*, 2009). They are usually rich in basic amino acid residues and often derived from proteins that are involved in signal transduction. Today, due to their high potential to efficiently cross membranes and transport cargoes, characterising and optimising CPPs has been a major goal of many different studies (Fotin-Mleczek *et al.*, 2005; Gupta *et al.*, 2005; Torchilin, 2007).

For that reason, defined experimental conditions should be established for the measurements of cellular CPP uptake, a necessary step for reproducibility and avoiding artefacts. Approximately 100,000 cells per millilitre (depending on the cell line) should be seeded one day before the experiment in order to reach about 80 % confluence on the day of measurement (12-well plates). Within one experiment, the same number of cells should always be seeded, since the uptake of CPPs depends on the peptide to cell ratio (Hallbrink *et al.*, 2004). In general, cells should not reach the confluent state to assure a complete internalisation without any hindrance by tight junction formation. For example, endocytotic internalisation was remarkably reduced especially in confluent Madin-Darby canine kidney (MDCK) epithelial cells. This effect was shown to be compound-unspecific, since other compounds (FITC-dextran, Tetramethylrhodamine isothiocyanate (TRITC)-transferrin etc.), known to be internalised by endocytosis, lost their internalisation efficiency (Foerg *et al.*, 2007). Also, trypsinisation or trypan blue quenching (depending on the method of measurement) after CPP incubation is required to avoid the measurement of external, membrane-bound CPPs. Finally, to acquire images for confocal microscopy, the cells should be viable (not fixed) due to the fact that formaldehyde or methanol fixation leads to cellular redistribution of the CPPs.

Toxic effects should be kept at a minimum if CPPs are used as drug delivery vehicles. For that reason and deduced from literature, for uptake experiments a final CPP concentration of 1 μM to 10 μM was used and an incubation time of 30 minutes.

To understand the mechanism(s) of cellular CPP uptake better, specific endocytotic pathways, the acidification or fusion of endosomes or all energy-dependent uptake routes can be specifically and individually blocked. The internalisation rates of the tested CPPs was mostly uninfluenced and never completely shut down, but sometimes

depending on CPP and cell line significantly reduced or even increased. Since CPPs often use different routes of uptake simultaneously (Letoha *et al.*, 2003), the blocking of one pathway might have resulted in the internalisation via a different route. However, at low concentrations (1 µM to 10 µM) CPPs seem to internalise via endocytosis (Abes *et al.*, 2006; Duchardt *et al.*, 2007). Unfortunately, combinations of different endocytosis inhibitors are toxic for the cells, making clear conclusions difficult. To fully understand internalisation pathways of the used CPPs, different techniques such as light scattering, microscopy (electromagnetic spectrum and atomic force microscopy), optical spectroscopies (circular dichroism, fourier transform infrared, fluorescence and rapid kinetics) in association with investigations dealing with peptide-lipid interactions (monolayer and langmuir films) need to be used (Deshayes *et al.*, 2005; Morris *et al.*, 2008).

4.1. Comparison of 22 CPPs in Seven Different Cell Types

For the delivery of the pro-apoptotic KLA peptide, the best CPP should be chosen. This is difficult, since a systematic evaluation of more than 11 different CPPs in more than six cell lines has never been done before (El-Andaloussi *et al.*, 2007; Fischer *et al.*, 2004; Fotin-Mleczek *et al.*, 2005; Maiolo *et al.*, 2005; Sarko *et al.*, 2010; Tunnemann *et al.*, 2008; Wender *et al.*, 2000). Therefore, 22 CPPs were evaluated in six cell lines and primary cells. The toxicity was analysed first, since it is crucial for the peptides' future use as delivery vehicles. Applying the CPPs for 4 hours at a concentration of 10 µM, no cytotoxicity (viability < 70 %) was observed in Cos-7, HEK293, HeLa, MDCK, MCF-7, RAW 264.7 and RAEC cells (Annex - Table 5 and Table 7). Only $S4_{13}PV$ revealed toxic effects at this concentration, which were not detectable in the CSLM pictures when using an incubation time of 30 min. At high concentrations toxic effects were observed on cell membranes and organelles as shown for transportan. 20-30 % of the cells revealed a huge accumulation of transportan (Figure 3, last row), which correlated with the vital dye trypan blue staining independently of the cell type. This is not surprising, since transportan penetrates the cell membrane by creating short-lived pores (Matsuzaki *et al.*, 1996).

The analytical evaluation of the CPP internalisation in the seven different cell types (Cos-7, HEK293, HeLa, MDCK, MCF-7, RAW 264.7, RAEC) resulted in a classification into three groups (Figure 2 and Figure 4) of which the first one comprises surprisingly the most CPPs: (I) CPPs with low cellular uptake [< 500 SI/mg protein; such as hCT(9-32), Tat, Pep-1]; (II) CPPs with medium internalisation (500 –

1,000 SI/mg protein; e.g. Rev, $S4_{13}PV$, R9 and integrin); (III) CPPs with high cellular uptake (> 1,000 SI/mg protein; MPG, penetratin, MAP and transportan).

Table 4: Uptake Classification of 22 CPPs in Seven Cell Types

CPPs	Uptake	Cos-7	HEK293	HeLa	MDCK	MCF-7	RAW 264.7	RAEC
pVEC-scrambled Polyomavirus Vp1 poly-P NF-kB SV40 HATF3 hCT(9-32) SynB1 DPV6 Tat Pep-1 Bac1-15 R7	Low < 500 SI/mg protein							
pVEC Rev $S4_{13}PV$ R9 Integrin	Medium 500 - 1,000 SI/mg protein							
MPG Penetratin MAP Transportan	High > 1,000 SI/mg protein							

Footnote: The internalisation of the 22 CPPs in the seven cell types can be classified in low (marked white), medium (marked grey) and high (marked black) cellular uptake. Even if transportan seems to be the more efficient CPP for all cell types, it should be taken into account that it is the most cytotoxic CPP (see Table 5 and Table 7 in the annex).

Altogether breast cancer cells show the highest uptake rates of all tested cells whereas MDCK cells show the lowest.

Comparing the results, some agreements with published reports can be found, but also some basic differences. For example, the commonly used CPPs such as penetratin, MAP and R9, also show the highest signal intensities in the analytical measurements, which is in agreement with the literature. The results of MCF-7 cells coincide with the

ones of Sarko et al (Sarko *et al.*), where the uptake hierarchy is defined by MAP > penetratin > R9, although they measured a higher uptake of Tat than of R9. Furthermore, lower uptake of Tat compared to penetratin and polyarginines was confirmed by different reports (Fischer *et al.*, 2004; Wender *et al.*, 2000) as well as the better internalisation of R9 compared to R7 (Tunnemann *et al.*, 2008).
When looking at the cellular CPP distribution, it was mainly of a punctuated pattern throughout the cytoplasm probably resulting from an entrapment of the CPPs in endosomes. Some CPPs were also located evenly disseminated in the cytoplasm and nucleus such as R9 in Cos-7, MDCK and MCF-7 cells suggesting endocytotic and non-endocytotic uptake routes (Jiao *et al.*, 2009; Vives *et al.*, 2008). Moreover, it has been speculated that often more than one uptake pathway is possible, dependent on factors such as the peptide concentration applied, the cell line used, the cargo attached and the overall incubation conditions (Jiao *et al.*, 2009; Tunnemann *et al.*, 2008; Walther *et al.*, 2009). This is in agreement with the measurement of different endocytosis inhibiting agents during cellular uptake revealing no distinguishing or mainly weak information on the internalisation mechanism [details in Table 3 of (Mueller *et al.*, 2008)].

To compare the uptake of the seven adherent cell types to a suspension cell line, Julia Triebus' results for the uptake of the 22 CPPs in human T-lymphocytes (Jurkat) are presented in Figure 14, page 59 (published in her diploma thesis: Quantitative and qualitative analysis of cell penetrating peptides in immune cells, FU Berlin, 2009).
The classification of the CPPs in the three uptake groups (low, medium and high) is completely different in the suspension Jurkat cells. Here, the first group (low uptake: mean fluorescence < 2,500) comprises only two CPPs and the control peptide pVEC-scrambled, whereas eleven CPPs are grouped in the third class (high uptake: mean fluorescence > 5,000). Many CPPs classified in the first group in the adherent cells show high uptake rates in the suspension cells [e.g. HATF3 or hCT(9-32)], which could be due to the larger cell surface area exposed to the CPPs. Surprisingly the uptake of transportan is low (2,031 ± 469 mean fluorescence), which used to be high in all the other adherent cell types.

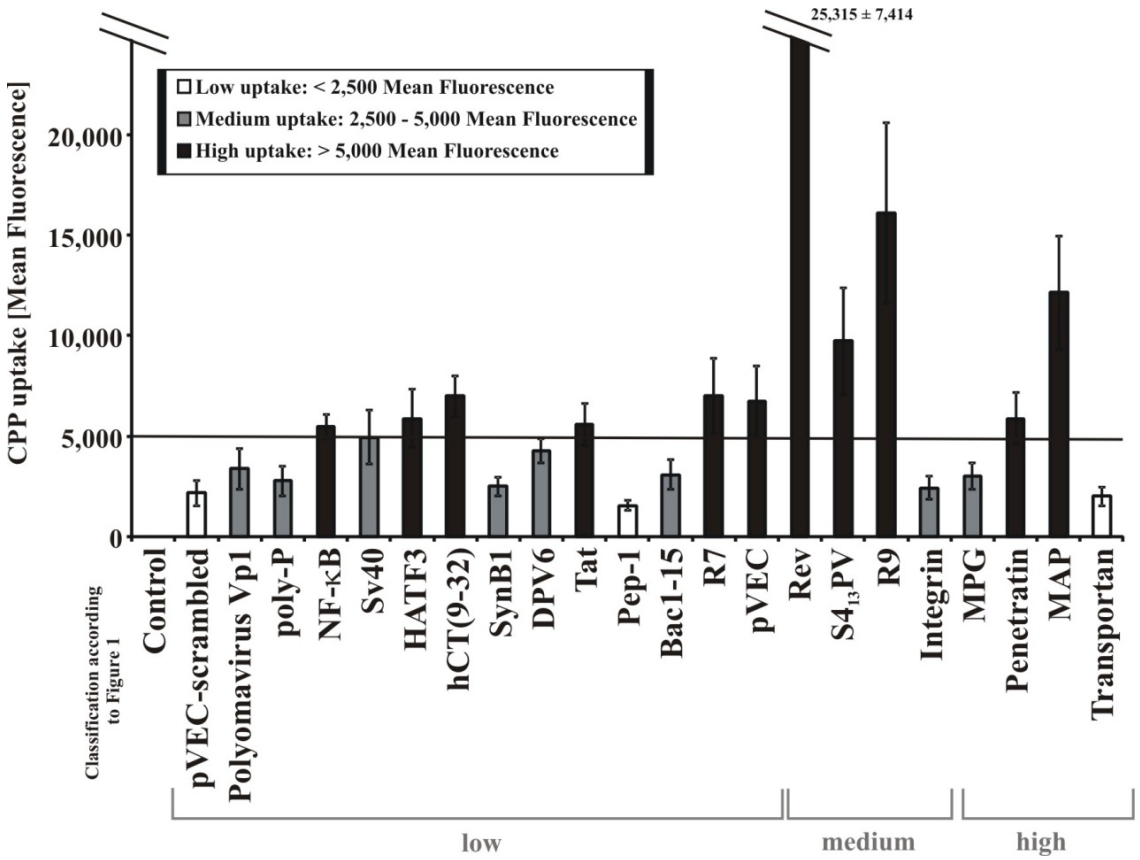

Figure 14. CPP Uptake in Suspension Jurkat Cells.
1×10^6 Jurkat cells were washed and incubated with 10 µM CF-CPPs for 30 min at 37°C. The cells were then washed and treated with trypsin (10 min at 37°C) to avoid the measurement of membrane bound, but not internalised CPPs. A total of 10,000 events were recorded on a FACS Canto II (BD Biosciences). In each analysis, nonviable (PI+) cells have been excluded. The uptake of a given CF-CPP into cells was assessed by the change of the median fluorescence of a cell sample treated with the peptide compared with an untreated control sample. The results are expressed as the mean change in median fluorescence ± standard deviation (n=3).

Altogether the cellular CPP uptake in suspension cells seems to be extremely different compared to the uptake in adherent cells - another proof for the importance to compare and select the optimal CPP for the desired application.

However, predicting cell penetrating properties of CPPs by analysing their primary amino acid sequence or the structural conformation is still a great challenge. For example, CPPs with similar isoelectric points (pI) show different uptake activities. For example, penetratin (pI = 12.31) shows high cellular internalisation in comparison to the low activity of poly-P (for sequence see Table 1, page 29) with the same pI value (pI = 12.30). These results demonstrate that the positive charges of CPPs (pI = 10 - 12), which are postulated to be important for the interaction with HSPGs on the cell surface, are not always the portal guiding endocytosis (Poon *et al.*, 2007). On the other hand,

CPPs with a low pI such as integrin (pI = 5.49) revealed good internalisation, especially in HEK293 cells.

The only point, which can be ruled out, is the correlation of the amino acid order within the primary sequence. pVEC's uptake in HeLa cells was 301 ± 53 SI/mg protein, whereas the scrambled version showed practically no uptake (53 ± 9 SI/mg protein). A similar effect could be observed with $S4_{13}PV$ (ALWKTLLKKVLKA-PKKKRKV) and SV40 T antigen (PKKKRKV): only the addition of the N-terminal, cell penetrating sequence induces the cell internalisation properties in most cell lines (Mano *et al.*, 2005). These results imply that the sequence and amphipacity of the CPP plays a more important role in cellular uptake than the accumulation of positive charge. However, it is also difficult to argue with the three dimensional structure since α-helices (e.g. transportan (Lindberg *et al.*, 2001) as well as β-structures (e.g. penetratin (Magzoub *et al.*, 2003) are reported to be important for cellular internalisation via membrane perturbation.

4.2. Importance of the C-Terminus

The analysis of the 22 CPPs in the seven cell types shows the importance of the appropriate CPP choice for a distinct application. Based on these results, six CPPs were selected, namely Tat, $S4_{13}PV$, R9, penetratin, integrin and MPG for further investigations. By trying to optimise their cellular uptake, the influence of the C-terminus (-COOH *versus* $-CONH_2$) on the internalisation was evaluated after the determination of the toxicity of CPP-$CONH_2$. The carboxyamidated form heavily enhanced the ability of CPP penetration for most, but not all tested CPPs (Figure 6). In primary RAEC cells only Int-$CONH_2$ internalised better than its carboxylated form, whereas the uptake rates of the other CPPs remained the same. Carboxyamidated CPPs are more toxic to the six cell lines than carboxylated CPPs with HeLa cells showing the most toxic effects. $S4_{13}PV$-$CONH_2$ caused the most viability reductions, though they are not linked to higher internalisation rates. Surprisingly, carboxyamidated CPPs are less toxic to primary RAEC cells, but the reduced toxicity of CPP-$CONH_2$ in RAEC cells cannot be explained by lower internalisation rates. Tat, being one of the most frequently used CPPs, shows again very low uptake rates independent of its C-terminus. However, the cellular distribution of the CPPs was not altered in the vast majority of cases when changing the C-termini (Figure 7). CPPs were mostly detected in a punctuated pattern hinting towards endosomal entrapment. Taken together, depending

on the CPP and cell line the C-terminus influences the cellular CPP uptake, toxicity and in a few cases the cellular localisation.

4.3. Delivery of the Pro-Apoptotic KLA Peptide by CPPs

CPPs are proven vehicles for the intracellular delivery of macromolecules such as oligonucleotides, peptides and proteins, low-molecular-weight drugs, nano-particles and liposomes (Langel, 2011). Even if there is no "golden rule" for the CPP application, the importance of CPPs for controlled and targeted delivery of therapeutic and imaging agents is very clear.

In this study, the delivery of the pro-apoptotic KLA peptide in breast adenocarcinoma cells, leukaemic macrophages and fibroblasts using the three best CPPs (MPG, integrin and penetratin) was compared and their therapeutic applicability was proven. Nowadays, the development and analysis of CPPs conjugated to anti-cancer drugs to serve as potential new chemotherapeutic agents becomes the focus of attention. In order to offer an alternative to covalent methods, a strategy for the delivery of the pro-apoptotic KLA peptide (Ellerby *et al.*, 1999) into mammalian cells on the basis of a simple co-incubation with the appropriate CPP was proposed.

After determining the optimal mixing ratios (1:1 and 1:2 of CPP:KLA), a 2- to 3-fold enhancement of the KLA uptake was demonstrated (Figure 8A). Unfortunately, a general rule for a successful KLA delivery was not perceived; different cell types needed different CPPs with different C-termini to deliver the KLA peptide effectively. Furthermore, the CPP uptake did not necessarily correlate with the KLA uptake. For example, MPG-$CONH_2$ having the highest internalisation properties in all cell lines (Figure 6), showed only an improvement of the KLA delivery in RAW264.7 cells compared to the other employed CPP:KLA pairs in all other cell lines (Figure 9A). In contrast, the Int-COOH:KLA mixture (1:1 or 1:2) revealed the best KLA delivery in Cos-7 cells, although Int-COOH alone seemed to have nearly no penetration ability (Figure 2). CLSM confirmed the measurements done before; KLA was successfully delivered into the cells, but showed mostly a punctuated pattern, which might have been due to endosomal entrapment (Abes *et al.*, 2006). Besides, a diffuse KLA-distribution was observed probably resulting from an endosomal KLA release (Figure 9B). By simply mixing the CPP and KLA peptides, it is highly likely to have had no proper complex formation as shown for CPP:ON complexes (Andaloussi *et al.*, 2011) nor a formation of aggregates as reported in (Kamei *et al.*, 2008). The KLA peptide was presumably endocytosed together with the CPP. Over the last years, it became clear that

CPPs are internalised at low concentrations via energy-dependent mechanisms (Brasseur *et al.*, 2010). Therefore, it can be assumed that the internalisation of the KLA peptide was facilitated by the endocytosis of the CPPs.

However, by looking at the pro-apoptotic properties of the internalised KLA peptide in MTT assays (Figure 10), one combination could be depicted, which was toxic to macrophages and cancer cells, but showed no toxicity in fibroblasts. The mixture of MPG-$CONH_2$:KLA (1:2) resulted in 42 % toxicity ($P < 0.001$ *versus* KLA alone) in MCF-7 cells and in 36 % toxicity ($P < 0.05$ *versus* KLA alone) in RAW 264.7 cells. This is particularly interesting since 10-fold lower concentrations were used as in the incubations with Cos-7 cells. For the Cos-7 cells only the combination of Int-COOH:KLA (1:2) revealed a reduction in cell viability of 32 %. These results were validated when microscopically examining the nuclear condensation, which is a hallmark of apoptosis. For the conditions causing toxicity in the MTT-viability measurements, a distinguished nucleus condensation in all three cell lines was detected (Figure 11). Furthermore, the KLA peptide induced active caspase-3 in Cos-7 cells, but not in MCF-7 cells. Contradictory results are presented in the literature, showing the detection of active Caspase-3 in MCF-7 cells (Wang *et al.*, 2009; Yang *et al.*, 2006) or the lack of caspase-3 due to a deletion in the CASP-3 gene (Janicke, 2009). These findings show the importance of apoptosis validation by different methods. Later the toxic effects in MCF-7 cells were assigned to apoptosis by annexin V stain and DNA-fragmentation assay.

To cross-validate the co-incubation approach, the toxicity of covalently coupled CF-MPG-KLA was determined in MCF-7 cells. Using the CF-MPG-KLA construct at a 5 µM concentration, a viability reduction could be clearly detected (39 % toxicity at day 0 and 44 % at day 1) - a phenomenon which was not obeserved at a 1 µM concentration. Since KLA is not even 1/3 of the CF-MPG-KLA sequence, the effective KLA concentration correspond to ~ 1.7 µM which is in the same range as in the co-incubation of MPG-$CONH_2$:KLA (1:2) (2 µM). These results confirm the non-covalent strategy as being as effective as the covalent approach and furthermore hint towards an advantage of the co-incubation strategy in an enclosed incubation environment, because of its simplicity in its application.

The comparison with published reports to validate the results is difficult, because the internalisation is usually done by a covalent linkage of the KLA peptide to CPPs (Cai *et al.*, 2010; Watkins *et al.*, 2009), to homing peptides (Ellerby *et al.*, 1999) or to self

assembling fibres (Standley *et al.*, 2010). Nevertheless, in all cases researchers used covalent-bound peptide concentrations comparable to this study (1 - 10 µM) (Futaki *et al.*, 2001; Pooga *et al.*, 2001; Snyder *et al.*, 2004) or even higher (50 µM in (Dutot *et al.*, 2009). By using the simple co-incubation strategy to administrate the KLA peptide in a low micromolar range (1 µM CPP + 2 µM KLA) - a pro-apoptotic effect of the KLA peptide was obtained ranging between 25 % and 60 %, which is in the same scope of induced toxicity as described in the other studies (Cai *et al.*, 2010; Ellerby *et al.*, 1999; Watkins *et al.*, 2009).

All together, the simple co-incubation strategy enabled the introduction of the pro-apoptotic KLA peptide in the carcinoma cell line MCF-7 and in the macrophagic cell line RAW264.7, both involved in cancer development and metastasis formation. For these cell lines a 36 % and 42 % cell viability reduction was reached, which coincides with the effect of KLA covalently coupled to CPPs (Cai *et al.*, 2010; Watkins *et al.*, 2009) or with KLA nanofibres (Standley *et al.*, 2010) even though much shorter incubation times were used. More importantly, this effect was not observable in fibroblastic Cos-7 cells even at 10-fold higher concentrations.

In summary, the co-incubation strategy may hold many benefits such as the combinatorial potential of different CPPs with different pro-apoptotic peptides, the use of targeting devices and associated cost savings due to shorter peptide sequence. These advantages are highly relevant in regard to a therapeutic application of pro-apoptotic peptides in cancer treatment. In the case of an occurring resistance to one therapeutic peptide, it can be quickly and easily replaced when the mixture is applied.

5. CONCLUSION

Despite the high number of biological applications using CPPs, the precise mechanism of entry still appears controversial and certainly requires further investigations. Contradictory results are often reported, and could stem from experimental variations: e.g. diversity of the CPP sequences, the wide variety of cell lines studied, the differing protocols applied to investigate the entry mechanism, etc.

A comparative screen using 22 CPPs in seven cell types under standardised conditions revealed the categorisation of the CPPs by their behaviour into three main groups showing high, medium and low cellular uptake. Also, the C-terminus of the CPPs is able to influence its uptake, toxicity and sometimes even its sub-cellular localisation. Compared to a carboxylated C-terminus, a carboxyamidated enhances the cellular uptake often. Furthermore, CPPs are able to deliver a second peptide by a simple co-incubation. Here as well, the delivery depends on CPP, C-terminus and cell type. Inside the cell, the delivered peptide is sometimes, but not always functionally active, here shown by the reduced cell viability caused by the pro-apoptotic KLA peptide, which was assigned to apoptosis in later tests. The activity of the KLA peptide did not correlate with its uptake rates.

This co-incubation approach represents a huge benefit for the future therapeutic utilisation: (I) It is much easier and quicker to co-incubate the appropriate CPP with the corresponding therapeutic peptide instead of newly synthesising the chosen set; (II) It is possible to change the pro-apoptotic peptide quickly in case resistance occurs.

These results show the difficulty scientists have when working with CPPs. Which CPP is the “best” one for the application? The comparison of different CPPs in the respective cell line is advisable whilst taking the C-terminus into account. This is aggravated by the fact that a chosen CPP might be perfect in its toxicity and uptake properties, but might not show the expected transportation capabilities. Therefore it is recommended to always include more than one CPP in the evaluation process.

6. REFERENCES

Abes, S, Turner, JJ, Ivanova, GD, Owen, D, Williams, D, Arzumanov, A, Clair, P, Gait, MJ, Lebleu, B (2007) Efficient splicing correction by PNA conjugation to an R6-Penetratin delivery peptide. *Nucleic Acids Res* **35**(13)**:** 4495-4502.

Abes, S, Williams, D, Prevot, P, Thierry, A, Gait, MJ, Lebleu, B (2006) Endosome trapping limits the efficiency of splicing correction by PNA-oligolysine conjugates. *J Control Release* **110**(3)**:** 595-604.

Andaloussi, SE, Lehto, T, Lundin, P, Langel, U (2011) Application of PepFect peptides for the delivery of splice-correcting oligonucleotides. *Methods Mol Biol* **683:** 361-373.

Bais, MV, Kumar, S, Tiwari, AK, Kataria, RS, Nagaleekar, VK, Shrivastava, S, Chindera, K (2008) Novel Rath peptide for intracellular delivery of protein and nucleic acids. *Biochem Biophys Res Commun* **370**(1)**:** 27-32.

Barany-Wallje, E, Gaur, J, Lundberg, P, Langel, U, Graslund, A (2007) Differential membrane perturbation caused by the cell penetrating peptide Tp10 depending on attached cargo. *FEBS Lett* **581**(13)**:** 2389-2393.

Barkett, M, Gilmore, TD (1999) Control of apoptosis by Rel/NF-kappaB transcription factors. *Oncogene* **18**(49)**:** 6910-6924.

Barua, S, Linton, RS, Gamboa, J, Banerjee, I, Yarmush, ML, Rege, K (2010) Lytic peptide-mediated sensitization of TRAIL-resistant prostate cancer cells to death receptor agonists. *Cancer Lett* **293**(2)**:** 240-253.

Bates, E, Bode, C, Costa, M, Gibson, CM, Granger, C, Green, C, Grimes, K, Harrington, R, Huber, K, Kleiman, N, Mochly-Rosen, D, Roe, M, Sadowski, Z, Solomon, S, Widimsky, P (2008) Intracoronary KAI-9803 as an adjunct to primary percutaneous coronary intervention for acute ST-segment elevation myocardial infarction. *Circulation* **117**(7)**:** 886-896.

Bohnlein, E, Berger, J, Hauber, J (1991) Functional mapping of the human immunodeficiency virus type 1 Rev RNA binding domain: new insights into the domain structure of Rev and Rex. *J Virol* **65**(12)**:** 7051-7055.

Brasseur, R, Divita, G (2010) Happy birthday cell penetrating peptides: already 20 years. *Biochim Biophys Acta* **1798**(12)**:** 2177-2181.

Cai, HW, Yang, H, Xiang, B, Li, SF, Liu, S, Wan, L, Zhang, J, Li, YP, Cheng, JQ, Lu, XF (2010) Selective Apoptotic Killing of Solid and Hematologic Tumor Cells by Bombesin-Targeted Delivery of Mitochondria-Disrupting Peptides. *Molecular Pharmaceutics* **7**(2)**:** 586-596.

Capecchi, MR (1980) High efficiency transformation by direct microinjection of DNA into cultured mammalian cells. *Cell* **22**(2 Pt 2)**:** 479-488.

Cardone, MH, Roy, N, Stennicke, HR, Salvesen, GS, Franke, TF, Stanbridge, E, Frisch, S, Reed, JC (1998) Regulation of cell death protease caspase-9 by phosphorylation. *Science* **282**(5392)**:** 1318-1321.

Chang, D, Cai, X, Consigli, RA (1993) Characterization of the DNA binding properties of polyomavirus capsid protein. *J Virol* **67**(10)**:** 6327-6331.

Chen, LB (1988) Mitochondrial membrane potential in living cells. *Annu Rev Cell Biol* **4:** 155-181.

Chen, X, Thakkar, H, Tyan, F, Gim, S, Robinson, H, Lee, C, Pandey, SK, Nwokorie, C, Onwudiwe, N, Srivastava, RK (2001) Constitutively active Akt is an important regulator of TRAIL sensitivity in prostate cancer. *Oncogene* **20**(42)**:** 6073-6083.

Cochrane, AW, Perkins, A, Rosen, CA (1990) Identification of sequences important in the nucleolar localization of human immunodeficiency virus Rev: relevance of nucleolar localization to function. *J Virol* **64**(2)**:** 881-885.

Copp, DH (1970) Endocrine regulation of calcium metabolism. *Annu Rev Physiol* **32:** 61-86.

Cryan, SA, Devocelle, M, Moran, PJ, Hickey, AJ, Kelly, JG (2006) Increased intracellular targeting to airway cells using octaarginine-coated liposomes: in vitro assessment of their suitability for inhalation. *Mol Pharm* **3**(2)**:** 104-112.

De Coupade, C, Fittipaldi, A, Chagnas, V, Michel, M, Carlier, S, Tasciotti, E, Darmon, A, Ravel, D, Kearsey, J, Giacca, M, Cailler, F (2005) Novel human-derived cell-penetrating peptides for specific subcellular delivery of therapeutic biomolecules. *Biochem J* **390**(Pt 2)**:** 407-418.

Derossi, D, Calvet, S, Trembleau, A, Brunissen, A, Chassaing, G, Prochiantz, A (1996) Cell internalization of the third helix of the Antennapedia homeodomain is receptor-independent. *J Biol Chem* **271**(30)**:** 18188-18193.

Derossi, D, Joliot, AH, Chassaing, G, Prochiantz, A (1994) The third helix of the Antennapedia homeodomain translocates through biological membranes. *J Biol Chem* **269**(14)**:** 10444-10450.

Deshayes, S, Heitz, A, Morris, MC, Charnet, P, Divita, G, Heitz, F (2004) Insight into the mechanism of internalization of the cell-penetrating carrier peptide Pep-1 through conformational analysis. *Biochemistry* **43**(6)**:** 1449-1457.

Deshayes, S, Morris, MC, Divita, G, Heitz, F (2005) Cell-penetrating peptides: tools for intracellular delivery of therapeutics. *Cell Mol Life Sci* **62**(16)**:** 1839-1849.

Deshayes, S, Plenat, T, Charnet, P, Divita, G, Molle, G, Heitz, F (2006) Formation of transmembrane ionic channels of primary amphipathic cell-penetrating peptides. Consequences on the mechanism of cell penetration. *Biochim Biophys Acta* **1758**(11)**:** 1846-1851.

Dietz, GP, Bahr, M (2004) Delivery of bioactive molecules into the cell: the Trojan horse approach. *Mol Cell Neurosci* **27**(2)**:** 85-131.

Duchardt, F, Fotin-Mleczek, M, Schwarz, H, Fischer, R, Brock, R (2007) A comprehensive model for the cellular uptake of cationic cell-penetrating peptides. *Traffic* **8**(7)**:** 848-866.

Dutot, L, Lecorche, P, Burlina, F, Marquant, R, Point, V, Sagan, S, Chassaing, G, Mallet, JM, Lavielle, S (2009) Glycosylated cell-penetrating peptides and their conjugates to a proapoptotic peptide: preparation by click chemistry and cell viability studies. *J Chem Biol* **3**(2)**:** 51-65.

Egeblad, M, Werb, Z (2002) New functions for the matrix metalloproteinases in cancer progression. *Nat Rev Cancer* **2**(3)**:** 161-174.

Eguchi, A, Dowdy, SF Efficient siRNA delivery by novel PTD-DRBD fusion proteins. *Cell Cycle* **9**(3)**:** 424-425.

El-Andaloussi, S, Jarver, P, Johansson, HJ, Langel, U (2007) Cargo-dependent cytotoxicity and delivery efficacy of cell-penetrating peptides: a comparative study. *Biochem J* **407**(2)**:** 285-292.

Ellerby, HM, Arap, W, Ellerby, LM, Kain, R, Andrusiak, R, Rio, GD, Krajewski, S, Lombardo, CR, Rao, R, Ruoslahti, E, Bredesen, DE, Pasqualini, R (1999) Anti-cancer activity of targeted pro-apoptotic peptides. *Nat Med* **5**(9)**:** 1032-1038.

Elmquist, A, Langel, U (2003) In vitro uptake and stability study of pVEC and its all-D analog. *Biol Chem* **384**(3)**:** 387-393.

Elmquist, A, Lindgren, M, Bartfai, T, Langel, U (2001) VE-cadherin-derived cell-penetrating peptide, pVEC, with carrier functions. *Exp Cell Res* **269**(2)**:** 237-244.

Endoh, T, Ohtsuki, T (2009) Cellular siRNA delivery using cell-penetrating peptides modified for endosomal escape. *Adv Drug Deliv Rev* **61**(9)**:** 704-709.

Fawell, S, Seery, J, Daikh, Y, Moore, C, Chen, LL, Pepinsky, B, Barsoum, J (1994) Tat-mediated delivery of heterologous proteins into cells. *Proc Natl Acad Sci U S A* **91**(2)**:** 664-668.

Feener, EP, Shen, WC, Ryser, HJ (1990) Cleavage of disulfide bonds in endocytosed macromolecules. A processing not associated with lysosomes or endosomes. *J Biol Chem* **265**(31)**:** 18780-18785.

Fernandez-Carneado, J, Kogan, MJ, Castel, S, Giralt, E (2004) Potential peptide carriers: amphipathic proline-rich peptides derived from the N-terminal domain of gamma-zein. *Angew Chem Int Ed Engl* **43**(14)**:** 1811-1814.

Ferrari, A, Pellegrini, V, Arcangeli, C, Fittipaldi, A, Giacca, M, Beltram, F (2003) Caveolae-mediated internalization of extracellular HIV-1 tat fusion proteins visualized in real time. *Mol Ther* **8**(2)**:** 284-294.

Fischer, R, Kohler, K, Fotin-Mleczek, M, Brock, R (2004) A stepwise dissection of the intracellular fate of cationic cell-penetrating peptides. *J Biol Chem* **279**(13)**:** 12625-12635.

Fischer, R, Mader, O, Jung, G, Brock, R (2003) Extending the applicability of carboxyfluorescein in solid-phase synthesis. *Bioconjug Chem* **14**(3)**:** 653-660.

Fittipaldi, A, Ferrari, A, Zoppe, M, Arcangeli, C, Pellegrini, V, Beltram, F, Giacca, M (2003) Cell membrane lipid rafts mediate caveolar endocytosis of HIV-1 Tat fusion proteins. *J Biol Chem* **278**(36)**:** 34141-34149.

Foerg, C, Ziegler, U, Fernandez-Carneado, J, Giralt, E, Merkle, HP (2007) Differentiation restricted endocytosis of cell penetrating peptides in MDCK cells corresponds with activities of Rho-GTPases. *Pharm Res* **24**(4)**:** 628-642.

Foillard, S, Sancey, L, Coll, JL, Boturyn, D, Dumy, P (2009) Targeted delivery of activatable fluorescent pro-apoptotic peptide into live cells. *Org Biomol Chem* **7**(2)**:** 221-224.

Fotin-Mleczek, M, Welte, S, Mader, O, Duchardt, F, Fischer, R, Hufnagel, H, Scheurich, P, Brock, R (2005) Cationic cell-penetrating peptides interfere with TNF signalling by induction of TNF receptor internalization. *J Cell Sci* **118**(Pt 15)**:** 3339-3351.

Frankel, AD, Pabo, CO (1988) Cellular uptake of the tat protein from human immunodeficiency virus. *Cell* **55**(6)**:** 1189-1193.

Futaki, S, Suzuki, T, Ohashi, W, Yagami, T, Tanaka, S, Ueda, K, Sugiura, Y (2001) Arginine-rich peptides. An abundant source of membrane-permeable peptides having potential as carriers for intracellular protein delivery. *J Biol Chem* **276**(8)**:** 5836-5840.

Gait, MJ (2003) Peptide-mediated cellular delivery of antisense oligonucleotides and their analogues. *Cell Mol Life Sci* **60**(5)**:** 844-853.

Gehring, WJ (1987) Homeo boxes in the study of development. *Science* **236**(4806)**:** 1245-1252.

Gennaro, R, Skerlavaj, B, Romeo, D (1989) Purification, composition, and activity of two bactenecins, antibacterial peptides of bovine neutrophils. *Infect Immun* **57**(10)**:** 3142-3146.

Gerbal-Chaloin, S, Gondeau, C, Aldrian-Herrada, G, Heitz, F, Gauthier-Rouviere, C, Divita, G (2007) First step of the cell-penetrating peptide mechanism involves Rac1 GTPase-dependent actin-network remodelling. *Biol Cell* **99**(4)**:** 223-238.

Gondeau, C, Gerbal-Chaloin, S, Bello, P, Aldrian-Herrada, G, Morris, MC, Divita, G (2005) Design of a novel class of peptide inhibitors of cyclin-dependent kinase/cyclin activation. *J Biol Chem* **280**(14)**:** 13793-13800.

Gottschalk, S, Sparrow, JT, Hauer, J, Mims, MP, Leland, FE, Woo, SL, Smith, LC (1996) A novel DNA-peptide complex for efficient gene transfer and expression in mammalian cells. *Gene Ther* **3**(5)**:** 448-457.

Green, I, Christison, R, Voyce, CJ, Bundell, KR, Lindsay, MA (2003) Protein transduction domains: are they delivering? *Trends Pharmacol Sci* **24**(5)**:** 213-215.

Green, M, Loewenstein, PM (1988) Autonomous functional domains of chemically synthesized human immunodeficiency virus tat trans-activator protein. *Cell* **55**(6)**:** 1179-1188.

Gros, E, Deshayes, S, Morris, MC, Aldrian-Herrada, G, Depollier, J, Heitz, F, Divita, G (2006) A non-covalent peptide-based strategy for protein and peptide nucleic acid transduction. *Biochim Biophys Acta* **1758**(3)**:** 384-393.

Gupta, B, Levchenko, TS, Torchilin, VP (2005) Intracellular delivery of large molecules and small particles by cell-penetrating proteins and peptides. *Adv Drug Deliv Rev* **57**(4)**:** 637-651.

Hai, TW, Liu, F, Coukos, WJ, Green, MR (1989) Transcription factor ATF cDNA clones: an extensive family of leucine zipper proteins able to selectively form DNA-binding heterodimers. *Genes Dev* **3**(12B)**:** 2083-2090.

Hallbrink, M, Floren, A, Elmquist, A, Pooga, M, Bartfai, T, Langel, U (2001) Cargo delivery kinetics of cell-penetrating peptides. *Biochim Biophys Acta* **1515**(2)**:** 101-109.

Hallbrink, M, Oehlke, J, Papsdorf, G, Bienert, M (2004) Uptake of cell-penetrating peptides is dependent on peptide-to-cell ratio rather than on peptide concentration. *Biochim Biophys Acta* **1667**(2)**:** 222-228.

Hariton-Gazal, E, Feder, R, Mor, A, Graessmann, A, Brack-Werner, R, Jans, D, Gilon, C, Loyter, A (2002) Targeting of nonkaryophilic cell-permeable peptides into the nuclei of intact cells by covalently attached nuclear localization signals. *Biochemistry* **41**(29)**:** 9208-9214.

Hawiger, J (1999) Noninvasive intracellular delivery of functional peptides and proteins. *Curr Opin Chem Biol* **3**(1)**:** 89-94.

Hed, J, Hallden, G, Johansson, SG, Larsson, P (1987) The use of fluorescence quenching in flow cytofluorometry to measure the attachment and ingestion phases in phagocytosis in peripheral blood without prior cell separation. *J Immunol Methods* **101**(1)**:** 119-125.

Hiromura, M, Okada, F, Obata, T, Auguin, D, Shibata, T, Roumestand, C, Noguchi, M (2004) Inhibition of Akt kinase activity by a peptide spanning the betaA strand of the proto-oncogene TCL1. *J Biol Chem* **279**(51)**:** 53407-53418.

Hogset, A, Prasmickaite, L, Selbo, PK, Hellum, M, Engesaeter, BO, Bonsted, A, Berg, K (2004) Photochemical internalisation in drug and gene delivery. *Adv Drug Deliv Rev* **56**(1)**:** 95-115.

Hopkins-Donaldson, S, Bodmer, JL, Bourloud, KB, Brognara, CB, Tschopp, J, Gross, N (2000) Loss of caspase-8 expression in highly malignant human neuroblastoma cells correlates with resistance to tumor necrosis factor-related apoptosis-inducing ligand-induced apoptosis. *Cancer Res* **60**(16)**:** 4315-4319.

Huber, O, Bierkamp, C, Kemler, R (1996) Cadherins and catenins in development. *Curr Opin Cell Biol* **8**(5)**:** 685-691.

Inagaki, K, Chen, L, Ikeno, F, Lee, FH, Imahashi, K, Bouley, DM, Rezaee, M, Yock, PG, Murphy, E, Mochly-Rosen, D (2003) Inhibition of delta-protein kinase C protects against reperfusion injury of the ischemic heart in vivo. *Circulation* **108**(19)**:** 2304-2307.

Janicke, RU (2009) MCF-7 breast carcinoma cells do not express caspase-3. *Breast Cancer Res Treat* **117**(1)**:** 219-221.

Jarver, P, Langel, U (2006) Cell-penetrating peptides--a brief introduction. *Biochim Biophys Acta* **1758**(3)**:** 260-263.

Jiao, CY, Delaroche, D, Burlina, F, Alves, ID, Chassaing, G, Sagan, S (2009) Translocation and endocytosis for cell-penetrating peptide internalization. *J Biol Chem* **284**(49)**:** 33957-33965.

Joliot, A, Prochiantz, A (2008) Homeoproteins as natural Penetratin cargoes with signaling properties. *Adv Drug Deliv Rev* **60**(4-5)**:** 608-613.

Jones, AT (2008) Gateways and tools for drug delivery: endocytic pathways and the cellular dynamics of cell penetrating peptides. *Int J Pharm* **354**(1-2)**:** 34-38.

Jones, AT (2007) Macropinocytosis: searching for an endocytic identity and role in the uptake of cell penetrating peptides. *J Cell Mol Med* **11**(4)**:** 670-684.

Kalderon, D, Roberts, BL, Richardson, WD, Smith, AE (1984) A short amino acid sequence able to specify nuclear location. *Cell* **39**(3 Pt 2)**:** 499-509.

Kamei, N, Morishita, M, Eda, Y, Ida, N, Nishio, R, Takayama, K (2008) Usefulness of cell-penetrating peptides to improve intestinal insulin absorption. *J Control Release* **132**(1)**:** 21-25.

Kaplan, IM, Wadia, JS, Dowdy, SF (2005) Cationic TAT peptide transduction domain enters cells by macropinocytosis. *J Control Release* **102**(1)**:** 247-253.

Kelemen, BR, Hsiao, K, Goueli, SA (2002) Selective in vivo inhibition of mitogen-activated protein kinase activation using cell-permeable peptides. *J Biol Chem* **277**(10)**:** 8741-8748.

Kim, AL, Raffo, AJ, Brandt-Rauf, PW, Pincus, MR, Monaco, R, Abarzua, P, Fine, RL (1999) Conformational and molecular basis for induction of apoptosis by a p53 C-terminal peptide in human cancer cells. *J Biol Chem* **274**(49)**:** 34924-34931.

Knight, DE, Scrutton, MC (1986) Gaining access to the cytosol: the technique and some applications of electropermeabilization. *Biochem J* **234**(3)**:** 497-506.

Kolevzon, N, Kuflik, U, Shmuel, M, Benhamron, S, Ringel, I, Yavin, E (2011) Multiple triphenylphosphonium cations as a platform for the delivery of a pro-apoptotic peptide. *Pharm Res* **28**(11)**:** 2780-2789.

Kolonin, MG, Saha, PK, Chan, L, Pasqualini, R, Arap, W (2004) Reversal of obesity by targeted ablation of adipose tissue. *Nat Med* **10**(6)**:** 625-632.

Lanford, RE, Kanda, P, Kennedy, RC (1986) Induction of nuclear transport with a synthetic peptide homologous to the SV40 T antigen transport signal. *Cell* **46**(4)**:** 575-582.

Langel, Ü (2002) *Cell-Penetrating Peptides: Processes and Applications*. 1st edn. CRC Press: Boca Raton, London, New York, Washington, D.C.

Langel, Ü (2011) *Methods in Molecular Biology*. Vol. 683. Springer: New York.

Law, B, Quinti, L, Choi, Y, Weissleder, R, Tung, CH (2006) A mitochondrial targeted fusion peptide exhibits remarkable cytotoxicity. *Mol Cancer Ther* **5**(8)**:** 1944-1949.

Lebleu, B, Moulton, HM, Abes, R, Ivanova, GD, Abes, S, Stein, DA, Iversen, PL, Arzumanov, AA, Gait, MJ (2008) Cell penetrating peptide conjugates of steric block oligonucleotides. *Adv Drug Deliv Rev* **60**(4-5)**:** 517-529.

Lee, MT, Hung, WC, Chen, FY, Huang, HW (2005) Many-body effect of antimicrobial peptides: on the correlation between lipid's spontaneous curvature and pore formation. *Biophys J* **89**(6)**:** 4006-4016.

Lemeshko, VV (2010) Potential-dependent membrane permeabilization and mitochondrial aggregation caused by anticancer polyarginine-KLA peptides. *Arch Biochem Biophys* **493**(2)**:** 213-220.

Lenardo, MJ, Baltimore, D (1989) NF-kappa B: a pleiotropic mediator of inducible and tissue-specific gene control. *Cell* **58**(2)**:** 227-229.

Letoha, T, Gaal, S, Somlai, C, Czajlik, A, Perczel, A, Penke, B (2003) Membrane translocation of penetratin and its derivatives in different cell lines. *J Mol Recognit* **16**(5)**:** 272-279.

Li, R, Boehm, AL, Miranda, MB, Shangary, S, Grandis, JR, Johnson, DE (2007) Targeting antiapoptotic Bcl-2 family members with cell-permeable BH3 peptides induces apoptosis signaling and death in head and neck squamous cell carcinoma cells. *Neoplasia* **9**(10)**:** 801-811.

Lindberg, M, Jarvet, J, Langel, U, Graslund, A (2001) Secondary structure and position of the cell-penetrating peptide transportan in SDS micelles as determined by NMR. *Biochemistry* **40**(10)**:** 3141-3149.

Lindgren, M, Hallbrink, M, Prochiantz, A, Langel, U (2000) Cell-penetrating peptides. *Trends Pharmacol Sci* **21**(3)**:** 99-103.

Lindsay, MA (2002) Peptide-mediated cell delivery: application in protein target validation. *Curr Opin Pharmacol* **2**(5)**:** 587-594.

Liu, AH, Cao, YN, Liu, HT, Zhang, WW, Liu, Y, Shi, TW, Jia, GL, Wang, XM (2008) DIDS attenuates staurosporine-induced cardiomyocyte apoptosis by PI3K/Akt signaling pathway: activation of eNOS/NO and inhibition of Bax translocation. *Cell Physiol Biochem* **22**(1-4)**:** 177-186.

Lundberg, P, El-Andaloussi, S, Sutlu, T, Johansson, H, Langel, U (2007) Delivery of short interfering RNA using endosomolytic cell-penetrating peptides. *FASEB J* **21**(11)**:** 2664-2671.

Lutz, RJ (2000) Role of the BH3 (Bcl-2 homology 3) domain in the regulation of apoptosis and Bcl-2-related proteins. *Biochem Soc Trans* **28**(2)**:** 51-56.

Magzoub, M, Eriksson, LE, Graslund, A (2003) Comparison of the interaction, positioning, structure induction and membrane perturbation of cell-penetrating peptides and non-translocating variants with phospholipid vesicles. *Biophys Chem* **103**(3)**:** 271-288.

Maiolo, JR, Ferrer, M, Ottinger, EA (2005) Effects of cargo molecules on the cellular uptake of arginine-rich cell-penetrating peptides. *Biochim Biophys Acta* **1712**(2)**:** 161-172.

Mano, M, Teodosio, C, Paiva, A, Simoes, S, Pedroso de Lima, MC (2005) On the mechanisms of the internalization of S4(13)-PV cell-penetrating peptide. *Biochem J* **390**(Pt 2)**:** 603-612.

Matsuzaki, K, Yoneyama, S, Murase, O, Miyajima, K (1996) Transbilayer transport of ions and lipids coupled with mastoparan X translocation. *Biochemistry* **35**(25)**:** 8450-8456.

Melikov, K, Chernomordik, LV (2005) Arginine-rich cell penetrating peptides: from endosomal uptake to nuclear delivery. *Cell Mol Life Sci* **62**(23)**:** 2739-2749.

Mor, A, Amiche, M, Nicolas, P (1994) Structure, synthesis, and activity of dermaseptin b, a novel vertebrate defensive peptide from frog skin: relationship with adenoregulin. *Biochemistry* **33**(21)**:** 6642-6650.

Morris, MC, Chaloin, L, Mery, J, Heitz, F, Divita, G (1999) A novel potent strategy for gene delivery using a single peptide vector as a carrier. *Nucleic Acids Res* **27**(17)**:** 3510-3517.

Morris, MC, Depollier, J, Mery, J, Heitz, F, Divita, G (2001) A peptide carrier for the delivery of biologically active proteins into mammalian cells. *Nat Biotechnol* **19**(12)**:** 1173-1176.

Morris, MC, Deshayes, S, Heitz, F, Divita, G (2008) Cell-penetrating peptides: from molecular mechanisms to therapeutics. *Biol Cell* **100**(4)**:** 201-217.

Morris, MC, Vidal, P, Chaloin, L, Heitz, F, Divita, G (1997) A new peptide vector for efficient delivery of oligonucleotides into mammalian cells. *Nucleic Acids Res* **25**(14)**:** 2730-2736.

Moulton, HM, Nelson, MH, Hatlevig, SA, Reddy, MT, Iversen, PL (2004) Cellular uptake of antisense morpholino oligomers conjugated to arginine-rich peptides. *Bioconjug Chem* **15**(2)**:** 290-299.

Mueller, J, Kretzschmar, I, Volkmer, R, Boisguerin, P (2008) Comparison of cellular uptake using 22 CPPs in 4 different cell lines. *Bioconjug Chem* **19**(12)**:** 2363-2374.

Mueller, J, Triebus, J, Kretzschmar, I, Volkmer, R, Boisguerin, P (2011) The agony of choice: how to find a suitable CPP for cargo delivery. *J Pept Sci* **in press**.

Murphy, MP, Smith, RA (2007) Targeting antioxidants to mitochondria by conjugation to lipophilic cations. *Annu Rev Pharmacol Toxicol* **47:** 629-656.

Murray, KD, Etheridge, CJ, Shah, SI, Matthews, DA, Russell, W, Gurling, HM, Miller, AD (2001) Enhanced cationic liposome-mediated transfection using the DNA-binding peptide mu (mu) from the adenovirus core. *Gene Ther* **8**(6)**:** 453-460.

Murriel, CL, Dowdy, SF (2006) Influence of protein transduction domains on intracellular delivery of macromolecules. *Expert Opin Drug Deliv* **3**(6)**:** 739-746.

Nagahara, H, Vocero-Akbani, AM, Snyder, EL, Ho, A, Latham, DG, Lissy, NA, Becker-Hapak, M, Ezhevsky, SA, Dowdy, SF (1998) Transduction of full-length TAT fusion proteins into mammalian cells: TAT-p27Kip1 induces cell migration. *Nat Med* **4**(12)**:** 1449-1452.

Oehlke, J, Krause, E, Wiesner, B, Beyermann, M, Bienert, M (1997) Extensive cellular uptake into endothelial cells of an amphipathic beta-sheet forming peptide. *FEBS Lett* **415**(2)**:** 196-199.

Oehlke, J, Krause, E, Wiesner, B, Beyermann, M, Bienert, M (1996) Nonendocytic, amphipathicity dependent cellular uptake of helical model peptides. *Protein and Peptide Letters* **3**(6)**:** 393-398.

Oehlke, J, Scheller, A, Wiesner, B, Krause, E, Beyermann, M, Klauschenz, E, Melzig, M, Bienert, M (1998) Cellular uptake of an alpha-helical amphipathic model peptide with the potential to deliver polar compounds into the cell interior non-endocytically. *Biochim Biophys Acta* **1414**(1-2)**:** 127-139.

Olson, ES, Aguilera, TA, Jiang, T, Ellies, LG, Nguyen, QT, Wong, EH, Gross, LA, Tsien, RY (2009) In vivo characterization of activatable cell penetrating peptides for targeting protease activity in cancer. *Integr Biol (Camb)* **1**(5-6)**:** 382-393.

Pittet, MJ, Swirski, FK, Reynolds, F, Josephson, L, Weissleder, R (2006) Labeling of immune cells for in vivo imaging using magnetofluorescent nanoparticles. *Nat Protoc* **1**(1)**:** 73-79.

Pooga, M, Hallbrink, M, Zorko, M, Langel, U (1998a) Cell penetration by transportan. *Faseb J* **12**(1)**:** 67-77.

Pooga, M, Kut, C, Kihlmark, M, Hallbrink, M, Fernaeus, S, Raid, R, Land, T, Hallberg, E, Bartfai, T, Langel, U (2001) Cellular translocation of proteins by transportan. *FASEB J* **15**(8)**:** 1451-1453.

Pooga, M, Soomets, U, Hallbrink, M, Valkna, A, Saar, K, Rezaei, K, Kahl, U, Hao, JX, Xu, XJ, Wiesenfeld-Hallin, Z, Hokfelt, T, Bartfai, T, Langel, U (1998b) Cell penetrating PNA constructs regulate galanin receptor levels and modify pain transmission in vivo. *Nat Biotechnol* **16**(9)**:** 857-861.

Poon, GM, Gariepy, J (2007) Cell-surface proteoglycans as molecular portals for cationic peptide and polymer entry into cells. *Biochem Soc Trans* **35**(Pt 4)**:** 788-793.

Pouny, Y, Rapaport, D, Mor, A, Nicolas, P, Shai, Y (1992) Interaction of antimicrobial dermaseptin and its fluorescently labeled analogues with phospholipid membranes. *Biochemistry* **31**(49)**:** 12416-12423.

Pujals, S, Giralt, E (2008) Proline-rich, amphipathic cell-penetrating peptides. *Adv Drug Deliv Rev* **60**(4-5)**:** 473-484.

Qian, YQ, Billeter, M, Otting, G, Muller, M, Gehring, WJ, Wuthrich, K (1989) The structure of the Antennapedia homeodomain determined by NMR spectroscopy in solution: comparison with prokaryotic repressors. *Cell* **59**(3)**:** 573-580.

Ragin, AD, Morgan, RA, Chmielewski, J (2002) Cellular import mediated by nuclear localization signal Peptide sequences. *Chem Biol* **9**(8)**:** 943-948.

Raucher, D, Moktan, S, Massodi, I, Bidwell, GL, 3rd (2009) Therapeutic peptides for cancer therapy. Part II - cell cycle inhibitory peptides and apoptosis-inducing peptides. *Expert Opin Drug Deliv* **6**(10)**:** 1049-1064.

Rawat, A, Vaidya, B, Khatri, K, Goyal, AK, Gupta, PN, Mahor, S, Paliwal, R, Rai, S, Vyas, SP (2007) Targeted intracellular delivery of therapeutics: an overview. *Pharmazie* **62**(9)**:** 643-658.

Richard, JP, Melikov, K, Brooks, H, Prevot, P, Lebleu, B, Chernomordik, LV (2005) Cellular uptake of unconjugated TAT peptide involves clathrin-dependent endocytosis and heparan sulfate receptors. *J Biol Chem* **280**(15)**:** 15300-15306.

Richard, JP, Melikov, K, Vives, E, Ramos, C, Verbeure, B, Gait, MJ, Chernomordik, LV, Lebleu, B (2003) Cell-penetrating peptides. A reevaluation of the mechanism of cellular uptake. *J Biol Chem* **278**(1)**:** 585-590.

Rols, MP (2006) Electropermeabilization, a physical method for the delivery of therapeutic molecules into cells. *Biochim Biophys Acta* **1758**(3)**:** 423-428.

Ross, MF, Filipovska, A, Smith, RA, Gait, MJ, Murphy, MP (2004) Cell-penetrating peptides do not cross mitochondrial membranes even when conjugated to a lipophilic cation: evidence against direct passage through phospholipid bilayers. *Biochem J* **383**(Pt. 3)**:** 457-468.

Rothbard, JB, Garlington, S, Lin, Q, Kirschberg, T, Kreider, E, McGrane, PL, Wender, PA, Khavari, PA (2000) Conjugation of arginine oligomers to cyclosporin A facilitates topical delivery and inhibition of inflammation. *Nat Med* **6**(11)**:** 1253-1257.

Rousselle, C, Clair, P, Lefauconnier, JM, Kaczorek, M, Scherrmann, JM, Temsamani, J (2000) New advances in the transport of doxorubicin through the blood-brain barrier by a peptide vector-mediated strategy. *Mol Pharmacol* **57**(4)**:** 679-686.

Ruben, S, Perkins, A, Purcell, R, Joung, K, Sia, R, Burghoff, R, Haseltine, WA, Rosen, CA (1989) Structural and functional characterization of human immunodeficiency virus tat protein. *J Virol* **63**(1)**:** 1-8.

Sadler, K, Eom, KD, Yang, JL, Dimitrova, Y, Tam, JP (2002) Translocating proline-rich peptides from the antimicrobial peptide bactenecin 7. *Biochemistry* **41**(48)**:** 14150-14157.

Said Hassane, F, Saleh, AF, Abes, R, Gait, MJ, Lebleu, B (2009) Cell penetrating peptides: overview and applications to the delivery of oligonucleotides. *Cell Mol Life Sci* **67**(5)**:** 715-726.

Saphire, AC, Guan, T, Schirmer, EC, Nemerow, GR, Gerace, L (2000) Nuclear import of adenovirus DNA in vitro involves the nuclear protein import pathway and hsc70. *J Biol Chem* **275**(6)**:** 4298-4304.

Sarko, D, Beijer, B, Garcia Boy, R, Nothelfer, EM, Leotta, K, Eisenhut, M, Altmann, A, Haberkorn, U, Mier, W (2010) The pharmacokinetics of cell-penetrating peptides. *Mol Pharm* **7**(6)**:** 2224-2231.

Sawant, R, Torchilin, V (2009) Intracellular transduction using cell-penetrating peptides. *Mol Biosyst* **6**(4)**:** 628-640.

Schulz, A, Adermann, K., Eulitz, M., Feller, S. M., and, Kardinal, C (2000) Preparation of disulfide-bonded polypeptide
heterodimers by titration of thio-activated peptides with
thiol-containing peptides. *Tetrahedron* **56**(24)**:** 3889-3891.

Schwarze, SR, Ho, A, Vocero-Akbani, A, Dowdy, SF (1999) In vivo protein transduction: delivery of a biologically active protein into the mouse. *Science* **285**(5433)**:** 1569-1572.

Selivanova, G, Iotsova, V, Okan, I, Fritsche, M, Strom, M, Groner, B, Grafstrom, RC, Wiman, KG (1997) Restoration of the growth suppression function of mutant p53 by a synthetic peptide derived from the p53 C-terminal domain. *Nat Med* **3**(6)**:** 632-638.

Selivanova, G, Ryabchenko, L, Jansson, E, Iotsova, V, Wiman, KG (1999) Reactivation of mutant p53 through interaction of a C-terminal peptide with the core domain. *Mol Cell Biol* **19**(5)**:** 3395-3402.

Sethuraman, VA, Bae, YH (2007) TAT peptide-based micelle system for potential active targeting of anti-cancer agents to acidic solid tumors. *J Control Release* **118**(2)**:** 216-224.

Simeoni, F, Morris, MC, Heitz, F, Divita, G (2003) Insight into the mechanism of the peptide-based gene delivery system MPG: implications for delivery of siRNA into mammalian cells. *Nucleic Acids Res* **31**(11)**:** 2717-2724.

Simmons, CG, Pitts, AE, Mayfield, LD, Shay, JW, Corey, DR (1997) Synthesis and membrane permeability of pna-peptide conjugates. *Bioorganic and Medicinal Chemistry Letters* **7**(23)**:** 3001-3006.

Skerlavaj, B, Romeo, D, Gennaro, R (1990) Rapid membrane permeabilization and inhibition of vital functions of gram-negative bacteria by bactenecins. *Infect Immun* **58**(11)**:** 3724-3730.

Smith, G, Wolf, CR, Deeni, YY, Dawe, RS, Evans, AT, Comrie, MM, Ferguson, J, Ibbotson, SH (2003) Cutaneous expression of cytochrome P450 CYP2S1: individuality in regulation by therapeutic agents for psoriasis and other skin diseases. *Lancet* **361**(9366)**:** 1336-1343.

Snyder, EL, Meade, BR, Saenz, CC, Dowdy, SF (2004) Treatment of terminal peritoneal carcinomatosis by a transducible p53-activating peptide. *PLoS Biol* **2**(2)**:** E36.

Standley, SM, Toft, DJ, Cheng, H, Soukasene, S, Chen, J, Raja, SM, Band, V, Band, H, Cryns, VL, Stupp, SI (2010) Induction of cancer cell death by self-assembling nanostructures incorporating a cytotoxic peptide. *Cancer Res* **70**(8)**:** 3020-3026.

Steinberg, DA, Hurst, MA, Fujii, CA, Kung, AH, Ho, JF, Cheng, FC, Loury, DJ, Fiddes, JC (1997) Protegrin-1: a broad-spectrum, rapidly microbicidal peptide with in vivo activity. *Antimicrob Agents Chemother* **41**(8)**:** 1738-1742.

Suk, JS, Suh, J, Choy, K, Lai, SK, Fu, J, Hanes, J (2006) Gene delivery to differentiated neurotypic cells with RGD and HIV Tat peptide functionalized polymeric nanoparticles. *Biomaterials* **27**(29)**:** 5143-5150.

Torchilin, VP (2005) Recent advances with liposomes as pharmaceutical carriers. *Nat Rev Drug Discov* **4**(2)**:** 145-160.

Torchilin, VP (2007) Tat peptide-mediated intracellular delivery of pharmaceutical nanocarriers. *Adv Drug Deliv Rev* **60**(4-5)**:** 548-558.

Torchilin, VP, Levchenko, TS, Rammohan, R, Volodina, N, Papahadjopoulos-Sternberg, B, D'Souza, GG (2003) Cell transfection in vitro and in vivo with nontoxic TAT peptide-liposome-DNA complexes. *Proc Natl Acad Sci U S A* **100**(4)**:** 1972-1977.

Trabulo, S, Resina, S, Simoes, S, Lebleu, B, Pedroso de Lima, MC (2010) A non-covalent strategy combining cationic lipids and CPPs to enhance the delivery of splice correcting oligonucleotides. *J Control Release* **145**(2)**:** 149-158.

Trehin, R, Krauss, U, Muff, R, Meinecke, M, Beck-Sickinger, AG, Merkle, HP (2004) Cellular internalization of human calcitonin derived peptides in MDCK monolayers: a comparative study with Tat(47-57) and penetratin(43-58). *Pharm Res* **21**(1)**:** 33-42.

Tunnemann, G, Ter-Avetisyan, G, Martin, RM, Stockl, M, Herrmann, A, Cardoso, MC (2008) Live-cell analysis of cell penetration ability and toxicity of oligo-arginines. *J Pept Sci* **14**(4)**:** 469-476.

Valero, JG, Sancey, L, Kucharczak, J, Guillemin, Y, Gimenez, D, Prudent, J, Gillet, G, Salgado, J, Coll, JL, Aouacheria, A (2011) Bax-derived membrane-active peptides act as potent and direct inducers of apoptosis in cancer cells. *J Cell Sci* **124**(Pt 4)**:** 556-564.

Veldhoen, S, Laufer, SD, Trampe, A, Restle, T (2006) Cellular delivery of small interfering RNA by a non-covalently attached cell-penetrating peptide: quantitative analysis of uptake and biological effect. *Nucleic Acids Res* **34**(22)**:** 6561-6573.

Vidal, P, Chaloin, L, Heitz, A, Van Mau, N, Mery, J, Divita, G, Heitz, F (1998) Interactions of primary amphipathic vector peptides with membranes. Conformational consequences and influence on cellular localization. *J Membr Biol* **162**(3)**:** 259-264.

Vives, E, Brodin, P, Lebleu, B (1997) A truncated HIV-1 Tat protein basic domain rapidly translocates through the plasma membrane and accumulates in the cell nucleus. *J Biol Chem* **272**(25)**:** 16010-16017.

Vives, E, Schmidt, J, Pelegrin, A (2008) Cell-penetrating and cell-targeting peptides in drug delivery. *Biochim Biophys Acta* **1786**(2)**:** 126-138.

Vlieghe, P, Lisowski, V, Martinez, J, Khrestchatisky, M (2009) Synthetic therapeutic peptides: science and market. *Drug Discov Today* **15**(1-2)**:** 40-56.

Vouilleme, L, Cushing, PR, Volkmer, R, Madden, DR, Boisguerin, P (2010) Engineering peptide inhibitors to overcome PDZ binding promiscuity. *Angew Chem Int Ed Engl* **49**(51)**:** 9912-9916.

Wadia, JS, Stan, RV, Dowdy, SF (2004) Transducible TAT-HA fusogenic peptide enhances escape of TAT-fusion proteins after lipid raft macropinocytosis. *Nat Med* **10**(3)**:** 310-315.

Wagner, E, Plank, C, Zatloukal, K, Cotten, M, Birnstiel, ML (1992) Influenza virus hemagglutinin HA-2 N-terminal fusogenic peptides augment gene transfer by transferrin-polylysine-DNA complexes: toward a synthetic virus-like gene-transfer vehicle. *Proc Natl Acad Sci U S A* **89**(17)**:** 7934-7938.

Walev, I, Bhakdi, SC, Hofmann, F, Djonder, N, Valeva, A, Aktories, K, Bhakdi, S (2001) Delivery of proteins into living cells by reversible membrane permeabilization with streptolysin-O. *Proc Natl Acad Sci U S A* **98**(6)**:** 3185-3190.

Walther, C, Ott, I, Gust, R, Neundorf, I (2009) Specific labeling with potent radiolabels alters the uptake of cell-penetrating peptides. *Biopolymers* **92**(5)**:** 445-451.

Wang, Q, Yin, H, Camelliti, P, Betts, C, Moulton, H, Lee, H, Saleh, AF, Gait, MJ, Wood, MJ (2010) In vitro evaluation of novel antisense oligonucleotides is predictive of in vivo exon skipping activity for Duchenne muscular dystrophy. *J Gene Med* **12**(4)**:** 354-364.

Wang, R, Wang, X, Li, B, Lin, F, Dong, K, Gao, P, Zhang, HZ (2009) Tumor-specific adenovirus-mediated PUMA gene transfer using the survivin promoter enhances radiosensitivity of breast cancer cells in vitro and in vivo. *Breast Cancer Res Treat* **117**(1)**:** 45-54.

Watkins, CL, Brennan, P, Fegan, C, Takayama, K, Nakase, I, Futaki, S, Jones, AT (2009) Cellular uptake, distribution and cytotoxicity of the hydrophobic cell penetrating peptide sequence PFVYLI linked to the proapoptotic domain peptide PAD. *J Control Release* **140**(3)**:** 237-244.

Weller, K, Lauber, S, Lerch, M, Renaud, A, Merkle, HP, Zerbe, O (2005) Biophysical and biological studies of end-group-modified derivatives of Pep-1. *Biochemistry* **44**(48)**:** 15799-15811.

Wells, DJ (2004) Gene therapy progress and prospects: electroporation and other physical methods. *Gene Ther* **11**(18)**:** 1363-1369.

Wender, PA, Mitchell, DJ, Pattabiraman, K, Pelkey, ET, Steinman, L, Rothbard, JB (2000) The design, synthesis, and evaluation of molecules that enable or enhance cellular uptake: peptoid molecular transporters. *Proc Natl Acad Sci U S A* **97**(24)**:** 13003-13008.

Wyber, JA, Andrews, J, D'Emanuele, A (1997) The use of sonication for the efficient delivery of plasmid DNA into cells. *Pharm Res* **14**(6)**:** 750-756.

Yamaguchi, K, Inoue, M, Goshima, N (2011) Efficient protein transduction method using cationic peptides and lipids. *J Biomed Biotechnol***:** 872065.

Yandek, LE, Pokorny, A, Almeida, PF (2008) Small changes in the primary structure of transportan 10 alter the thermodynamics and kinetics of its interaction with phospholipid vesicles. *Biochemistry* **47**(9)**:** 3051-3060.

Yang, HL, Chen, CS, Chang, WH, Lu, FJ, Lai, YC, Chen, CC, Hseu, TH, Kuo, CT, Hseu, YC (2006) Growth inhibition and induction of apoptosis in MCF-7 breast cancer cells by Antrodia camphorata. *Cancer Lett* **231**(2)**:** 215-227.

Yang, SW, Lee, SM, Choi, EY, Lee, KH, Kim, SH, Shin, MJ, Han, YS, Kang, SM, Chung, JH (2011) Matrix metalloproteinase-1 induces cleavage of exogenous alphaB-crystallin transduced by a cell-penetrating peptide. *J Cell Biochem* **112**(9)**:** 2454-2462.

Youngblood, DS, Hatlevig, SA, Hassinger, JN, Iversen, PL, Moulton, HM (2007) Stability of cell-penetrating peptide-morpholino oligomer conjugates in human serum and in cells. *Bioconjug Chem* **18**(1)**:** 50-60.

Zeira, E, Manevitch, A, Khatchatouriants, A, Pappo, O, Hyam, E, Darash-Yahana, M, Tavor, E, Honigman, A, Lewis, A, Galun, E (2003) Femtosecond infrared laser-an efficient and safe in vivo gene delivery system for prolonged expression. *Mol Ther* **8**(2)**:** 342-350.

Zhang, C, Tang, N, Liu, X, Liang, W, Xu, W, Torchilin, VP (2006) siRNA-containing liposomes modified with polyarginine effectively silence the targeted gene. *J Control Release* **112**(2)**:** 229-239.

Zhang, L, Torgerson, TR, Liu, XY, Timmons, S, Colosia, AD, Hawiger, J, Tam, JP (1998) Preparation of functionally active cell-permeable peptides by single-step ligation of two peptide modules. *Proc Natl Acad Sci U S A* **95**(16)**:** 9184-9189.

Ziegler, A (2008) Thermodynamic studies and binding mechanisms of cell-penetrating peptides with lipids and glycosaminoglycans. *Adv Drug Deliv Rev* **60**(4-5)**:** 580-597.

Zorko, M, Langel, U (2005) Cell-penetrating peptides: mechanism and kinetics of cargo delivery. *Adv Drug Deliv Rev* **57**(4)**:** 529-545.

7. ANNEX

Table 5. Viability Test of 22 CPPs in Cos-7, HEK293, HeLa and MDCK Cells.

	Cos-7				HEK293				HeLa				MDCK			
CPPs	**1 µM**	**10 µM**	**25 µM**	**50 µM**	**1 µM**	**10 µM**	**25 µM**	**50 µM**	**1 µM**	**10 µM**	**25 µM**	**50 µM**	**1 µM**	**10 µM**	**25 µM**	**50 µM**
pVEC-scrambled	79 ± 24	80 ± 8	90 ± 9	**37 ± 8**	72 ± 11	78 ± 26	74 ± 19	82 ± 29	103 ± 18	99 ± 15	102 ± 22	76 ± 15	103 ± 7	95 ± 22	94 ± 10	93 ± 10
Polyomavirus Vp1	106 ± 15	81 ± 9	106 ± 24	89 ± 1	108 ± 26	90 ± 15	97 ± 17	88 ± 16	102 ± 22	88 ± 3	90 ± 4	91 ± 20	95 ± 11	106 ±13	122 ±24	98 ± 11
poly-P	104 ± 03	106 ± 15	94 ± 21	**47 ± 10**	87 ± 19	96 ± 23	82 ± 10	80 ± 9	92 ± 18	94 ± 21	92 ± 10	107 ± 20	98 ± 7	97 ± 10	99 ± 8	106 ± 7
NF-kB	102 ± 05	98 ± 10	67 ± 27	**54 ± 25**	93 ± 8	111 ± 0	89 ± 3	70 ± 9	103 ± 9	90 ± 12	90 ± 18	95 ± 15	104 ± 12	98 ± 20	102 ± 22	101 ± 11
SV40	105 ± 17	101 ± 29	103 ± 23	87 ± 14	106 ± 14	88 ± 9	104 ± 20	109 ± 9	87 ± 12	86 ± 6	89 ± 1	86 ± 18	101 ± 2	86 ± 8	102 ± 21	100 ± 6
HATF3	71 ± 01	83 ± 22	**49 ± 16**	**39 ± 20**	80 ± 16	76 ± 5	88 ± 17	81 ± 9	87 ± 15	100 ± 28	101 ± 10	105 ± 27	104 ± 20	102 ± 7	114 ± 15	120 ± 25
hCT(9-32)	118 ± 21	110 ± 4	111 ± 4	92 ± 10	89 ± 24	89 ± 2	78 ± 12	83 ± 25	95 ± 17	108 ± 10	100 ± 10	96 ± 10	96 ± 1	93 ± 8	102 ± 1	108 ± 13
SynB1	108 ± 11	86 ± 11	96 ± 21	104 ± 4	109 ± 22	81 ± 17	90 ± 15	80 ± 3	105 ± 16	105 ± 21	87 ± 25	96 ± 25	100 ± 8	102 ± 11	99 ± 8	103 ± 19
DPV6	97 ± 07	83 ± 9	88 ± 10	93 ± 14	104 ± 20	115 ± 6	134 ± 7	114 ± 1	94 ± 8	92 ± 20	106 ± 16	102 ± 9	112 ± 13	84 ± 10	106 ± 18	117 ± 12
Tat	105 ± 12	99 ± 6	115 ± 10	93 ± 2	82 ± 15	83 ± 15	90 ± 13	94 ± 8	100 ± 20	80 ± 16	**63 ± 22**	**50 ± 10**	100 ± 0	100 ± 5	106 ± 6	100 ± 14
Pep-1	98 ± 01	97 ± 15	93 ± 19	**78 ± 11**	87 ± 12	99 ± 1	81 ± 9	91 ± 18	96 ± 15	98 ± 17	104 ± 18	109 ± 27	106 ± 20	104 ± 19	105 ± 10	100 ± 14
Bac1-15	116 ± 17	91 ± 14	105 ± 2	100 ± 12	88 ± 21	104 ± 9	90 ± 13	73 ± 21	95 ± 15	99 ± 11	81 ± 27	88 ± 23	86 ± 9	89 ± 13	89 ± 11	93 ± 16
R7	91 ± 12	97 ± 4	93 ± 8	94 ± 7	89 ± 14	84 ± 0	80 ± 9	**69 ± 11**	97 ± 14	87 ± 17	93 ± 26	97 ± 24	105 ± 7	101 ± 22	103 ± 12	110 ± 16
pVEC	98 ± 26	91 ± 5	78 ± 9	**52 ± 12**	79 ± 14	71 ± 18	**68 ± 12**	**52 ± 15**	114 ± 26	112 ± 17	116 ± 30	94 ± 24	101 ± 9	102 ± 4	102 ± 4	97 ± 2
Rev	114 ± 10	101 ± 11	98 ± 3	98 ± 20	94 ± 25	93 ± 26	78 ± 28	**26 ± 13**	85 ± 7	94 ± 16	74 ± 15	**34 ± 0**	94 ± 1	100 ± 10	76 ± 12	**51 ± 11**
$S4_{13}PV$	97 ± 23	89 ± 17	**63 ± 21**	**12 ± 27**	94 ± 9	95 ± 6	**50 ± 26**	**11 ± 17**	105 ± 12	**64 ± 24**	**0**	**0**	106 ± 4	**33 ± 16**	**11 ± 1**	**5 ± 2**
R9	91 ± 19	102 ± 8	108 ± 13	88 ± 17	99 ± 18	89 ± 10	72 ± 22	78 ± 9	92 ± 14	111 ± 1	98 ± 19	73 ± 23	104 ± 15	91 ± 6	81 ± 12	**61 ± 25**
Integrin	97 ± 4	119 ± 16	117 ± 12	106 ± 3	76 ± 7	75 ± 1	95 ± 11	105 ± 15	96 ± 1	113 ± 22	98 ± 9	118 ± 25	105 ± 5	110 ± 4	101 ± 0	99 ± 4
MPG	108 ± 15	101 ± 2	116 ± 5	132 ± 5	97 ± 14	100 ± 17	95 ± 26	118 ± 16	99 ± 17	96 ± 13	111 ± 26	103 ± 15	103 ± 5	102 ± 6	83 ± 9	90 ± 12
Penetratin	114 ± 10	99 ± 7	110 ± 23	114 ± 11	113 ± 17	141 ± 11	105 ± 25	101 ± 17	94 ± 16	95 ± 22	76 ± 3	72 ± 26	98 ± 5	89 ± 10	112 ± 9	120 ± 19
MAP	99 ± 25	106 ± 11	**55 ± 23**	**6 ± 7**	107 ± 17	110 ± 7	113 ± 3	83 ± 16	92 ± 26	99 ± 19	**34 ± 10**	**6 ± 10**	102 ± 1	97 ± 14	**66 ± 10**	**46 ± 14**
Transportan	104 ± 12	86 ± 15	**20 ± 25**	**0**	90 ± 5	97 ± 7	**50 ± 29**	**14 ± 11**	108 ± 21	88 ± 19	**0**	**0**	102 ± 60	116 ± 13	**14 ± 1**	**7 ± 2**

Footnote: Measurement of the viability using the CCK-8 solution (Fluka). 100 % shows no influence of the CPPs. Four different CPP concentrations were used (1, 10, 25 and 50 µM) for each cell line. The data represent the mean of 3-5 independent experiments ± the standard deviation; bold data indicated a viability ≤ 70 %.

Table 6. Effects of Endocytosis Modulators on Cellular Uptake - Raw Data.

Cell lines	Conditions	Control	pVEC-scrambled	DPV6	Tat	R7	Rev	$S4_{13}PV$	R9	Integrin	MPG	Penetratin	MAP	Transportan
Cos-7	37°C	20 ± 5	60 ± 10	34 ± 6	64 ± 11	129 ± 10	95 ± 20	481 ± 132	145 ± 42	51 ± 1	1,411 ± 116	472 ± 114	1,600 ± 393	7,349 ± 18
	4°C	18 ± 5	123 ± 22	123 ± 18	197 ± 23	134 ± 118	301 ± 47	217 ± 23	374 ± 66	58 ± 12	614 ± 113	534 ± 138	4,127 ± 479	24,813 ± 115
	Chlorpromazine	16 ± 3	77 ± 4	52 ± 20	46 ± 11	49 ± 4	279 ± 47	344 ± 99	144 ± 20	51 ± 23	738 ± 118	975 ± 138	875 ± 98	9,533 ± 592
	Chloroquine	20 ± 3	226 ± 43	67 ± 10	190 ± 12	164 ± 24	529 ± 122	320 ± 32	800 ± 212	47 ± 13	1,435 ± 232	718 ± 200	4,309 ± 920	10,109 ± 2,236
	Nystatin	16 ± 3	119 ± 16	20 ± 2	23 ± 2	23 ± 5	49 ± 4	479 ± 27	128 ± 38	38 ± 8	507 ± 138	357 ± 27	1,668 ± 61	7,388 ± 1,061
	Heparin	20 ± 4	144 ± 23	226 ± 19	255 ± 18	344 ± 31	477 ± 17	208 ± 58	325 ± 28	29 ± 2	377 ± 43	414 ± 43	1,677 ± 119	19,844 ± 5,408
	Wortmannin	17 ± 3	41 ± 12	31 ± 9	29 ± 8	30 ± 8	96 ± 18	157 ± 18	99 ± 21	86 ± 8	236 ± 14	386 ± 114	569 ± 57	27,805 ± 4,067
HEK293	37°C	23 ± 6	42 ± 1	95 ± 21	125 ± 4	189 ± 3	645 ± 145	689 ± 179	713 ± 190	1,638 ± 360	928 ± 171	1,269 ± 137	2,795 ± 677	6,197 ± 799
	4°C	19 ± 5	97 ± 26	36 ± 7	34 ± 1	68 ± 7	211 ± 24	135 ± 24	214 ± 44	205 ± 45	1,240 ± 195	798 ± 121	18,761 ± 3,000	18,862 ± 2,919
	Chlorpromazine	18 ± 3	204 ± 39	62 ± 12	30 ± 9	36 ± 3	378 ± 99	519 ± 44	477 ± 109	79 ± 14	588 ± 27	1,380 ± 331	1,422 ± 259	8,412 ± 201
	Chloroquine	21 ± 4	136 ± 9	64 ± 15	60 ± 16	145 ± 21	438 ± 75	792 ± 121	461 ± 7	1,908 ± 153	783 ± 25	1,084 ± 274	2,210 ± 598	17,034 ± 1,732
	Nystatin	19 ± 4	61 ± 6	76 ± 15	47 ± 8	39 ± 5	108 ± 17	984 ± 68	165 ± 8	70 ± 16	571 ± 129	1,042 ± 69	1,949 ± 356	2,589 ± 542
	Heparin	20 ± 5	250 ± 16	128 ± 5	150 ± 25	589 ± 154	761 ± 83	362 ± 27	637 ± 76	779 ± 29	2,386 ± 479	324 ± 56	4,661 ± 968	11,838 ± 3,794
	Wortmannin	11 ± 3	40 ± 11	59 ± 8	24 ± 5	39 ± 8	117 ± 23	348 ± 4	112 ± 22	930 ± 183	519 ± 102	492 ± 45	552 ± 22	25,970 ± 3,059
HeLa	37°C	21 ± 4	53 ± 9	81 ± 9	59 ± 11	48 ± 7	715 ± 217	1,052 ± 172	1,409 ± 322	595 ± 35	1,257 ± 160	3,335 ± 831	4,199 ± 361	10,529 ± 1,047
	4°C	21 ± 5	63 ± 10	107 ± 24	90 ± 3	104 ± 13	267 ± 56	808 ± 198	839 ± 159	173 ± 40	1,068 ± 209	1,374 ± 326	4,798 ± 304	19,985 ± 4,514
	Chlorpromazine	22 ± 4	66 ± 15	32 ± 5	100 ± 15	92 ± 2	113 ± 12	1,017 ± 207	1,774 ± 296	51 ± 23	1,517 ± 361	1,178 ± 175	3,121 ± 216	7,709 ± 1,731
	Chloroquine	20 ± 6	154 ± 18	55 ± 9	117 ± 26	215 ± 63	697 ± 104	1,447 ± 305	2,011 ± 339	1,071 ± 313	1,209 ± 270	3,415 ± 51	1,388 ± 379	21,840 ± 4,276
	Nystatin	21 ± 6	127 ± 36	43 ± 5	102 ± 17	106 ± 26	502 ± 137	411 ± 98	578 ± 123	859 ± 94	1,396 ± 237	1,294 ± 141	5,534 ± 570	21,635 ± 2,816
	Heparin	19 ± 6	328 ± 85	262 ± 74	312 ± 95	405 ± 56	545 ± 115	1,134 ± 123	345 ± 56	61 ± 13	194 ± 18	1,734 ± 424	569 ± 106	14,634 ± 3,406
	Wortmannin	17 ± 3	46 ± 2	42 ± 12	27 ± 3	45 ± 4	135 ± 15	780 ± 99	224 ± 44	1,211 ± 221	749 ± 75	597 ± 179	1,084 ± 180	29,113 ± 1,025
MDCK	37°C	17 ± 5	61 ± 9	28 ± 4	28 ± 5	32 ± 8	65 ± 6	686 ± 110	66 ± 15	274 ± 39	435 ± 59	311 ± 22	839 ± 108	4,637 ± 78
	4°C	15 ± 3	55 ± 16	20 ± 3	25 ± 7	45 ± 3	57 ± 12	1,064 ± 153	68 ± 7	96 ± 27	574 ± 78	715 ± 72	245 ± 26	13,036 ± 2,744
	Chlorpromazine	19 ± 6	83 ± 7	47 ± 8	40 ± 8	49 ± 6	168 ± 45	650 ± 187	220 ± 62	156 ± 20	706 ± 57	556 ± 98	1,472 ± 436	19,713 ± 1,654
	Chloroquine	20 ± 4	51 ± 9	27 ± 3	30 ± 4	26 ± 7	114 ± 7	188 ± 53	81 ± 16	23 ± 7	285 ± 50	359 ± 78	1,430 ± 190	28,270 ± 3,237
	Nystatin	18 ± 2	46 ± 13	31 ± 6	26 ± 1	26 ± 4	58 ± 8	1,008 ± 179	63 ± 11	46 ± 6	199 ± 20	936 ± 135	6,618 ± 1,768	6,046 ± 688
	Heparin	20 ± 4	62 ± 17	27 ± 3	29 ± 3	53 ± 1	45 ± 13	46 ± 12	144 ± 38	84 ± 25	209 ± 61	549 ± 96	2,691 ± 798	22,499 ± 1,930
	Wortmannin	22 ± 3	33 ± 1	34 ± 1	31 ± 7	33 ± 8	49 ± 10	448 ± 65	69 ± 9	726 ± 194	534 ± 107	386 ± 72	1,106 ± 284	23,952 ± 4,476

Footnote: The cells were treated with the reagents at the given concentrations and later CPPs (10 µM) were added to the medium. The cells were incubated for another 30 min and subjected to quantification (for more details see 2.4 Endocytosis Inhibitor Test). The data represent the mean of 3-5 independent experiments ± the standard deviation.

Table 7. Viability Test of 22 CPPs in MCF-7, RAW264.7 and RAEC Cells.

	MCF-7				RAW 264.7				RAEC			
CPPs	**1 µM**	**10 µM**	**25 µM**	**50 µM**	**1 µM**	**10 µM**	**25 µM**	**50 µM**	**1 µM**	**10 µM**	**25 µM**	**50 µM**
pVEC-scrambled	84 ± 10	83 ± 10	88 ± 23	112 ± 12	98 ± 5	103 ± 11	100 ± 11	89 ± 6	95 ± 4	72 ± 18	**65 ± 19**	**65 ± 15**
Polyomavirus Vp1	107 ± 14	101 ± 5	89 ± 8	93 ± 19	94 ± 10	93 ± 10	92 ± 9	94 ± 13	89 ± 8	99 ± 12	106 ± 12	97 ± 4
poly-P	97 ± 15	101 ± 11	96 ± 21	102 ± 26	112 ± 15	101 ± 5	103 ± 8	102 ± 8	111 ± 15	107 ± 6	91 ± 8	89 ± 23
NF-kB	105 ± 14	97 ± 4	88 ± 12	91 ± 24	87 ± 10	95 ± 8	96 ± 8	95 ± 13	90 ± 5	70 ± 20	76 ± 19	83 ± 11
SV40	91 ± 22	96 ± 7	88 ± 10	89 ± 24	98 ± 16	96 ± 10	92 ± 10	94 ± 11	87 ± 18	**61 ± 6**	75 ± 11	79 ± 17
HATF3	95 ± 12	101 ± 6	106 ± 21	71 ± 22	102 ± 13	87 ± 15	**61 ± 9**	**52 ± 6**	83 ± 12	73 ± 12	73 ± 15	74 ± 13
hCT(9-32)	101 ± 10	98 ± 8	86 ± 17	84 ± 25	106 ± 12	105 ± 6	96 ± 6	96 ± 9	85 ± 16	73 ± 17	**69 ± 18**	**76 ± 12**
SynB1	105 ± 20	96 ± 8	110 ± 19	100 ± 27	100 ± 22	95 ± 20	86 ± 19	89 ± 17	98 ± 29	97 ± 20	105 ± 32	103 ± 9
DPV6	86 ± 3	99 ± 8	99 ± 10	127 ± 5	94 ± 4	87 ± 10	86 ± 14	89 ± 15	90 ± 15	110 ± 19	81 ± 24	**68 ± 1**
Tat	92 ± 17	105 ± 11	95 ± 17	86 ± 9	88 ± 7	89 ± 9	88 ± 14	88 ± 16	96 ± 15	103 ± 20	91 ± 11	**66 ± 15**
Pep-1	94 ± 23	103 ± 10	100 ± 20	113 ± 10	95 ± 13	94 ± 2	92 ± 7	98 ± 7	95 ± 12	103 ± 10	102 ± 15	97 ± 23
Bac1-15	86 ± 20	106 ± 16	109 ± 24	117 ± 5	97 ± 7	92 ± 7	87 ± 10	90 ± 12	90 ± 22	90 ± 7	89 ± 11	85 ± 19
R7	97 ± 11	104 ± 3	88 ± 21	84 ± 15	100 ± 8	95 ± 3	88 ± 10	**76 ± 1**	124 ± 15	134 ± 38	132 ± 33	125 ± 27
pVEC	97 ± 16	105 ± 8	102 ± 24	129 ± 13	101 ± 9	101 ± 9	98 ± 3	**60 ± 6**	85 ± 85	**65 ± 20**	76 ± 11	73 ± 13
Rev	100 ± 14	96 ± 8	86 ± 25	**35 ± 8**	98 ± 10	93 ± 4	81 ± 10	**62 ± 6**	89 ± 4	70 ± 16	**67 ± 20**	**71 ± 18**
$S4_{13}PV$	94 ± 17	**56 ± 16**	**0**	**0**	88 ± 7	72 ± 17	**46 ± 8**	**43 ± 10**	103 ± 19	90 ± 18	78 ± 11	**66 ± 5**
R9	123 ± 7	98 ± 4	105 ± 17	**69 ± 11**	99 ± 9	100 ± 2	92 ± 8	90 ± 12	92 ± 4	70 ± 12	**65 ± 13**	**74 ± 9**
Integrin	98 ± 13	104 ± 7	110 ± 3	124 ± 30	98 ± 6	94 ± 3	99 ± 3	95 ± 6	97 ± 6	78 ± 18	90 ± 7	92 ± 11
MPG	107 ± 18	104 ± 8	99 ± 15	109 ± 32	102 ± 10	103 ± 6	95 ± 13	74 ± 7	83 ± 17	76 ± 11	75 ± 13	79 ± 13
Penetratin	94 ± 13	103 ± 3	103 ± 29	112 ± 19	87 ± 9	82 ± 11	**59 ± 12**	**52 ± 6**	98 ± 9	106 ± 12	98 ± 16	102 ± 8
MAP	95 ± 14	94 ± 7	77 ± 21	**16 ± 4**	88 ± 9	76 ± 5	72 ± 17	**59 ± 9**	105 ± 8	117 ± 36	84 ± 16	**22 ± 4**
Transportan	97 ± 5	95 ± 2	90 ± 12	74 ± 16	88 ± 10	82 ± 13	75 ± 14	**64 ± 7**	86 ± 16	105 ± 27	73 ± 18	**51 ± 14**

Footnote: Measurement of the viability using the CCK-8 solution (Fluka). 100 % shows no influence of the CPPs. Four different CPP concentrations were used (1, 10, 25 and 50 µM) for each cell line. The data represent the mean of 3-5 independent experiments ± the standard deviation; bold data indicated a viability ≤ 70 %.

Table 8. Toxicity of the Carboxyamidated CPPs.

	Cos-7				HEK293			
CPPs	**1 µM**	**10 µM**	**25 µM**	**50 µM**	**1 µM**	**10 µM**	**25 µM**	**50 µM**
Penetratin	98 ± 22	95 ± 21	**62 ± 19**	**53 ± 11**	79 ± 11	79 ± 11	**67 ± 4**	**65 ± 17**
Tat	93 ± 16	87 ± 15	75 ± 18	78 ± 7	93 ± 20	102 ± 14	101 ± 14	107 ± 24
$S4_{13}PV$	92 ± 22	93 ± 22	73 ± 20	**23 ± 3**	84 ± 14	76 ± 14	**44 ± 3**	**35 ± 10**
R9	119 ± 18	99 ± 13	94 ± 18	96 ± 16	81 ± 7	98 ± 21	84 ± 21	**51 ± 12**
MPG	100 ± 24	94 ± 6	102 ± 18	92 ± 6	89 ± 5	77 ± 1	75 ± 5	**57 ± 4**
Integrin	89 ± 15	99 ± 6	100 ± 7	91 ± 0	87 ± 20	84 ± 19	73 ± 20	**57 ± 9**
	HeLa				**MDCK**			
CPPs	**1 µM**	**10 µM**	**25 µM**	**50 µM**	**1 µM**	**10 µM**	**25 µM**	**50 µM**
Penetratin	93 ± 14	86 ± 24	**42 ± 5**	**10 ± 2**	93 ± 4	89 ± 8	87 ± 10	87 ± 10
Tat	71 ± 4	79 ± 24	**61 ± 9**	**48 ± 13**	96 ± 6	93 ± 19	98 ± 3	87 ± 10
$S4_{13}PV$	80 ± 12	**39 ± 12**	**0 ± 0**	**0 ± 0**	95 ± 8	75 ± 13	**31 ± 12**	**0 ± 0**
R9	103 ± 5	76 ± 10	**52 ± 13**	**13 ± 3**	110 ± 12	100 ± 18	74 ± 21	**53 ± 7**
MPG	85 ± 3	82 ± 13	**49 ± 10**	**39 ± 7**	91 ± 18	89 ± 10	73 ± 20	**52 ± 10**
Integrin	101 ± 6	125 ± 24	116 ± 26	94 ± 5	97 ± 5	99 ± 5	94 ± 9	**66 ± 15**
	MCF-7				**RAW 264.7**			
CPPs	**1 µM**	**10 µM**	**25 µM**	**50 µM**	**1 µM**	**10 µM**	**25 µM**	**50 µM**
Penetratin	95 ± 19	96 ± 20	97 ± 24	**24 ± 2**	99 ± 5	79 ± 4	**39 ± 2**	**30 ± 1**
Tat	114 ± 12	123 ± 20	114 ± 12	88 ± 20	98 ± 4	93 ± 6	94 ± 2	85 ± 12
$S4_{13}PV$	131 ± 2	**65 ± 8**	**0 ± 0**	**0 ± 0**	92 ± 10	**37 ± 3**	**28 ± 1**	**29 ± 1**
R9	127 ± 19	90 ± 0	78 ± 9	**38 ± 10**	97 ± 4	88 ± 3	**51 ± 3**	**31 ± 2**
MPG	111 ± 20	106 ± 31	93 ± 26	76 ± 21	96 ± 5	90 ± 8	**58 ± 5**	**34 ± 2**
Integrin	108 ± 12	105 ± 11	98 ± 11	90 ± 14	97 ± 4	95 ± 5	96 ± 5	89 ± 4
	RAEC							
CPPs	**1 µM**	**10 µM**	**25 µM**	**50 µM**				
Penetratin	100 ± 2	96 ± 6	99 ± 6	100 ± 5				
Tat	99 ± 3	95 ± 6	96 ± 3	96 ± 5				
$S4_{13}PV$	94 ± 2	94 ± 2	73 ± 14	**0 ± 2**				
R9	90 ± 5	90 ± 8	91 ± 5	95 ± 7				
MPG	95 ± 4	92 ± 1	89 ± 4	89 ± 3				
Integrin	108 ± 10	106 ± 9	100 ± 12	103 ± 12				

Footnote: Measurement of the viability using the CCK-8 solution (Fluka). 100 % shows no influence of the CPPs. Four different CPP concentrations were used (1, 10, 25 and 50 µM) for each cell line. The data represent the mean of 3-5 independent experiments ± the standard deviation; bold data indicated a viability ≤ 70 %.

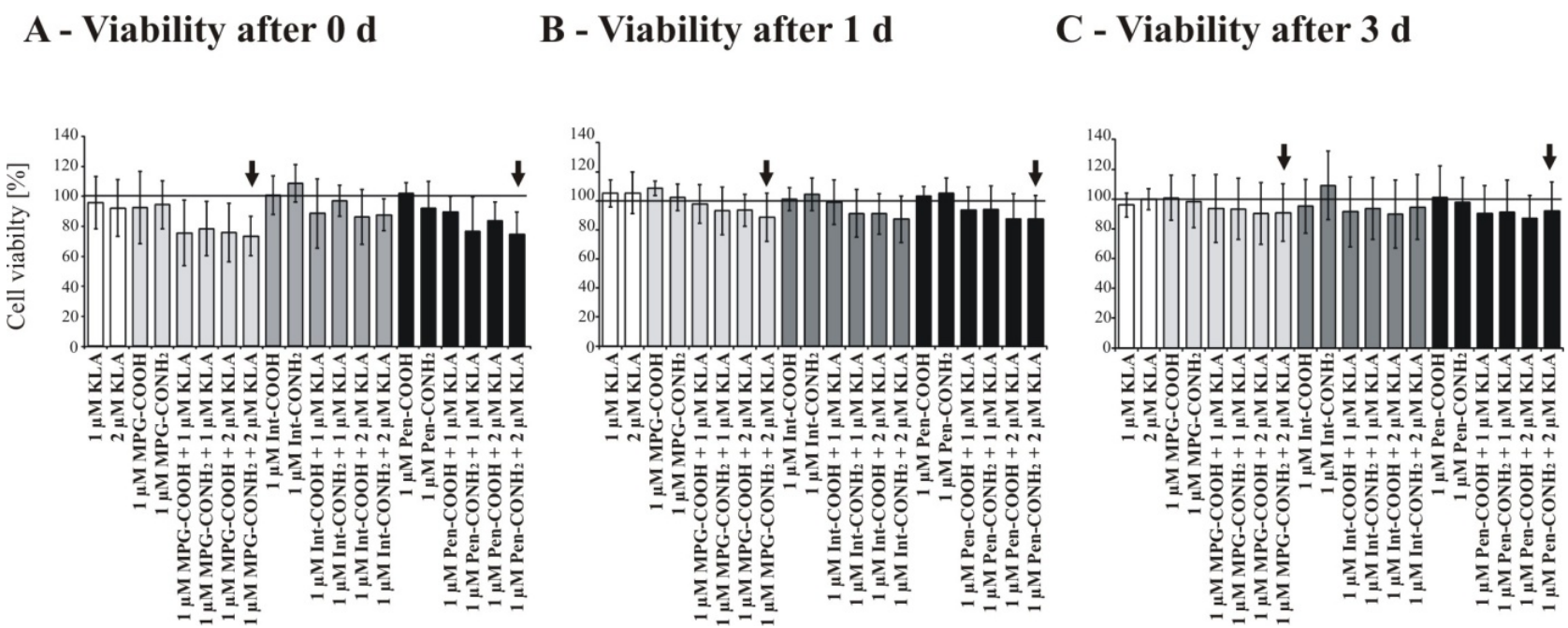

Figure 15. Viability after CPP:KLA in RAW 264.7 Cells Depending on the Incubation Duration.
CPP and KLA were simultaneously incubated for 1 h with RAW 264.7 cells and cell viability was detected using the MTT-test. 100 % cell viability corresponds to no toxic effect of the peptides. The cell viability was measured immediately after peptide incubation and removal of the peptides solution (0 days) (**A**), as well as 1 day (**B**) or 2 days (**C**) later. The highest pro-apoptotic effect of the KLA peptide is seen directly after the incubation and is probably a short-time effect or due to a fast growth of the remaining unaffected cells. Data shown are the means ± SEM (n=3).

8. ACKNOWLEDGEMENT

I gratefully thank Prof. Dr. Hans-Dieter Volk for his supervision of my thesis.

My special thanks goes to Dr. Rudolf Volkmer for giving me the opportunity to carry out my PhD thesis in the Molecular Libraries and Recognition Group at the Institute for Medical Immunology at the Charité in Berlin as well as for his kindness, discussion and support as well as the DFG for financial support.

My most heartfelt thanks belongs to Dr. Prisca Boisguérin for her excellent training, outstanding advice and her effort and positivity. She did not only become a good friend, but will always be a person one can learn from and look up to. Without her, this work would have never been accomplished.

Furthermore, I would like to thank Prof. Andreas Herrmann for his friendly assessment of this work, who also gave me the opportunity to use the confocal microscope in his laboratory. Dr. Thomas Korte introduced me to this technique and I am very grateful for his friendly and detailed approach.

My thanks also goes to Prof. Dr. Gerald Grütz for his welcoming assessment of this work.

I thank Ines Kretzschmar for the synthesis of the peptides as well as her kind introduction into the daily laboratory routine.

In particular, I want to thank Dr. Livia Otte for her help in protein expression techniques, which I particularly enjoyed, as well as Christiane Landgraf, Dr. Bernhard Ay, Marc Hovestädt, Dr. Zerrin Fidan, Dr. Carsten C. Mahrenholz, Oliver Korrt, Anja Heiduk, Annette Hayungs and Dr. Rolf-Dietrich Stigler for their discussion, support and laughter.

I am indebted to Prof. Dr. Martina Seifert for leaving me the primary RAEC cells.

I would also like to sincerely thank Prof. Dr. Bernard Lebleu for giving me the opportunity to work in his laboratory at the UMR 5235 CNR in Montpellier, use his equipment and discover new exciting methods as well as the great French life style.

Finally, I thank my fiancé Nick for his love, patience and encouragement as well as my parents for their support.

9. SCIENTIFIC CONTRIBUTIONS

Mueller, J, Triebus, J, Kretzschmar, I, Volkmer, R, Boisguerin, P (2011) The agony of choice: how to find a suitable CPP for cargo delivery. *J Pept Sci* **in press**.

Mueller, J, Kretzschmar, I, Volkmer, R, Boisguerin, P (2010) Non-covalent peptide delivery by CPPs. *Poster, 31st EPS-Satellite Symposium on Cell Penetrating Peptides*, Copenhagen, Denmark.

Mueller, J, Kretzschmar, I, Volkmer, R, Boisguerin, P (2010) Non-covalent strategy to deliver the pro-apoptotic KLA-peptide. *Poster, 12th Naples Workshop on Bioactive Peptides*, Naples, Italy.

Mueller, J, Kretzschmar, I, Volkmer, R, Boisguerin, P (2009) Analytical screening of the cellular CPP uptake. *Poster, PepVec 2009*, Montpellier, France.

Mueller, J, Kretzschmar, I, Volkmer, R, Boisguerin, P (2009) Comparing the Cellular Uptake of CPPs. *Poster, 9th German Peptide Symposium*, Göttingen, Germany.

Boisguerin P, **Mueller J**, Volkmer R (2008) Quantitative evaluation cellular uptake of 22 CPPs in 4 different cell lines. *J Pep Sci* 14(8), 5-5.

Mueller, J, Kretzschmar, I, Volkmer, R., Boisguerin, P (2008) Comparison of cellular uptake using 22 CPPs in 4 different cell lines. *Bioconjug Chem* 19(12) 2363-2374.

10. DECLARATION OF HONESTY

(EIDESSTATTLICHE VERSICHERUNG)

Hereby I declare that I have written this thesis by myself, marked the sources of any quotations or content obtained otherwise and mentioned any personal help by name.

(Ich erkläre hiermit, dass ich die vorliegende Doktorarbeit selbständig verfasst, die wörtlich oder inhaltlich anderen Quellen entnommenen Stellen als solche kenntlich gemacht und die Inanspruchnahme persönlicher Hilfe namentlich aufgeführt habe.)

Berlin, February 29th 2012

Judith Müller